Xe-100 Licensing Topical Report GOTHIC and Flownex Analysis Codes Qualification

Document ID Number	**:**	**008585**
Configuration Classification	**:**	**XE00-GL-GL-GL-GL-GL-X**
Revision	**:**	**2**
Security Classification	**:**	**Non Proprietary**
Status	**:**	**Approved**
Date Created	**:**	**21-May-2024**
Project	**:**	**XE-100**

This document is the property of X Energy, LLC. The content may not be reproduced, disclosed, or used without the Company's prior written approval.

E-SIGNATURES

Document Approval Signees

Action	Designation	Name	Signature	Date
Preparer	Principal Consultant	Charles DeDeaux	Maintained in Team Center	May 21, 2024
Reviewer	Manager, Mechanical Engineering	Andrew Dercher	Maintained in Team Center	May 21, 2024
Reviewer	Nuclear Safety Analysis Engineer	Brian Mays	Maintained in Team Center	May 21, 2024
Reviewer	Licensing Project Manager	Jessica Maddocks	Maintained in Team Center	May 21, 2024
Approver	Director, Licensing	Steve Vaughn	Maintained in Team Center	May 21,2024

Copyright Notice

This document is the property of X Energy LLC (X-energy) and was prepared for review by the U.S. Nuclear Regulatory Commission (NRC) and use by X-energy, its contractors, its customers, and other stakeholders as part of regulatory engagements for the Xe-100 reactor plant design. Other than by the NRC and its contractors as part of such regulatory reviews, the content herein may not be reproduced, disclosed, or used without prior written approval of X-energy. This report has been reviewed for proprietary and controlled information and determined to be available for unrestricted release.

10 CFR 810 Export-Controlled Information Disclaimer

This document was reviewed for information containing technology subject to U.S. export controls governed by the Export Administration regulations (15 CFR Part 730 et seq.) and/or the Department of Energy regulations (10 CFR Part 810) and does not contain information classified as Export Controlled Information. For specific information, contact X-energy at (301) 358-5600.

Department of Energy Acknowledgement and Disclaimer

This material is based upon work supported by the Department of Energy under Award Number DE-NE0009040.

This report was prepared as an account of work sponsored by an agency of the United States Government. Neither the United States Government nor any agency thereof, nor any of their employees, makes any warranty, express or implied, or assumes any legal liability or responsibility for the accuracy, completeness, or usefulness of any information, apparatus, product, or process disclosed, or represents that its use would not infringe privately owned rights. Reference herein to any specific commercial product, process, or service by trade name, trademark, manufacturer, or otherwise does not necessarily constitute or imply its endorsement, recommendation, or favoring by the United States Government or any agency thereof. The views and opinions of authors expressed herein do not necessarily state or reflect those of the United States Government or any agency thereof.

SYNOPSIS

This Licensing Topical Report (LTR) provides X-energy, LLC's (X-energy) approach to developing the GOTHIC and Flownex models that represents the thermal-hydraulic phenomena associated with the Transient and Safety Analysis (TSA) Evaluation Model (EM) for the Xe-100 reactor. The Xe-100 is a 200 MWt (80 MWe) pebble bed high temperature gas-cooled reactor design.

This report supports the EM Development and Assessment Process (EMDAP) described in U.S. Nuclear Regulatory Commission Regulatory Guide (RG) 1.203, "Transient and Accident Analysis Methods," as applicable, to prepare the Xe-100 plant TSA EM. The following three elements are addressed within the report that support the TSA EM:

1. Transient and Safety Analysis Code (GOTHIC and Flownex) Methodology (methods and theory)
2. Transient and Safety Analysis Codes (GOTHIC and Flownex) Qualification (verification and validation)
3. Transient and Safety Analysis Codes Quality Assurance

Additionally, the approach X-energy has provided for developing the TSA codes methodology is in accordance with the regulatory requirements discussed in Section 2. As a starting point, this report provides the overall framework and approach taken by X-energy to develop specific code methodologies, models, and Verification and Validation (V&V).

X-energy is seeking U.S. Nuclear Regulatory Commission review and approval of the proposed use of the GOTHIC and Flownex codes to perform TSA for the Xe-100 reactor. This information will be used as content for future Safety Analysis Reports (SARs) to fulfill the regulatory requirements for prospective Xe-100 licensing applications under 10 CFR 50, 10 CFR 52, and/or possibly a future licensing application under 10 CFR 53.

CONFIGURATION CONTROL/DOCUMENT CHANGE HISTORY

Document Change History

Rev.	Date	Preparer	Page/Section Revised	Description
1	29-Sep-2023	C. DeDeaux	N/A	Initial issue.
2	21-May-2024	C. DeDeaux	All	Revised to add more model details. Changed air cooled RCCS to water cooled RCCS. Updated boundaries. Revised Regulatory Section to be more focused. Revised GOTHIC Validation Plan Section to match current plan.

Table of Contents

Appendices

List of Tables

List of Figures

Abbreviations/Acronyms

Abbreviations/Acronyms

Short Form	Phrase
AOO	Anticipated Operational Occurrence
AR	Advanced Reactor
ARCAP	Advanced Reactor Content of Application Project
BC	Boundary Condition
BV	Bypass Valve
CB	Core Barrell
CFD	Computational Fluid Dynamics
CFR	Code of Federal Regulations
CI	Conventional Island
COL	Combined Operating License
CP	Construction Permit
CRW	Control Rod Withdrawal
DA	Deaerator
DBA	Design Basis Accident
DBE	Design Basis Event
DC	Design Certification
DCS	Distribution Control System
DID	Defense in Depth
DLOFC	Depressurized Loss of Forced Circulation
DOE	Department of Energy
EES	Engineering Equation Solver

Short Form	Phrase
EM	Evaluation Model
EMDAP	Evaluation Model Development and Assessment Process
ESP	Early Site Permit
FCV	Flow Control Valve
FR	Flow Restrictors
FSAR	Final Safety Analysis Report
FOM	Figure of Merit
FW	Feedwater
FWIV	Feedwater Isolation Valve
GDC	General Design Criteria
GUI	Graphical User Interface
HPB	Helium Pressure Boundary
HPFWP	High Pressure Feedwater Pump
HSS	Helium Service System
HTGR	High Temperature Gas-Cooled Reactor
HTR-10	10 MW High Temperature Gas-Cooled Reactor Test Module
HTTR	High Temperature Engineering Test Reactor
HX	Heat Exchanger
IPS	Investment Protection System
IV	Isolation Valve
LBE	Licensing Basis Event
LOCA	Loss of Coolant Accident
LOFC	Loss of Forced Coolant

Short Form	Phrase
LTR	Licensing Topical Report
LWR	Light Water Reactor
MCR	Maximum Continuous Rating
MSL	Main Steam Line
NEI	Nuclear Energy Institute
NEIMA	Nuclear Energy Innovation and Modernization Act
NGNP	Next Generation Nuclear Plant
NI	Nuclear Island
NIAB	Nuclear Island Auxiliary Building
NNR	National Nuclear Regulator
NRC	Nuclear Regulatory Commission
PIRT	Phenomena Identification and Ranking Table
PK-PIRT	Phenomena and Key Parameter Identification and Ranking Table
PLOFC	Pressurized Loss of Forced Cooling
PRA	Probabilistic Risk Assessment
PRV	Pressure Relief Valve
PSAR	Preliminary Safety Analysis Report
QA	Quality Assurance
QAP	Quality Assurance Program
QAPD	Quality Assurance Program Description
RB	Reactor Building
RCCS	Reactor Cavity Cooling System
RCS	Reactivity Control System

Short Form	Phrase
RCSS	Reactivity Control and Shutdown System
RG	Regulatory Guide
ROT	Reactor Outlet Temperature
RPS	Reactor Protection System
RPV	Reactor Pressure Vessel
RSS	Reserve Shutdown System
SAR	Safety Analysis Report
SDS	Software Design Specification
SEMP	Systems Engineering Management Plan
SG	Steam Generator
SRP	Standard Review Plan
SSC	Structure, System, and Component
SSS	Startup and Shutdown System
TB	Turbine Building
TI-RIPB	Technology-Inclusive, Risk-Informed, and Performance-Based
TRISO	TRistructural ISOtropic
TSA	Transient and Safety Analysis
UCO	Uranium Oxy-Carbide
V&V	Verification and Validation
X-energy	X Energy, LLC

1. Introduction

1.1 Purpose

The purpose of this report is to describe the methodology (including theory) of the GOTHIC and Flownex Analysis Codes that support the Safety Analysis EM for the Xe-100 described in the "Xe-100 Licensing Topical Report Transient and Safety Analysis Methodology,"[2]. Additionally, this report references the code manuals and associated validation and qualifications for GOTHIC and Flownex.

1.2 Scope

The GOTHIC and Flownex methodology described herein support the TSA EM described in Reference [2]. The TSA EM analyzes accident and transient behavior of the Xe-100. This report does not provide all the details of the specific codes used to perform safety analyses or how specific analyses have been categorized or performed.

The GOTHIC and Flownex methodology, utilized in the TSA EM, provided in this report are applicable to the Xe-100 reactor in deployments of a single-unit through multi-unit plants.

The conclusions presented in this report will support the Xe-100 Transient and Safety Analysis (TSA).

1.3 Interfacing Documents

This Licensing Topical Report (LTR) is one of several reports covering key regulatory issues submitted to the U.S. Nuclear Regulatory Commission (NRC) staff as part of Xe-100 pre-application process. The evaluation of the transient and accident analysis in accordance with R.G. 1.203 [3] is part of the overall approach to implement a risk-informed and performance-based design licensing basis as described in Nuclear Energy Institute (NEI) 18-04 [7] and endorsed and clarified by NRC Regulatory Guide (RG) 1.233 [14]. This report incorporates insights from several sources as described in the Reference section (Section 8) and throughout the report. This LTR interfaces with the follow documents:

- Xe-100 Licensing Topical Report, “Transient and Safety Analysis Methodologies”[2], describes the methods and models used to determine offsite dose and control room dose resulting from licensing basis events (LBEs) identified in the Probabilistic Risk Assessment (PRA) and related safety analyses.
- Xe-100 Licensing Topical Report, "Reactor Core Design Methods and Analysis" [84], describes the reactor core design analysis methodology and computer codes used to analyze the Xe-100 reactor at the beginning of life, startup, power ascension, and at equilibrium conditions.
- Xe-100 Licensing Topical Report, “Principal Design Criteria”[20], describes the development of the principal design criteria (PDC) for the X energy Xe-100 pebble bed, high-temperature gas cooled reactor (HTGR).

1.4 Document Layout

This report documents the Analysis Codes used to perform the analysis for transient and accident analysis for the Xe-100 plant. This report presents the high-level approach that X-energy is applying to develop the GOTHIC and Flownex models that perform the analysis for review by the NRC staff through the guidance of RG 1.203 [3]. It summarizes the relevant regulatory requirements and guidance, the theory for Code

Methodologies and Code Models of the Xe-100 plant, V&V, and quality assurance (QA) performed to support the Xe-100 plant. The following sections are provided in this document.

- This Section is followed by an overview of applicable regulatory requirements, Section 2.
- An overview of the safety analysis codes models is presented in Section 3.
- Section 4 describes the Code Manuals and Qualification for Flownex.
- Section 5 describes the Code Manuals and Qualification for GOTHIC.
- Section 6 describes the X-energy Quality Assurance Program (QAP).
- Conclusions are documented in Section 7.
- References are listed in Section 8.

1.5 Outcome Objectives

X-energy is requesting the NRC review and approval of the GOTHIC and Flownex Codes in support of the Xe-100 TSA Evaluation Model as described in the "Xe-100 Licensing Topical Report Transient and Safety Analysis Methodology" [2].

2. Overview of Regulatory Requirements and Guidance

The following sections provide an overview of the NRC regulatory framework. This report utilizes the regulatory framework described in this section to demonstrate how the GOTHIC and Flownex Analysis Codes provide input into the TSA Evaluation Models.

2.1 10 CFR Regulatory Requirements

The Xe-100 GOTHIC and Flownex Analysis Codes Qualification LTR supports the Xe-100 safety analyses required to comply with the appropriate sections of:

- 10 CFR 50.34(a) (Construction Permits)
- 10 CFR 50.34(b) (Operating Licenses)
- 10 CFR 52.17(a)(1)(ix) (Early Site Permits)
- 10 CFR 52.47(a)(2)(iv) (Design Certifications)
- 10 CFR 52.79(a)(1)(vi) (Combined Licenses)
- 10 CFR 52.137(a)(2)(iv) (Design Approvals)
- 10 CFR 52.157(d) (Manufacturing Licenses)
- 10 CFR 100 (Reactor Site Criteria)

2.2 Regulatory Guidance

2.2.1 Policy Statement on the Regulation of Advanced Reactors

The Advanced Reactor Policy Statement [11] provides overarching direction to advanced reactor (AR) developers like X-energy and informs the approach to regulation and addressing regulatory requirements. The final policy statement includes multiple design attributes that could assist the NRC to establish the acceptability and/or ability to license advanced reactor designs. These attributes inform the manner in which X-energy assessed the 10 CFR Part 50 technical requirements associated with design and programmatic elements of the Xe-100.

2.2.2 NRC Regulatory Guide 1.203, Transient and Accident Analysis Methods

Regulatory Guide 1.203 [3] describes a process that the NRC staff considers acceptable for use in developing and assessing EMs that may be used to analyze transient and accident behavior that is within the design basis of a nuclear power plant.

The EM establishes the basis for methods used to analyze a particular event or class of events. This concept is described in 10 CFR 50.46 [12] for Loss of Coolant Accident (LOCA) analysis but can be generalized for all analyzed events described in the Standard Review Plan (SRP) [18] and other regulatory guidance.

An EM is the calculational framework for evaluating the behavior of the reactor system during a postulated transient or design-basis accident. As such, the EM may include one or more computer programs, special models, and all other information needed to apply the calculational framework to a specific event.

The entirety of an EM ultimately determines whether the results are in compliance with applicable regulations. Therefore, the development, assessment, and review processes must consider the entire EM.

To produce a viable model, certain principles should be addressed during the model development and assessment processes. Specifically, the NRC has identified six basic principles described in Section B of Reference [3] important to follow in the process of developing and assessing an EM:

A summary of the EMDAP is shown in Figure 1 of Reference [3].

2.2.3 RG 1.233, Guidance for a Technology-Inclusive Risk-Informed, and Performance-Based Methodology to Inform the Licensing Basis and Content of Applications for Licenses, Certifications, and Approvals for Non-Light Water Reactors

RG 1.233 [15] provides the NRC staff's guidance on using a TI-RIPB methodology to inform the licensing basis and content of applications for non-LWRs, including, but not limited to, molten salt reactors, HTGRs, and a variety of fast reactors. The RG is for use by non-LWR applicants applying for permits, licenses, certifications, and approvals under 10 CFR Part 50, "Domestic Licensing of Production and Utilization Facilities" and 10 CFR Part 52, "Licenses, Certifications, and Approvals for Nuclear Power Plants."

RG 1.233 endorses the guidance of NEI 18-04 as one acceptable method for informing the licensing basis and determining the appropriate scope and level of detail for parts of applications for licenses, certifications, and approvals for non-LWRs. The NRC staff had no significant exceptions to the guidance in NEI 18-04 but did provide clarifications and points of emphasis as detailed in the RG. X-energy provided responses to these clarifications in its topical report on the subject [16]. NEI 18-04 outlines an approach for use by reactor developers to select Licensing Basis Events (LBEs), classify Structures, Systems, and Components (SSCs), determine special treatments and programmatic controls, and assess the adequacy of a design in terms of providing layers of Defense in Depth (DID). The methodology described in NEI 18-04 and RG 1.233 also provides a general approach for identifying an appropriate scope and depth of information that applications for licenses, certifications, and approvals should provide.

X-energy is implementing the NEI 18-04 approach and uses safety analysis methods as described in References [6] and [2] as a means of evaluating plant performance and response to various LBEs.

2.2.4 Regulatory Guide 1.253, Guidance For A Technology-Inclusive Content-Of-Application Methodology To Inform The Licensing Basis And Content Of Applications For Licenses, Certifications, And Approvals For Non-Light-Water Reactors

Regulatory Guide 1.253 [14] endorses the methodology described in NEI 21-07, with clarifications and additions, where applicable, as one acceptable process for use in developing certain portions of the SAR for an application for a non-LWR construction permit or operating license.

The guidance indicates source term information should cover all radioactive material inventories and include the type, quantity, and timing of the release of radioactive material from the facility during LBEs. Analysis methodologies, assumptions, bases, and justifications associated with transport of radioactive material from its point of origin to the accessible environment should be included. For an LMP-based safety analysis, the use of a mechanistic source term, consistent with the advanced non-LWR PRA standard definition should be included.

2.3 Additional NRC Guidance

2.3.1 DANU-ISG-2022-01, Review of Risk-Informed, Technology Inclusive Advanced Reactor Applications-Roadmap

The U.S. NRC staff is providing this interim staff guidance [13] for two reasons. First, this interim staff guidance (ISG) provides guidance to facilitate the preparation of non-light water reactor (non-LWR) applications for construction permits or operating licenses under Title 10 of the Code of Federal Regulations (CFR) Part 50, "Domestic Licensing of Production and Utilization Facilities," or combined licenses, manufacturing licenses, standard design approvals, and design certifications under 10 CFR Part 52, "Licenses, Certifications, and Approvals for Nuclear Power Plants." Second, this ISG provides guidance to NRC staff on how to review such an application.

The guidance in this ISG provides (1) a general overview of the information that should be included in a non-LWR application submitted under 10 CFR Part 50 or 10 CFR Part 52; (2) a review roadmap for NRC staff with the principal purpose of ensuring consistency, quality, and uniformity of staff reviews; and (3) a well-defined base from which the staff can evaluate proposed differences in the scope of reviews (e.g., construction permit versus operating license). Specific sections of the information described in this ISG are primarily aligned with the Licensing Modernization Project methodology as endorsed in RG-1.233, "Guidance for a Technology-Inclusive, Risk Informed, and Performance-Based Methodology To Inform the Licensing Basis and Content of Applications for Licenses, Certifications, and Approvals for Non-Light-Water Reactors," issued June 2020, as one acceptable process for applicants to use when developing portions of an application. Nonetheless, the concepts and general information in this ISG may also be used to inform the review of an application submitted using other methodologies (as applicable) such as one based on a maximum hypothetical accident or deterministic approaches.

X-energy will utilize DANU-ISG-2022-01 [13] for guidance in preparing the Xe-100 applications under 10 CFR 50 or 52, as applicable.

2.4 US HTGR Precedents

The X-energy team evaluated multiple reactor technology SARs and, when available, safety evaluation documents. The extensive experience gained through the General Atomics' Modular HTGR review, as documented in NUREG-1338 [24], and Next Generation Nuclear Plant (NGNP) licensing strategy, including white paper development for technical and policy considerations, provided useful insight for the Xe-100 approach to meeting regulatory requirements. Of particular interest are the Phenomena Identification and Ranking Tables (PIRT) of relevant phenomena common among HTGRs matured through the NGNP program. X-energy is undertaking an activity to screen the NGNP PIRTs to determine where further progress has been made in the state of knowledge and understanding of HTGR and TRistructural ISOtropic (TRISO) fuel technology.

Exelon transmitted a general description of the South African version of the Pebble Bed Modular Reactor (PBMR) to the NRC as an introduction to the PBMR [25]. It was transmitted for information only and no formal review was requested. The body of the document stated, " This document presents an overview of the PBMR, the concept, the basic principles of design, safety analysis, and operation. It is not intended to be used (or maintained) as a design document."

3. Overview of Safety Analysis Code Models

3.1 Introduction

Two of the codes utilized for the Xe-100 Safety Analysis integrated plant transients are GOTHIC and Flownex. Flownex provides the short-term transient response and GOTHIC provides the long-term transient response. The short-term transient is defined as the period at which SSCs are actively responding to an initiating event, forced cooling remains available or the primary system is actively depressurizing. The long-term transient is defined as the period at which passive heat transfer begins and no additional active plant responses to the initiating event are considered. The safety analysis team is primarily utilizing Flownex to capture the short-term transient response of the plant, focusing on the primary system conditions and key secondary side systems such as the Steam Generator (SG).

Flownex uses 1D Finite Volume discretization in general and 2D axi-symmetric discretization for the reactor. Flownex also solves the partial differential equations for mass, momentum, and energy conservation to obtain the mass flow, pressure, and temperature distributions throughout Xe-100. Flownex is used to model the Xe-100 for use in evaluating transient and accident analysis.

GOTHIC is a hybrid code that bridges the gap between computational fluid dynamics (CFD) and standard thermal-hydraulic systems analysis codes. Lumped parameter and 3-D regions can be combined into a single model to allow for detailed analysis in regions of interest. As a result, assuming proper care is taken in development of the model, a relatively fast running simulation can be produced. These features allow for the development of models suitable for sensitivity studies and design change analyses.

With Flownex, the Reactor Cavity Cooling System (RCCS) is water-cooled system that is modeled with constant flow rates and tuned to CFD results to approximate its behavior, benchmarked to normal operating conditions.

Model experience has shown that the fuel temperatures are not strongly affected by moderate deviations in the RCCS performance over short time frames. Vessel temperatures, on the other hand, will be strongly affected by it.

3.2 Flownex – Xe-100 Transient and Safety Analysis

The Flownex Code is used to calculate mass flows, temperatures, and pressures in the reactor core during expected operational modes and states, as well as under accident conditions. It is used for both steady state and transient simulations. Below is a brief description of Flownex. A more detailed discussion is found in Appendix C and a brief discussion of the theory is found in Appendix A.

3.2.1 Flownex Theory

The Flownex Simulation Environment program is an engineering simulation program that represents thermo-fluid systems as networks of one-dimensional components. It is used for Xe-100 safety analysis and is capable of modelling reactor kinetics and thermal-hydraulic phenomena. The complete Xe-100 thermal-hydraulic architecture, including the primary system, secondary system and power conversion cycle, is modelled with the Flownex SE code. Flownex is used to predict the overall system response of the reactor when integrated with the primary and secondary heat transport systems for the Xe-100 safety analyses. It is also used to provide thermal and flow BCs to other codes. To support the use of Flownex for Xe-100 safety analyses, Flownex validation for a steady-state fuel temperature calculation is performed by using the 10 MW High Temperature Gas-Cooled Reactor Test Module (HTR-10 benchmark). The theory for Flownex is briefly discussed in Appendix A.

3.2.2 Flownex Model – Xe-100 Transient and Safety Analysis

Sections 3.2.3 through 3.2.12 briefly discusses the Xe-100 Flownex Model. This is discussed in more detail in Appendix C ([6], [26], [27], [29], [30], [31], [32]) .

3.2.3 Deaerator

The Deaerator (DA) was removed from the Flownex model. The DA tank, and all upstream piping between the SSS and Turbine Bypass have been removed from the model. The removal of the DA tank component assumes that all the steam through the turbine bypass and turbine goes to the DA tank. [26] [6]

3.2.4 Reactor Cavity Cooling System

The RCCS is designed as a water-cooled Non-Safety Related system with Special Treatment (NSRST) active design for normal operations and Anticipated Operational Occurrences (AOOs) with a Safety Related (SR) passive mode that provides a 72-hour (3 day) boil off volume for Design Basis Event (DBE) and DBA conditions. After seventy-two (72) hours in a DBE or DBA (in a passive mode), it is assumed that on site staff will be able to connect equipment to re-fill the RCCS with water. [33] [81]

The RCCS model is still under development. The steady state model contains a general purpose and layout of the system. The liquid is single phase while in steady state with a network of pumps, pipes, and heat exchangers (HXs) removing a known quantity of parasitic heat loss from the RPV. Thus, for purposes of the safety analysis, only BCs are utilized.

3.2.5 Startup/Shutdown System

The safety analysis base model includes a simplified representation of the SSS to simulate the effects of decay heat removal and sensible heat removal from the Xe-100 reactor. The purpose of the simulated SSS is to provide secondary heat removal when main loop cooling capabilities are unavailable. [6] [27].

3.2.6 Steam Generator

In the SG, the heat transfer is assumed to be uniform in the radial direction in the tube coil region, so only the axial subdivisions were defined regarding the number of axial nodes. In addition, the water/steam side of the SG tube coils are modeled. Similar to the helium volume, the heat transfer is assumed to be uniform in the radial direction in tube coil region. Axially, this volume was divided into axial nodes to match the axial regions for the helium side of the tube coils.

A negligible amount of volume (~1.0 L) was added to the nodes in the relief valve lines to improve numerical stability in the low flow lines between the steam lines and the relief valve discharge nodes. The discharge BCs were set with a superheated temperature of 130°C to prevent two-phase conditions out of the relief valves, which have been observed to lead to model errors. [6] [29]

3.2.7 Material Properties

All fluid and solid material properties in the model are inherited from Reference [31], excluding the exceptions detailed in Section 2.4 of Reference [6]. The exceptions are related to the modeling of irradiation-induced aging effects of graphite within the Xe-100 reactor. Certain graphite properties are strongly dependent on the amount of irradiation damage that incurs during their operational lifetimes. Updates have been made to the model to allow for a detailed accounting of these effects and their impacts on plant response and heat transfer. [6] [34]

3.2.8 Reactor and Helium Pressure Boundary

The Flownex reactor model models the neutronic response of the Xe-100 reactor using a point kinetics script that is delivered as part of the Flownex software package. It uses inputs derived from other neutronics simulation software (primarily VSOP) to calculate the reactor fission and decay power. [6] [31] [84]

3.2.9 Flow Paths

It is assumed that the model will be based on a two-dimensional axially symmetric coordinate system rather than a full three-dimensional cylindrical coordinate system. This implies that all variations in geometry or material properties around the perimeter of the reactor will be spread evenly around the circumference at that radius to form a material with constant properties at a given height and radius. [38]

3.2.10 Heat Transfer

In Flownex, heat transfer through graphite is not significantly affected by density changes and is not accounted for because irradiation damage does not affect the mass of the graphite just the volume a given mass occupies.

Reactor Pressure Vessel (RPV) temperatures are reported by aggregating the nodal results from the appropriate components. The heat transfer coefficients for convection, radiation, and conduction are unchanged from the upstream model. [6]

In the absence of forced helium flow, heat transfer within the pebble bed is dominated by radiative and conductive mechanisms. The complexities of these phenomena may be represented in a simplified manner using an effective thermal conductivity between pebble nodes that varies as a function of fuel pebble surface temperature [73]. Additional information for pebble-to-pebble heat transfer is found in Reference [6].

3.2.11 Boundary Conditions

Boundary Condition components in the model are described in Appendix C and Reference [6], along with their values for select circumstances. The BC values correspond to the parameters used to establish the 100% power controlled operating conditions. They are derived from the upstream model conditions at 100% power and the various sub-models. Most of these BCs will remain unchanged during an LBE unless the LBE specifically requires a change. The BCs and component inputs must be set when performing a steady state solution. [6] [35]

3.2.12 Nodes

Flownex uses nodes and elements to represent a thermal-fluid network graphically. Elements are components such as pipes, pumps, valves, compressors, or HXs, while nodes are the end points of elements. Elements can be connected in any way at common nodes to form a network.

Flownex solves the momentum equation in each element and the continuity and energy equation at each node. Although components may be represented at the systems level as a single entity, they may actually be complex sub-networks. The main network with embedded sub-networks is treated as one large network in the solution algorithm. [38]

3.3 GOTHIC – Xe-100 Transient and Safety Analysis

GOTHIC was developed and is maintained under Numerical Advisory Solutions, LLC QA Program that conforms to the requirements of 10 CFR 50 Appendix B and 10 CFR 50 Part 21. GOTHIC is a hybrid code that bridges the gap between CFD and standard thermal-hydraulic systems analysis codes. Lumped parameter and 3-D regions can be combined into a single model to allow for detailed analysis in regions of interest. As a result, a relatively fast running simulation can be produced. These features allow for the development of models suitable for sensitivity studies and design change analyses. The purpose of this model is to provide a relatively fast running tool to provide insight into dose analysis, and RCCS and RB analyses. [7]

Thermal-hydraulic analysis is needed for a variety of reasons; to address certain safety issues such as plant response following a transient or accident; to predict the plant response to a change in operating conditions; to model the behavior of plant; or for a wide variety of situations that involve the response of a system to applied mass and energy sources. In these analyses, the focus may be on the maximum pressure or temperature, pressure loadings on internal structures due to jet impingement or pressure gradients, local temperature variation, equipment temperatures, buildup of volatile gases or a variety of other conditions of interest.

The information below briefly discusses the application of the GOTHIC theory specifically required for the GOTHIC Reactor System Mode used in TSA. Appendix B discusses the model theory. A description of the Xe-100 GOTHIC Methodologies and Model are found in Appendix D.

3.3.1 Volumes

The volume of the pebble bed region of the core is modeled. The fuel pebbles are assumed to occupy a defined region (cylindrical), because the cone region is not explicitly modeled. However, the pebble bed is meshed radially with the dimensions equal to that used in the VSOP model [36]. Volume summaries used in the GOTHIC model are described Appendix D.

3.3.2 Steam Generator

GOTHIC models the helium space. In the SG, the heat transfer is assumed to be uniform in the radial direction in the tube coil region, so only the axial subdivisions are defined regarding the number of axial nodes. Sensitivity studies were performed to determine the number of nodes required to achieve acceptable heat transfer performance. In addition, the water/steam side of the SG tube coils are modeled. Similar to the helium volume, the heat transfer is assumed to be uniform in the radial direction in tube coil region. Axially, this volume was divided into 30 axial nodes to match the axial regions for the helium side of the tube coils.

3.3.3 Reactor Cavity Cooling System

The RCCS model was run using GOTHIC computer code. The RCCS is described in Section 3.2.4.

3.3.4 Reactor Building

A detailed 3-D model of the Reactor Building (RB) was developed using the GOTHIC computer code for the purpose of evaluating pressure and temperature response as well as helium, fission product and dust transport. Additionally, a (lumped volume) O-D model of the RB was developed for faster runs of sensitivity studies, which is adequate for building response. This representation could be combined with a GOTHIC model of the HPB to provide an integrated system response of the HPB and RB.

3.3.5 Flow Paths

Development of the Flow Paths are provided in Appendix D.

3.3.6 Conductors

A. **Conductors**

Appendix D provides a summary of the conductors defined for the GOTHIC reactor system model. Conductor numbers with a “s” appended refer to subdivided conductors.

1. Pebble Bed Fuel Conductors

The geometry of conductors in GOTHIC is limited to slabs, cylinders, cylindrical shells and spherical. The process is described in Appendix D.

2. Side Reflector Conductors

The helium gap between the outer graphite surface of the side reflector and the inner surface of the core barrel is not explicitly modelled as a separate volume. This is due to uncertainties concerning graphite expansion and fissuring due to radiation exposure along with uncertainties concerning helium bypass around the graphite blocks into the helium gap. Therefore, a composite conductor consisting of the side reflector graphite inner blocks, graphite outer blocks, helium gap, and core barrel is defined. The side reflector support rings and wedges are not explicitly modelled. Additional information is found in Appendix D.

B. **Surface Options**

GOTHIC surface options define the heat transfer coefficients along with various heat transfer options and are defined for both sides of the conductor. The surface options are described in Appendix D.

3.3.7 Boundary Conditions

The GOTHIC BCs are listed with the GOTHIC Model Designator (e.g., 1F, 2F, 3P…) with a brief description in Appendix D.

3.3.8 Components

Information on the valve and pumps modeled in GOTHIC (including model designators) are included in Appendix D.

4. Flownex Code Manuals and Qualifications

4.1 Flownex Code User Manuals

4.1.1 Flownex Simulation Environment General User Manual

The general user manual, which describes the functionality of the Flownex Simulation Environment (SE), includes [37]:

- Descriptions of all the graphical user interface (GUI) components.
- Methods to create a Flownex SE project.
- Chart and lookup table functionality.
- Methods to create dynamic simulations.
- Descriptions and examples of Flownex Simulation Environment utilities, this includes the Designer, Optimizer, Scheduler, Sensitivity Analysis, Excel Network Importer, Aspen Fluid Generator, Excel Reporting and Alarms.
- Procedures to create graphs, set-up compound components, log results.
- Methods to link third party software.

4.1.2 Flownex Library Manual

The Flownex library manual describes the functionality of Flownex library components this includes [38]:

- Descriptions of all components within the Flownex library.
- Component theory.
- Component input properties.
- Component results.
- Flownex charts and lookup tables.

4.1.3 Flownex Theory Manual

The Flownex theory manual describes the theory used by the Flownex solver this includes [39]:

- Governing equations theory
- Two phase flow theory
- Combustion modeling theory
- Dynamic modeling theory
- Slurry modeling theory

4.2 Verification and Validation

4.2.1 V&V Scope

It is important to distinguish between "Software V&V" and "Model and Data V&V." Software V&V is done to ensure the integrity and consistency of the simulation software. However, the accuracy of simulation results is not only dependent on the integrity of the software itself, but also on the way the software is used to setup a simulation model, as well as the component model input values for the specific simulation model. This area is covered by Calculation Model and Data V&V.

Calculation Model and Data V&V is unique to each simulation model and is the responsibility of the software user. Calculation Model and Data V&V includes verification that the calculation model was set up in such a way that all the important phenomena for the specific case are appropriately accounted for and ensuring that the input values for each component are accurate.

4.2.2 Vendor-Based V&V Efforts

Flownex is developed under an NQA-1 quality management system at M-Tech Industrial (software design authority) which include:

- test plans and procedures,
- code reviews, user testing,
- automated testing and regression testing.

More than 1000 networks are tested between each release of Flownex to ensure that the new version of Flownex gives the same, or more accurate, results as compared to the previous version. V&V is a crucial part in the development of Flownex.

More than 40-person years of work was done on the V&V of Flownex. In the V&V process of Flownex, verification is the process of ensuring that the controlling physical equations have been correctly translated into computer code or in the case of hand calculations, correctly incorporated into the calculation procedure. Validation is defined as the evidence that demonstrates that the code or calculation method is fit for purpose. This includes confirmation that the results from the verified model agrees with the benchmarks.

To ensure that all phenomena for each component in Flownex are validated for the various extremities is a comprehensive exercise. Furthermore, V&V of the individual components as well as integrated systems of components, for both steady-state and dynamic analysis are required.

V&V forms part of the overall Flownex development process and includes the verification activities that form part of the software engineering process, as well as all related verification that is done as part of the derivation and implementation of the theory for component models or model enhancements.

Validation of Flownex is performed by comparing the results of the implemented theoretical models in Flownex with benchmark data obtained from appropriate methods or sources such as analytical data, experimental data, plant data and data obtained from other codes such as Spectra, XNet, and Star CD. To further enhance the Flownex V&V effort, and to ensure that the Flownex capabilities comply with the latest requirements on HTGR analysis, M-Tech is an active participant in international conferences, like CRP-5, ICAPP, and HTR-TN.

4.3 Existing Code Verification and Validation

4.3.1 X-energy Flownex Validation Plan – Service Receipt Inspection Report

This report lays out the validation plan for Flownex [40]. The postulated accident cases for validation of Flownex are as follows:

A. Loss of Feedwater
B. Circulator Trip
C. Primary Side Depressurization Events
D. Steam Generator Tube Rupture (SGTR)
E. Seismic Events

For all LBEs, the primary metric is dose at the EAB. Because dose is not calculated by Flownex, parameters predicted by Flownex which have a significant impact on subsequent dose assessments should therefore be considered as candidates for validation. Such parameters are those which measure conditions under which radionuclide release becomes more probable. With these considerations, candidates for FOM in validation are:

A. Fuel Temperature
B. Primary Coolant Temperature
C. Primary Coolant Flow
D. Primary Side Coolant Pressure
E. Reactor Power
F. Break Discharge (Primary and Secondary)
G. Reactor Pressure Vessel Wall Temperature
H. Reactor Cavity Temperature

4.3.2 Flownex Fuel Temperature Validation Exercise Report

The PIRT for the Xe-100 safety analysis is documented in Table 17 of Reference [42]. The phenomena modelled by Flownex have been extracted from the overall PIRT documented in an earlier version of Reference [42] and are presented in Table 1 of Reference [42]. There are no differences in the phenomena relevant to this validation exercise and Table 1 of Reference [41].

The validation method used compares the Flownex pebble temperature predictions against a mathematical solution for a stylized problem. Specifically, the computer program predictions were compared to the relevant solutions to standard or benchmark problems.

The stylized problem uses pebble dimensions and material properties for the Pebble Bed Modular Reactor (PBMR) design, which uses 60 mm pebbles, consisting of a 5 mm thick graphite shell and an inner fuel matrix containing TRISO particles. The pebble dimensions are the same as the pebble dimensions for the Xe-100.

The pebbles in the stylized problem differ from the Xe-100 pebbles with respect to the number of TRISO particles. The stylized problem assumes 15,000 TRISO particles per pebble compared to the approximate 19,000 TRISO particles in the Xe-100 pebble. The difference is dispositioned in Section 6.2.1 of Reference [41].

The stylized problem in Reference [44] uses BCs which result in a change in pebble temperature from 0°C to approximately 160°C. To extend the range over which the validation is performed, the calculations applied to the stylized problem in Reference [44] have been extended to cover pebble temperature of up to approximately 1200°C. The extended calculations are described further in Section 2.0 of Reference [41].

Use of the stylized problem for validation of the Flownex internal pebble temperatures demonstrates that given the correct thermal properties of the pebble, and the correct BCs to the pebble, an accurate prediction of the internal pebble temperature is obtained.

The validation exercise for the Flownex predictions of fuel temperature demonstrate that discretization of the pebble model strongly influences the bias in the code predictions. For the 6-node model applied in Xe-100 safety analysis, the accuracy in the code predictions is summarized in Table 5 and Table 6 of Reference [41]. The prediction bias is a strong function of fuel power and therefore at low powers that would occur following a reactor trip or fuel temperature induced power reduction, the prediction bias is not as significant. [46]

4.3.3 Flownex Reflector Structure Temperature Validation Exercise Report Using HTR-10 Benchmark at Steady State Conditions

A comparison of the Flownex temperature predictions to temperature measurements is an acceptable method of validation and is consistent with ASME NQA-1. As discussed in Section 1.1 of Reference [45], the phenomena to be validated are thermal conduction (HT1), convection (HT2) and radiation (HT3), and the FOM is temperature at selected locations in the HTR-10 core.

There are significant similarities in the HTR-10 and Xe-100 reactor with some differences, as summarized in Table 3 of Reference [45]. They are both a graphite moderated and helium-cooled pebble bed reactor, employing the similar fuel type of 60-mm diameter pebbles, consisting of a 5 mm graphite shell and an inner fuel matrix containing TRISO particles with a pebble packing fraction of [[ ]]^{P}. The overall reactor structure is very similar such that the reactor core is a cylindrical shape with the active core in the center, surrounded by the top/bottom/side reflectors inside the Core Barrell (CB) and RPV. The reactor and SG are housed in two separate steel pressure vessels, which are arranged side by side and connected to each other by a horizontal hot gas duct pressure vessel. The main differences are largely due to the reactor power: 10 MWt for the HTR-10 and 200 MWt for the Xe-100. So, the Xe-100 reactor has higher power, larger core size, and higher reactor power density (2.0 MW/m3 for HTR-10 versus 4.8 MW/m3 for Xe-100). Therefore, the Xe-100 operates at higher coolant flow rate and higher pressure in the primary system: 4.32 kg/s at 3.0 MPa(a) for HTR-10 versus 78.91 kg/s at 6.0 MPa(a) for Xe-100. However, the operational reactor inlet and outlet temperatures in the primary side are similar in both reactors: e.g., 250/700°C for HTR-10 versus 260/750°C for Xe-100. Therefore, References [43] and [47] determined that the HTR-10 benchmark data [48] should be relevant for the heat transfer V&V of the Flownex code based on the similarities in the reactor type, the operational range and geometrical features.

The HTR-10 and the associated experimental data were gathered at actual operating conditions, with a steady state temperature distribution within the pebble bed. The measured data included solid material temperatures adjacent to the pebble bed for a full power initial core. The HTR-10 operational data provides integral test results for V&V of the Flownex code since the data represents the entire pebble bed core with power and flow at nominal conditions or at a percent fraction of nominal conditions. The validation focused on the total heat transfer including conduction, convection, and radiation, providing axial and radial temperature profiles in the core and in the graphite.

The reference heat conduction calculation model used by the Chinese Institute of Nuclear and New Technology (INET) is shown in Figure 3 of Reference [38]: note INET is the host organization of the HTR-10 benchmark problem. It includes the fuel zone and non-fuel zone of the core, reflectors, carbon bricks, cavity, thermal shield, CB, RPV, RCCS, and coolant flow paths, etc. The 2D axi-symmetric heat conduction model in the R-Z geometry for the HTR-10 consists of 33 radial and 57 axial mesh points, and there are 44 different calculating regions. The pebble bed, reflectors and gas cavity are treated to be homogeneous media whose heat capacities can be determined according to the void fraction in these regions. The heat transfer of conduction, radiation and natural convection is considered in this model. This model is used as the basis to construct a Flownex model for HTR-10 validation exercise.

The validation exercises for the HTR-10 benchmark problem demonstrate that Flownex can predict the temperature distribution in the HTR-10 reactor core reasonably well within ±15% prediction error (224°C – 882°C) for steady-state operation at full power of 10 MWt. Generally, a coarse node model is employed for the HTR-10 reactor core model, and the discretization error is estimated to be approximately 9°C for predicting fuel pebble centerline temperature (coarse grid underprediction of temperature). The code bias for the side reflector temperatures was determined to be 29.8°C (overprediction), while the bias is -37.6°C (underprediction) for the top and bottom reflectors. The Euclidian difference between the experiment and simulation is 12.8%.

The Flownex HTR-10 benchmark study is compared against the previous two benchmark study results (INET and CEA): INET employed the modular code THERMIX, while CEA completed the benchmark problem using the CFD code ARCTURUS. Overall, the predicted temperatures by all three codes agree well with those measured temperatures within ±15% prediction errors (224°C – 882°C). The code bias and its variation in all three benchmark studies are similar.

The sensitivity studies on two key parameters (i.e., core bypass flow and natural convection cooling in air cavities) show that the extent of core bypass flow can have a relatively significant impact on predicting the maximum pebble centerline and surface temperatures in the reactor core during steady-state operation. Selection of a thermal conductivity model (e.g., correlation for the side reflector versus correlation for the top/bottom reflectors) does not have appreciable impact on the reactor core temperature prediction by Flownex during the steady-state operation. The steady-state condition is dominated by convection heat transfer, which transports orders of magnitude more heat than conduction.

4.3.4 Initial Flownex Validation Exercise Report Using HTR-10 Benchmark – Prediction and Quantification of Code Accuracy for Reactor Power Transients

As discussed in [43], a test at the 10 MWt HTGR Test Module (HTR-10) was identified as appropriate for Flownex validation to support Xe-100 safety analyses. The HTR-10 tests were published in the formal IAEA benchmark report [49]. The benchmark study included steady-state operation at full power (10 MWt) and transients following a LOFC without scram and single CRW without scram at partial load of 30% of full power (3 MWt). The transient tests for Loss of Forced Coolant (LOFC) without scram and single Control Rod Withdrawal (CRW) without scram were performed for which the measured relative reactor power is available. All-important phenomena (see Section 1.1 of Reference [48]) relevant to the LOFC and single CRW safety analyses were active in the transient tests. Although not measured, a key parameter in these tests is the fuel temperature because the reactivity feedback induced by the change in fuel temperature causes the reactor to shut down during the test. The tests are therefore suitable for indirectly assessing the fuel temperature reactivity feedback effect on the reactor power prediction. [48]

The validation exercise to assess the Flownex predictions of the temperature in the graphite structures within the reactor vessel for steady-state operation at full power operation was documented in [83]. The report documents the validation exercise to assess the Flownex predictions of the reactor power transients following the LOFC without scram and single CRW without scram by using Flownex code version 8.14.0.4675 [51]. The work documented in this report follows the Flownex validation plan [43] with the exception that the neutronic input parameters were obtained as described in Reference [48].

4.3.5 Pebble Bed Temperature Prediction Validation with SANA

Flownex is supported by a large V&V program directed by M-Tech. Much of the activity is focused on exercises which align with verification, as opposed to validation. However, the program also contains a significant number of validation exercises against experimental test data. The validation exercises that are based on experimental data, or independent analytical solutions, are identified in Reference [40]. The phenomena active in the validation exercises are noted and the associated FOM relevant to the validation is also identified.

Validation supporting the accuracy of graphite pebble temperature predictions in a pebble bed in the absence of forced flow is available in Reference [44]. The validation is based on the SANA experimental test data and is summarized in the code applicability section of Reference [54]. The SANA test rig is illustrated in Figure 1 of Reference [40]. The validation spanned pebble temperatures from 60°C to 1200°C. Both steady state and transient predictions of pebble temperature are compared at various axial and radial locations in the bed. The validation addressed conductive and radiative heat transfer phenomena in the pebble bed using the Zehner-Schlünder correlation. The convective heat transfer phenomenon under natural circulation conditions, which would occur in a loss of flow event, was present in the test and was captured in the validation using the Kugeler and Schulten correlation. The fluid resistance phenomenon was modelled using the KTA-Ergun equation, which is also known as the PBR equation, although only under natural circulation conditions. The temperature measurements were compared to the Flownex predictions at the pebble surface. Examples of plots for steady state and transient validation cases are shown in Figure 2 and Figure 3 of Reference [40]. The accuracy of the pebble temperature predictions was reported in terms of the maximum normalized point difference and Euclidian difference.

The range of pebble surface temperatures in the SANA experiments exceeds the range of maximum fuel average temperatures predicted in the depressurized loss of flow analysis reported in Reference [54]. The SANA experiments are therefore sufficient to fully cover the required range of applicability for the DLOFC with respect to validation of the heat transfer models in the pebble bed.

4.3.6 Blowdown Pressure Prediction Validation

Validation supporting the accuracy of Flownex pressure predictions in the Flownex nodes under pressurization and depressurization transients is available in Reference [55]. The accuracy of the pressure predictions in this validation exercise also illustrates that accuracy of the break discharge modelling.

The volume blowdown test rig is illustrated in Figure 4 of Reference [40]. The piping connecting the three tanks in the test rig contain sharp edged orifices and isolation valves (IVs). The tanks are initially at different pressures as shown in the test matrix reproduced in Table 3 of Reference [40]. As noted in the table end notes, the test pressures ranged between approximately zero (vacuum) and 1 MPa(a). The test matrix shown in the table contains cases in which the tanks are initially filled with different gases, allowing the Flownex models for the mixing phenomenon to be assessed. Each test case is initiated by simultaneously and quickly opening the valves between the tanks. The tests were simulated with Flownex using ideal gas models, including modelling of discharge through the orifices. Using ideal gas modelling is consistent with the approach applied in the safety analysis documented in Reference [54]. Discharge through an orifice is also used for break modelling in the safety analysis [54].

An example of a plot from Reference [55] comparing Flownex predictions to the test results are reproduced in Figure 5 of Reference [40]. The accuracy of the gas pressure predictions was reported in terms of the maximum point difference and Euclidian difference.

The test is appropriate for assessing break discharge modelling for breaks in which the gas behaves as an ideal gas. Gases approximate ideal gas behavior for low pressures or high temperature, relative to the critical pressure and temperature of the gas. The range of conditions covered in the validation and in the safety analysis is discussed further below.

The blowdown tests were performed at low, ambient temperatures. At the higher temperatures predicted in the safety analysis, the gases will continue to approximate an ideal gas. The maximum primary pressure in the blowdown tests was 1 MPa(a). For comparison, the maximum pressure in the SGTR case reported in Reference [54] was approximately 8.4 MPa(a). Although the range of pressures in the safety analysis exceeds the pressures in the blowdown test, the gas temperatures in the safety analysis are much higher than in the ambient temperatures applied in the test. At the high temperatures predicted in the safety analysis, the gases continue to approximate ideal gas behavior. To illustrate this, at 8.4 MPa(a) and 800°C the volume occupied by one gmol of steam was calculated based on steam tables. The volume was then used to calculate the pressure of one gmol of steam at 800°C using the ideal gas law. The pressure predicted by the ideal gas law was 2% higher than that from the steam tables. The small overprediction is conservative in the context of assessment of pressure boundary integrity. The deviation from the ideal gas law for the primary coolant, helium, will be smaller than that for the larger steam molecules.

4.3.7 Integrated System Validation with PBMM

Validation supporting the accuracy of temperature and pressure predictions in an integrated system is available in Reference [55]. The validation was executed using data from the Pebble Bed Micro Model (PBMM), which is illustrated in Figure 8 of Reference [40]. The PBMM is based on the Brayton power cycle. The nitrogen is compressed, heated, and then expanded in a series of turbines. It is then cooled to complete the cycle. The nitrogen temperatures ranged from approximately 25°C to 600°C. The nitrogen pressures ranged from approximately atmospheric up to approximately 300 kPa(a). Further details are provided in Reference [55]. Examples of plots from Reference [55] comparing Flownex predictions to the test results are reproduced in Figure 9 and Figure 10 of Reference [40]. The accuracy of the gas temperature and pressure predictions after each step of the cycle were reported in terms of the maximum point difference and Euclidean point difference [57].

4.3.8 Integrated System Startup Validation with PBMM

Validation supporting the accuracy of temperature and pressure predictions in an integrated system is available in Reference [58]. Reference [58] provides a comparison of Flownet[1] predictions with measurements from the PBMM during startup. The code was used to determine the point at which the PBMM was "bootstrapped" during startup. The point at which the system is bootstrapped is defined as the point during startup at which the circulation in the system becomes self-sustaining without the need for the startup blower.

The manner in which bootstrapping is achieved is described in Reference [58] and is reproduced here. Refer to Figure 11 of Reference [40] for the location of the components discussed in the following quote from Reference [58]: "During startup the inline valve (IV) is closed and the startup blower system is used to circulate the gas through the cycle. The startup blower system is a positive displacement device; thus the flowrate remains essentially constant. Heat is then added to the gas in the heater. This energy is converted in the turbines into shaft work to power the compressors. For startup, the power to the heater is kept constant at about 180kW. As the system heats up, the outlet temperature of the heater rises as the inlet temperature rises and the pressure increase across the IV drops. The cycle spirals towards selfsustained circulation and the startup blower system is disengaged when the pressure drop over the valve is 0kPa. At this condition the cycle is said to have bootstrapped."

Reference [58] proposes that the exit temperature of the heater is the most important parameter with respect to defining of the bootstrap point because the energy that the turbines can deliver depends on the inlet gas temperature.

An estimation of the bootstrap temperature was made using Flownet by calculating the pressure increases over the IV as a function of heater outlet temperature. The results of the comparison are shown in Figure 12 of Reference [40].

4.3.9 Integrated System Nitrogen Injection Transient with PBMM

Validation supporting the accuracy of pressure predictions in an integrated system is available in Reference [59]. Reference [59] presents a comparison of Flownex with PBMM test results for a case in which nitrogen is injected transiently into the circuit. Nitrogen is injected into the cycle just upstream of the pre-Cooler (see Figure 11 of Reference [40]) in order to increase the inventory of nitrogen in the cycle. As the mass of nitrogen in the cycle increases, the power output of the power turbine also increases. Before injection commences, the plant is run at steady state. The steady state conditions prior to the two transient tests that were performed are reproduced in Table 4 of Reference [40]. For the transient, nitrogen was injected into the cycle at a rate of 0.0227 kg/s for about a minute.

The transient results from Reference [59] are shown in Figure 13, Figure 14 and Figure 15 of Reference [40] for the case with an initial low pressure compressor suction pressure of 94 kPa(a). Reference [59] indicated that a probable cause of the difference between measured and predicted values in the transient was that the connecting pipe work between the turbo machines is very short. The flow profile of the gas

[1] Flownet is the original name for Flownex.

entering the turbine is therefore not properly developed and the actual characteristics will be different from the characteristics as determined by the supplier and implemented in the model.

4.3.10 Pressure in Branched Piping Network Validation

Validation supporting the accuracy of the pressure predictions in a branched network of piping is available in References [60] and [61]. The test rig used in the experiment is part of the test rig in Section 3.2 of Reference [40]. The portion of the test rig used to collect the piping pressure data is the piping which exhausts Tank C, illustrated in Figure 6 of Reference [40]. Valve VAL-111 is quickly opened, creating a pressure wave in the downstream piping which is recorded at the location of the pressure taps shown in Figure 6. The pressures encountered during the tests ranged from a maximum of approximately 387 kPa(a) to atmospheric. Examples of plots comparing Flownex predictions to the test results are reproduced in Figure 7 of Reference [40]. The accuracy of the gas pressure predictions was reported in terms of the maximum point difference and Euclidian difference.

4.3.11 Mass Flow for Compressible Gas in a Piping Network Validation

A validation exercise for mass flow is summarized in Reference [62]. The network balancing experiment was to validate the Flownex node component for the mass flow balancing behavior of a compressible gas in a complex pipe network. A schematic of the test rig is shown in Figure 16 of Reference [40]. A fan supplying 0.045 kg/s of air at a total pressure of 102.36 kPa(a) is positioned at the inlet of plenum A. The flow network configuration was altered by opening and closing valves in each of the fifteen pipes resulting in different network flow configurations. The results for two flow configurations were reported in Reference [62]. Examples of plots comparing Flownex predictions to experimental measurements are reproduced in Figure 17 of Reference [40]. The accuracy of the gas pressure predictions was calculated in terms of the maximum point difference and Euclidian difference but only the maximum point difference was reported in Reference [62]

The tests were performed at low, ambient temperatures. At the higher temperatures predicted in the safety analysis, the gas will continue to approximate an ideal gas. This provides confidence in the mass flow predictions in a high temperature gas reactor.

4.3.12 Transient Temperature Predictions in Heat Exchanger Validation

A benchmarking exercise for temperature predictions in a pipe-in-pipe counter flow HX is summarized in Reference [62]. A schematic of the experimental setup is shown in Figure 18 of Reference [40]. The fluid in the experiment was water. The test was performed with both fluid streams at 26°C. The temperature of one stream was then increased from 26°C to 60°C. Additional test conditions are specified in Reference [62]. A plot comparing Flownex predictions to experimental measurements is shown in Figure 19 of Reference [40]. The accuracy of the water Temperature predictions for both streams exiting the HX was reported in terms of the maximum point difference and Euclidian difference in Reference [62]. The test exercises the convective and conductive heat transfer phenomena with respect to the prediction of fluid temperature.

4.3.13 Existing Validation Against Analytical Solutions

The 2021 Validation and Verification documentation [63] includes multiple cases in which the equations from Flownex are solved external to the code using the Engineering Equation Solver (EES). EES is an engineering analysis software developed by F-Chart Software for educational and commercial applications. It is a general equation solver that can solve thousands of coupled non-linear algebraic and differential equation and includes a library of thermodynamic and transport properties for hundreds of fluids and solid materials. In the majority of applications of EES, the exercises would be better categorized as verification since they confirm the correct implementation of the equations in the code by demonstrating that the code produces the same result as obtained when EES is used to solve the Flownex equations external to the code. These verification exercises have significant value because they demonstrate the correct function of the code, they are not discussed here. Rather, the exercises noted below are those which compare the code predictions to analytical solutions.

The following are Examples of existing validation against analytical solutions. Validation against analytical solutions is also reported in Reference [64] for assessment of the choked flow phenomenon and phenomena related to compressible flow in the pipe with heat transfer to the pipe.

- Step change in inlet temperature to a fixed adiabatic volume with constant inlet and outlet helium mass flowrates [66]. The benchmark solution was not accessible for review but was stated to be documented in Reference [66]. The high-level description of the approach to the benchmark solutions provided in Reference [66] provides some confidence in the independence of the analytical solutions from Flownex. Predicted node temperature change and pressure change were the FOMs.
- Step change in heat transfer to a fixed volume with constant inlet and outlet helium mass flowrates [65]. The benchmark solution was not accessible for review but was stated to be documented in Reference [66]. The high-level description of the approach to the benchmark solutions provided in Reference [66] provides some confidence in the independence of the analytical solutions from Flownex. Predicted node temperature change and pressure change were the FOMs.
- Fixed volume with constant helium mass inlet flowrate and no outlet flow [65]. The benchmark solution was not accessible for review but was stated to be documented in Reference [66]. The high-level description of the approach to the benchmark solutions provided in Reference [66] provides some confidence in the independence of the analytical solutions from Flownex. Predicted node temperature change and pressure change were the FOMs.
- Sudden mass injection into a tank [70]. Predicted node temperature change and pressure change were the FOMs.

4.4 Planned Flownex Code Verification and Validation

4.4.1 Flownex Simulations

The Flownex simulation will be performed with pebble properties and BCs which are identical to those applied in the analytical solution. Flownex calculates a fuel temperature for each fuel node in the Flownex model. The fuel center node temperatures of both the fuel matrix and the fuel kernel are therefore available for direct comparison with the benchmark calculations. The average fuel temperature, used for determining the fuel temperature reactivity feedback, is the temperature of either the fuel matrix node temperature or the fuel kernel node temperature (as selected by the user) and is the volume-weighted-average over the heated region [27]. These average temperatures are available for direct comparison with the weighted average benchmark temperatures. The Flownex model for the validation exercise has identified the fuel kernel nodes in the TRISO particles as the group of nodes for determining the fuel average temperature. [43]

4.4.2 Calculation of Bias and Variation in the Bias

The mean bias and the variation in the bias will be calculated based on the residual differences between the Flownex predictions and analytical values. The maximum normalized point difference and the Euclidian difference, as defined in Reference [71], will also be calculated for consistency with existing Flownex validation. Calculation of the bias is discussed in Reference [41].

5. GOTHIC Code Manuals and Qualifications

5.1 GOTHIC Code Manuals

5.1.1 GOTHIC Thermal Hydraulic Analysis Package User Manual

The user manual describes the functionality and use of GOTHIC Program [67]:

- Describes the GOTHIC Environment
- Instructions for the preprocessor
- Instructions for the thermal-hydraulics program
- Instructions for the graphics program to model nuclear reactor systems and auxiliary buildings
- Procedure for setting up and input model, running the solver, and accessing the results

5.1.2 GOTHIC Thermal Hydraulic Analysis Package Technical Manual

The GOTHIC technical manual describes the equations and models in GOTHIC S and the numerical methods used to solve them [68]:

- Modeling Overview
- Governing equations theory
- Models for Engineered Safety Equipment
- Models for Thermal Conductors
- Models for Interfacial Mass, Energy and Momentum Transfer, and Wall Heat Transfer and Drag
- Mechanics and Assumptions for the Multiple Drop Fields
- Models for Viscous and Turbulence Stress and Diffusion
- Models for Hydrogen Burn
- Model Theory for Neutron Point Kinetics
- Description of Various Fluid Property Functions
- Description of Control Models
- Description Finite Volume Formulations
- Description of the Numerical Methods Used to Solve the Equations

5.2 Verification and Validation

5.2.1 V&V Scope

It is important to distinguish between “Software V&V” and “Model and Data V&V”. Software V&V is done to ensure the integrity and consistency of the simulation software. However, the accuracy of simulation results is not only dependent on the integrity of the software itself, but also on the way the software is used to setup a simulation model, as well as the component model input values for the specific simulation model. This area is covered by Calculation Model and Data V&V.

Calculation Model and Data V&V is unique to each simulation model and is the responsibility of the software user. Calculation Model and Data V&V includes verification that the calculation model was set up in such a way that all the important phenomena for the specific case are appropriately accounted for and ensuring that the input values for each component are accurate.

The GOTHIC Qualification Report [74] includes benchmarks for a diverse set of physical phenomena to experimental data. The end user to determines which experiments are applicable and will supplement the information with additional benchmarking as needed to cover any gaps identified for the intended application. [69]

5.3 Existing GOTHIC Code Verification and Validation

Prior to identifying new validation work to be executed, existing validation work is reviewed. GOTHIC's Qualification Report [74], which documents verification & validation (V&V) for a wide range of single and two-phase flow situations and supports the application of GOTHIC to a variety of thermal-hydraulic situations. The validation set includes comparisons with experimental data for separate and multi-effect tests, comparisons with analytic solutions and functional tests primarily for GOTHIC equipment models. The GOTHIC Qualification Report (QR) is updated and released with each version of the software.

In this section the relevant validation is described. The phenomena active in the validation exercises are noted and the associated figure of merit relevant to the validation is also identified.

Since many of the tests involve multiple phenomena identified in the PIRTs, Table 1 provides a list of relevant GOTHIC validation tests with the included phenomena itemized. [69]

Table 1: Existing Applicable GOTHIC Validation

Test	Description	Related PIRT Items*	Comments
Wall Effects and Velocity Profile	Comparison of GOTHIC to analytical solutions for laminar and turbulent flow in a channel between infinitely wide parallel plates.	FF-1, FF-2, FF-3, NOC-2, and NOC-7	Excellent agreement with analytic solution that verifies and validates the hydraulic models in GOTHIC.
Square Cavity Natural Convection	Small scale experiments with measurements of velocity and temperature profiles inside the cavity.	HT-1, HT-2, HT-3, FF-4, FF-5, GLOFC-6, and PLOFC-2	Sensitivity studies were performed on surface-to-surface radiative heat transfer and 2D conduction. A nodalization study was also performed.
Thermally Driven Cavity	Air filled, 2.5m high cavity between two vertical walls maintained at 72.9 C and 27.1 C. Measurements include the steady vertical velocity profile and the temperature profile at the cavity vertical mid plane.	HT-1, HT-2, HT-3, FF-2, FF-4, FF-5, GLOFC-6, and PLOFC-2	Very good agreement for both profiles using a 20x20 uniform mesh

Test	Description	Related PIRT Items*	Comments
Natural Convection through horizontal and vertical openings	Heat transmission through vertical and horizontal opening between adjacent compartments was measured. Adjacent compartment wall temperatures were maintained to provide a constant temperature differential.	HT-2, FF-2, FF-3, FF-4, and FF-5	Calculated results were within the 20% data uncertainty band for a wide range of opening size and temperature differentials (1e6<Gr<1e8).
Turbulence Generation	Measured turbulent kinetic energy in air and water flow downstream of a rectangular grid in a rectangular duct.	FF-3	Very good agreement with the measured turbulent kinetic energy over a range of 10 to 100 times the grid spacing.
Natural convection heat transfer from a horizontal cylinder	The steady heat transfer rate from a heated horizontal cylinder to the surrounding cooled walls was measured. The test was configured for 2-dimensional natural circulation in the closed test chamber.	HT-2, FF-2, and FF-4	Calculated heat transfer rate is about 10% higher than measured but within the test uncertainty.
Plane turbulent jet	Measures air velocity profiles downstream of a slot jet in a rectangular duct.	FF-6 and WI-2	Very good agreement with the jet centerline velocity profile and for velocity profiles across the jet at various distances downstream of the slot.
Fluid Thermal Diffusion	Analytic solution for 1D transient conduction.	HT-1 and GLOFC-1	Calculated transient temperature matches the analytic solution. The test described in QR is for conduction in the liquid phase, however, similar tests were done to confirm conduction in the vapor phase and molecular diffusion of gas components in the vapor phase with similar results.
Aerosol Deposition	Analytic solution for gravitational settling velocity (1D model).	DLOFC-5 and WI-2	Calculated results for the aerosol fall velocity and the deposition rate match analytic results with specified aerosol termination velocity versus particle diameter.
Drop Heat and Mass Transfer	Tests by Spillman and IRSN experiments measured diameters of drops falling through air/steam mixtures. Depending on the initial drop temperature, vapor temperature and steam content, drops may shrink due to evaporation or grow due to condensation	DLOFC-5 and WI-2	Good agreement for drop size versus distance from injection level.
BFMC Test 6	Axisymmetric two compartment test with hydrogen injection over 2 hours into the lower compartment. The upper compartment was initialized at a higher temperature to establish thermally stratified conditions. Hydrogen penetration into the upper compartment is impeded by the stratified temperature conditions.	FF-2, FF-3, FF-4, FF-5, NOC-8, NOC-11, and AI-9	The two-compartment test geometry is modeled with a single 2D subdivided volume (coarse noding) with blockages to match the test. Good agreement with test data for hydrogen concentration in upper and lower compartments. Initial thermal stratification is maintained so the migration of hydrogen into the upper compartment is mainly by diffusion.

Test	Description	Related PIRT Items*	Comments
BFMC Tests 12 and 20	Multicompartment test with hydrogen injection over 50 hours into one of the lower compartments. For Test 12 the compartments were initialized with uniform conditions. For test 20, the upper compartments were initialized at ~20 C higher. Hydrogen was injected in a lower compartment.	FF-2, FF-3, FF-4, FF-5, NOC-8, and AI-9	A lumped model was used for Test 12 with parallel flow paths for circulation through horizontal connections. GOTHIC results are in good agreement with data for the well mixed conditions throughout. For Test 20 some compartments were modeled with coarse 1 or 2 dimensional subvolumes. GOTHIC results show agreement with restricted mixing due to the initial thermal stratification although there is some variation in the local hydrogen concentrations in the upper volumes. The simulation would probably benefit from more detailed noding.
HEDL HM 5 and 6	Two compartment facility to simulate hydrogen mixing in an ice condenser containment geometry. Ice was not included in the test. Steam and hydrogen were injected into the lower compartment as a jet (horizontal for HM-5, vertical for HM-6). Deck fans between the upper and lower compartment were on.	FF-1, FF-2, FF-3, FF-4, FF-5, NOC-8, and AI-9	Good agreement with local hydrogen concentration in the lower compartment during the jet injection and after. Initial temperature vertical variation was not modeled due to lack of sufficient test information. This may impact the post jet vertical variation as well.
NUPEC Tests	The NUPEC facility is a large multicompartment vessel (1,300 m3) representative of a large, dry PWR containment. The modeled tests (M- 7-1, M-4-3, M-8-1, M-8-2-2, M-2-2) include varying initial conditions, varying steam and helium injection at various locations. Sprays were active in 2 of the tests (M-7-1 an M- 8-2), but the test response and GOTHIC predictions for the period prior to the spray injection are still applicable to the Xe-100.	FF-2, FF-3, FF-4, FF-5, NOC-8, and AI-9	Agreement with data for pressure, vapor temperature and helium concentration is good to very good over all of the simulated tests. For some helium concentrations the variation was larger in the subvolumes for the injection compartment and nearby compartments. The measurements are for a specific point in the volume and the coarse grid may not match up with the measurement location. This is shown in the results by the inclusion of GOTHIC results from multiple cells for comparison with the point data.
CVTR	The containment for the Carolina Virginia Tube Reactor is a 277,000 ft3 PWR type building with a solid deck near the mid plane. A gap between the deck and wall and an open hatch connect the upper containment to the lower containment. Superheated steam was injected through a diffuser in the upper containment. Tests 3, 4 and 5 are included in the validation set. For tests 4 and 5, the upper containment was sprayed starting at 30 seconds after the end of the steam injection, but the test response and GOTHIC predictions for the period prior to the spray injection are still applicable to the Xe-100.	FF-2, FF-3, FF-4, FF-5, NOC-8, and AI-9	Lumped models give peak pressures that are significantly higher than measured for all test cases. Calculated pressure response is slightly overpredicted with the 3D models. The lumped models are unable to account for the stratification that is important in these tests.

Test	**Description**	**Related PIRT Items***	**Comments**
TOSQAN	This test is Part 1 of ISP-47. The 7 m3 steel vessel has temperature controlled walls. For the ISP the upper and lower walls were maintained at a high temperature and the mid level wall was maintained at a lower temperature. Condensate runoff from the bottom of the cold wall was collected and removed from the vessel. The test consisted of a series of 4 steady state conditions with varying steam injection. In order to match the steady vessel pressure, the calculated wall heat transfer and condensation must be consistent with the test. Helium was injected into the vessel between steady states 3 and 4. The vertical steam and helium injection was close to the vessel mid plane elevation. The test geometry was axisymmetric.	HT-2, FF-2, FF-3, FF4, FF-5, and AI-9	The calculated steady pressure, temperature, steam concentration and helium concentrations are in very good agreement with measurements.
THAI	This test is Part 3 of ISP-47. The 9 m high, 60 m^3, vessel has a domed top and bottom with an extended sump volume, an internal cylinder, open at the top and bottom, and concentric with the vessel that is locate in the lower 2/3 of the cylindrical portion of the vessel and a deck at the mid plane of the annulus region with 4 equally spaced 30 degree sector openings. The transient test had 4 phases: 1) 0-2700 s, helium injection from an off center vertical tube in the upper part of the vessel, 2) 2700- 4700s, steam injection from an off center vertical tube in the upper part of the vessel, diametrically opposed to the helium injection, 3) 4700-5700 s, steam injection from a horizontal tube located a short distance below the annular region and 4) a stabilization period with no injections. The early phase helium and steam injection established a highly stratified condition that is eventually broken up by the lower steam jet/plume.	HT-2, FF-2, FF-3, FF4, FF-5, and AI-9	The calculated pressure, temperature and helium/steam concentrations are in generally good agreement with measurements. The calculated breakup of the stratified layer occurs earlier than in the test. The stratification breakup is sensitive to the split of the lower steam plume between the inner cylinder interior and the annulus region.
THAI Helium Stratification Test	This test did not include the condensation collector trays used in the THAI ISP-47 test. Phase 1 of the test established a steady natural circulation driven by wall heaters at the lower portion of the vessel and wall coolers at the upper level of the vessel. In phase 2, helium was injected in the upper part of the vessel over a period of 4 minutes to establish a stratified layer of helium. In phase 3, the stratification was gradually eroded over a period of about 1 hour.	HT-1, HT-3, FF-4, FF-5, GLOFC-6, and AI-9	GOTHIC was used for blind and open test simulations. The referenced paper shows the measured erosion of the stratified layer and calculated results from participants using a variety of CFD and lumped parameter codes. GOTHIC gives very good agreement with the observed erosion of the stratified region.

Test	Description	Related PIRT Items*	Comments
SP-43	This was a downcomer mixing test facility that included 265 thermocouples (TCs) to quantify the thermal mixing that occurred due to cold water injection. In the most highly instrumented levels, TCs are positioned every 15 degrees (24 TCs around the circumference), and in the less instrumented levels, TCs are spaced every 30 degrees. Although the test was for hot/cold liquid, the same molecular and turbulent diffusion models exist in GOTHIC for the liquid and vapor phases. Therefore, the benchmark is still applicable for demonstrating GOTHIC's capability for modeling turbulence, mixing and buoyancy driven flow.	FF-2, FF-3, FF-4, and FF-5	Generally, good agreement between GOTHIC predictions and experimental data for both the spatial mixing profiles and transient response. The GOTHIC simulations use about 3 orders of magnitude fewer computational cells compared other CFD tools that participated in the benchmark, but GOTHIC proved to be at least as accurate if not more accurate than the CFD results.
TN-24P	The TN-24P is a dry cask, designed and constructed by Transnuclear Inc., for the storage of Pressurized Water Reactor (PWR) spent fuel. A series of experiments were performed using the TN-24P cask by EPRI looking at different orientations (vertical and horizontal) as well as different fill gases (helium, nitrogen and vacuum). These are steady-state validation benchmark of the TN-24P cask design for helium and nitrogen fill gas conditions. Axial temperature profile comparisons between the GOTHIC and measured results	HT-1, HT-3, FF-2, FF-4, FF-5, GLOFC-18, and PLOFC-2	Axial temperature profile comparisons show the characteristic difference between the helium and nitrogen cases. The nitrogen case has a higher peak because heat removal is predominantly by convection versus the helium case which has a lower peak because conduction is more dominant. There is generally good temperature agreement for the nitrogen filled case, but the results are slightly lower than the experiment for the helium case. Results could be improved with a more detailed calculation for the loss coefficients for circulating flow through the assemblies.
STF	Two sets of NSTF tests were performed. The first set of tests consisted of a heated wall section with a constant heat flux along the length of the heated wall. The second set of tests consisted of a heated wall with a constant wall surface temperature along the length of the heated wall. A wide range of heated wall heat fluxes and surface temperatures were included in the test sets. In addition, the two test sets were performed with a range of inlet form losses.	HT-2, HT-3, FF-4	GOTHIC results compare well with the heat transfer coefficients from the test.

*Related PIRT Items are defined in Reference [2] and Reference [69]

5.3.1 In addition to the validation data listed above, there has been practical experience applying GOTHIC for other HTGR evaluations, including [69]:

- Work performed by Texas A&M University to model a 1/28-scaled next generation nuclear plant NGNP HTGR reactor building test facility to analyze the depressurization scenarios and validate them against experimental data. This including air ingress (AI) related phenomena.
- Work performed by Oregon State University benchmarking GOTHIC to an asymmetric heating test at the High Temperature Test Facility (HTTF) during a pressurized conduction cooldown.

- Work performed by Framatome using GOTHIC to analyze their HTGR design and building response.

5.3.2 Reactor Cavity Cooling System Validation

The Argonne National Laboratory (ANL) Natural convection Shutdown heat removal Test Facility (NSTF) has initiated testing of a RCCS which is driven entirely by natural circulation. The test rig is air water cooled, similar as is to the current RCCS design for the Xe-100. The test rig is focused only on the RCCS operation and is not suitable for validating prediction of heat losses from the RPV to the RCCS. [69]

5.3.3 Reactor Building Validation

Some examples of tests included in the current Qualification Report at Battelle-Frankfurt Model Containment (BFMC) Test, hydrogen mixing tests at the Hanford Engineering Development Laboratory (HEDL) Containment Systems Test Facility, Nuclear Power Engineering Corporation (NUPEC) Test, Heissdampfreaktor (HDR) full-scale multicompartment containment experiments, and International Standard Problem-47, which includes the ThAI, MISTRA, and TOSQUAN tests. These provide a comprehensive basis for GOTHIC’s accuracy and applicability for modelling natural convection, mixing, and stratification. [69]

5.4 Planned GOTHIC Code Verification and Validation

5.4.1 Helium Pressure Boundary

This section describes additional validation that may be performed to support GOTHIC’s use for HPB modeling for the Xe-100. Table 1 provides validation data that covers much of the PIRT elements; however, additional validation of the effective thermal conductivity modeling for the pebble bed core region is recommended. Additional benchmarking of GOTHIC to Integrated Effects Testing (IET) for a high temperature gas reactor would be beneficial.

5.4.2 Pebble Bed Temperature Prediction Validation with SANA

The GOTHIC Validation for the Pebble Bed Temperature Prediction will be performed consistent with Flownex [39]; which, was based on the SANA experimental test data. Please refer Section 4.3.5 for more details.

Validation supporting the accuracy of graphite pebble temperature predictions in a pebble bed in the absence of forced flow can be based on the (Selbsttätige Abfuhr der Nachwäre) SANA experimental test data [40]. The experimental data covers pebble surface temperatures from 60°C to 1200°C. Both steady state and transient predictions of pebble temperature are compared at various axial and radial locations in the bed. The SANA experiments would provide validation of the heat transfer models in the pebble bed for both normal operating conditions and loss of forced circulation (LOFC) transients. The SANA experimental program has been widely used as a benchmark to support code developments intended for thermodynamic analysis of pebble bed HTGRs.

The main component of the test facility is a cylindrical steel vessel containing a pebble bed 1.5 m in diameter and 1.0 m high. The SANA experiments selected for validation used 60 mm graphite pebbles, corresponding to the pebble size in the Xe-100, with either helium or nitrogen as the coolant. For the cases used in this validation, the vessel was heated by an electrical heating element located along the central axis of the pebble bed. The heat could be applied in different locations (i.e., top half, bottom half, or full length) between tests. The FOM for the comparison would be the pebble temperature, measured radially at elevations close to the bottom, center and close of the top of the pebble bed.

There is also a series of tests with the same SANA experimental setup as discussed above, but with a step change increase or decrease in heating element power, allowing the transient response of the pebble bed to be assessed. Two validation cases were performed with nitrogen and two with helium. Pebble temperatures at the center height of the pebble bed and at seven radius points between the inner radius and the outer radius of the bed were compared over the sixty-hour transients.

A GOTHIC model of the SANA facility will be constructed, and benchmarks will be performed to the tests that used 60 mm graphite pebbles with helium coolant. [69]

5.4.3 Reactor Temperature and Power Validation using HTR-10

The 10 MW High Temperature Gas-Cooled Reactor Test Module (HTR-10) is an integrated effects test appropriate for validating GOTHIC to support the Xe-100 safety analysis. HTR-10 is a graphite moderated and helium-cooled pebble bed reactor. The reactor and SG are housed in two separate steel pressure vessels, which are arranged side by side and connected to each other by a horizontal hot gas duct pressure vessel. These three vessels make up the primary pressure boundary of the HTR-10.

The HTR-10 test was published in a formal IAEA benchmark report [49]. Steady state temperature measurements are available at various locations in the graphite structures within the reactor vessel. The active phenomena which directly influence the measurements include those related to conductive, convective, and radiative heat transfer. The measurements are indirectly related to the fuel temperature and primary coolant temperature FOM. Accurate prediction of the temperatures of the internal reactor structures provides confidence in the accuracy of the predicted fuel and coolant temperatures within the reactor.

A transient test was also performed for a loss of flow and CRW without scram. All-important phenomena relevant to the loss of flow and CRW safety analysis are active in the transient test for both events. Although not directly measured, a key parameter in the tests are the fuel temperature since the increase in fuel temperature causes the reactor to shutdown during the test. The tests are therefore suitable for assessing the fuel temperature reactivity feedback effect on the reactor power prediction.

VSOP has already been used to derive the appropriate input data for the point kinetics model to support a comparable Flownex validation case

A GOTHIC model may be built of the HTR-10. The GOTHIC model will incorporate correlations and modelling approaches that are consistent with those applied in the Xe-100 analysis. Comparisons of measured and predicted data for steady state, transient Loss of Flow without Scram Test, and Transient CR withdrawal without Scram Test will be performed with GOTHIC. [69]

6. Quality Assurance

X-energy developed and implemented a QAP which implements X-energy's Topical Report XEQAPD-NP, “Quality Assurance Program Description,” Revision 3 submitted to the NRC in August of 2020 [26]. The X-energy QAPD is based on the applicable portions of both Appendix B, “Quality Assurance Criteria for Nuclear Power Plants and Fuel Reprocessing Plants,” to, Title 10 of the Code of Federal Regulations Part 50, “Domestic Licensing of Production and Utilization Facilities,” (10 CFR 50) and American Society of Mechanical Engineers (ASME) NQA-1-2015, “Quality Assurance Program Requirements for Nuclear Facilities,” as endorsed by NRC Regulatory Guide (RG) 1.28, “Quality Assurance Program Criteria (Design and Construction),” Revision 5. The NRC reviewed this report and determined that X-energy XEQAPD Revision 3 satisfies the quality assurance requirements of Appendix B to 10 CFR 50 (ADAMS Accession No. ML20233A910). The activities described in this LTR are subject to, and conducted in accordance with, the provisions of the approved X-energy QAPD.

7. Conclusions and Limitations

7.1 Conclusions

The GOTHIC and Flownex Analysis Codes can support the Xe-100 TSA Evaluation Model. The LTR describes the methodology (including theory) of the GOTHIC and Flownex Analysis Codes that support the Safety Analysis EM for the Xe-100 described in the "Xe-100 Licensing Topical Report Transient and Safety Analysis Methodology,"[2]. Additionally, this report describes the code manuals and associated qualifications for GOTHIC and Flownex.

7.2 Limitations

X-energy is requesting the NRC review and approval of the GOTHIC and Flownex Codes in support of the Xe-100 TSA Evaluation Model as described in the "Xe-100 Licensing Topical Report Transient and Safety Analysis Methodology" [2]. Until this review and approval by the NRC is complete, the codes described herein cannot be used to support a final safety analysis report.

8. Cross References and References

	Document Title Cross References: X-energy documents that may impact the content of this document. References: X-energy or other documents that will not impact the content of this document	Document No.	Rev./ Date of Issuance	Cross Reference/ Reference
[1]	Contents of applications; technical information	10 CFR 50.34		Reference
[2]	Xe-100 Licensing Topical Report Transient and Safety Analysis Methodology	007834	Rev 1 04/29/2024	Cross Reference
[3]	Transient and Accident Analysis Methods	1.203	December 2005	Reference
[4]	Xe-100 Mass & Heat Balance Report"	000311	Rev 10 12/09/2021	Cross Reference
[5]	Xe-100 Flownex Control System Implementation Report	003037	Rev 3 02/16/2023	Cross Reference
[6]	Safety Analysis Flownex Base Model Report	003221	Rev 3 07/18/2023	Cross Reference
[7]	Preliminary GOTHIC8.4a(QA) Reactor System Model Report	005504	Rev 3 01/05/2024	Cross Reference
[8]	Risk-Informed Performance-Based Technology Inclusive Guidance for Non-Light Water Reactor Licensing Basis Development	NEI 18-04	Rev 1 August 2019	Reference
[9]	Xe-100 200MWth MCNP RCCS Preliminary Analysis Report	001827	Rev 1 05/31/2022	Cross Reference
[10]	DIT Xe-100 Preliminary Scoping VSOP Outputs for Safety Analysis	006529	Rev 5 03/24/2023	Reference
[11]	Policy Statement on the Regulation of Advanced Reactors	73 FR 60612	2008	Reference
[12]	Acceptance criteria for emergency core cooling systems for light-water nuclear power plants	10 CFR 50.46		Reference
[13]	Review of Risk-Informed, Technology-Inclusive Advanced Reactor Applications – Roadmap	DANU-ISG-2022-01	March 2024	Reference
[14]	Guidance For a Technology-Inclusive Content-Of-Application Methodology To Inform The Licensing Basis And Content Of Applications For Licenses, Certifications, And Approvals For Non-Light-Water Reactors	1.253	Rev 0 March 2024	Reference

	Document Title Cross References: X-energy documents that <u>may</u> impact the content of this document. References: X-energy or other documents that <u>will not</u> impact the content of this document	Document No.	Rev./ Date of Issuance	Cross Reference/ Reference
[15]	Guidance for a Technology-Inclusive, Risk-Informed, and Performance-Based Methodology to Inform the Licensing Basis and Content of Applications for Licenses, Certifications, and Approvals for Non-Light Water Reactors	1.233	Rev 0 June 2020	Reference
[16]	Xe-100 Licensing Topical Report Risk-Informed Performance-Based Licensing Basis Development, XE00-R-R1ZZ-RDZZ-L	001522	Rev 2 12/07/2021	Reference
[17]	Preliminary Scoping Steam Generator Check Valve Flow Based Design Analysis Information Transmittal	004011	1 11/21/2022	Reference
[18]	Standard Review Plan for the Review of Safety Analysis Reports for Nuclear Power Plants: LWR Edition	NUREG-0800		Reference
[19]	Xe-100 Steam Generator System Design Description	000003	Rev 4 04/12/2022	Cross Reference
[20]	X-energy Licensing Topical Report, “Xe-100 Principal Design Criteria Licensing Topical Report”	004799	Rev. 3 02/15/2024	Reference
[21]	Xe-100 Required Safety Functions and PRA Safety Functions	001279	Rev 5 01/26/2024	Cross Reference
[22]	Supplier Audit Report M-Tech Industrial April 19-22, 2022	005066	Rev 1 06/07/2022	Reference
[23]	Xe-100 Protection Systems Trip Matrix Report,	001490	Rev 4 02/05/2024	Cross Reference
[24]	Preapplication Safety Evaluation Report for the Modular High- Temperature Gas-Cooled Reactor	NUREG-1338	Draft March 1989	Reference
[25]	Introduction to the Pebble Bed Modular Reactor (ML012530326)	Exelon Letter from K.F. Borton to USNRC Document Control Desk	August 20, 2001	Reference
[26]	X-Energy, LLC, *Flownex DA Preliminary Scoping Model Report*	002109	Rev 4 04/27/2023	Cross Reference

Document Title Cross References: X-energy documents that may impact the content of this document. References: X-energy or other documents that will not impact the content of this document		Document No.	Rev./ Date of Issuance	Cross Reference/ Reference
[27]	Flownex Preliminary SSS Scoping Model Report	005802	Rev 1 04/06/2023	Cross Reference
[28]	Thermal Conductivity of Neutron-irradiated Graphite at Temperatures Between 50 and 1000°C		1972	Reference
[29]	X-Energy, LLC, Flownex SG Scoping Model Report	002056	Rev 5 06/15/2023	Cross Reference
[30]	Turbine Generator System Siemens Heat Balance Diagram – Service Receipt Inspection Report	001915	Rev 1 09/03/2021	Cross Reference
[31]	Flownex Reactor Scoping Model Report	000807	Rev 5 04/25/2023	Cross Reference
[32]	Flownex TB Scoping Model Report	002058	Rev 2 08/25/2022	Cross Reference
[33]	Reactor Cavity Cooling System Design Reconfiguration to Support Dow Gate 6 Design Information Transmittal	009728	Rev 1 03/13/2024	Cross Reference
[34]	Preliminary Reflector Graphite Material Properties Report	005616	Rev 2 09/13/2022	Cross Reference
[35]	Preliminary Scoping Steady State Flownex Integrated Plant Model with Air Cooled Condenser Report	005644	Rev 3 08/31/2023	Cross Reference
[36]	Xe-100 200MWt Steady-State Core Design Report	000288	Rev 5 02/17/2022	Cross Reference
[37]	Flownex Simulation Environment, General User Manual		March 2022	Reference
[38]	Flownex Simulation Environment, Flownex Library Manual	`	March 2021	Reference
[39]	Flownex Simulation Environment, Flownex Theory Manual		March 2022	Cross Reference
[40]	X-energy LLC, X-energy Flownex Validation Plan – Service Receipt Inspection Report	002102	Rev 2 05/15/2022	Cross Reference

Document Title Cross References: X-energy documents that <u>may</u> impact the content of this document. References: X-energy or other documents that <u>will not</u> impact the content of this document		Document No.	Rev./ Date of Issuance	Cross Reference/ Reference
[41]	Flownex Fuel Temperature Validation Exercise Report	K-640207/RP/0005	Rev 0 04/08/2022	Cross Reference
[42]	Xe-100 Safety Analysis Phenomena Identification and Key Parameter Identification and Ranking Tables	007086	Rev 1 05/12/2023	Reference
[43]	Flownex Software Validation Plan	K- 640207/PL/0006	Rev 0 08/11/2021	Reference
[44]	R. Stainsby, S. MacIntosh, A. Grief, B. McLaughlin, Investigation of Local Heat Transfer Phenomena in a Pebble Bed HTGR Core	NR001/RP/002	Rev 1 05/15/2009	Reference
[45]	Flownex Reflector Structure Temperature Validation Exercise Report Using HTR-10 Benchmark at Steady State Conditions	004843	Rev 1 08/05/2022	Reference
[46]	I.B. Celik, et al., Procedure for Estimation and Reporting of Uncertainty Due to Discretization in CFD Applications	Journal of Fluids Engineering, Vol. 130, No. 7, 078001 (4 pages)	July 2008	Reference
[47]	B. Neykov, Heat Transfer Database Literature Review Report	XE00-B-G1-GL-D000089	Rev 1 May 2018	Reference
[48]	Initial Flownex HTR-10 Benchmark Report- Evaluation of Code Accuracy for Transients	006477	Rev ision1 01/05/2023	Cross Reference
[49]	International Atomic Energy Agency, Evaluation of High Temperature Gas Cooled Reactor Performance - Benchmark Analysis Related to the PBMR-400, PBMM, GT-MHR, HTR-10 and the ASTRA Critical Facility	IAEA-TECDOC-1694, Vienna	April 2013	Reference
[50]	Xe-100 Preliminary Helium Circulator Design and Analysis	000967	Rev 4 06/30/2022	Cross Reference
[51]	N. Leeb, Flownex SE Version 8.14.0 Release Notes, M-Tech Industrial	FN 8.14.0-RN095	Rev 1 March 2022	Reference
[52]	Xe-100 Flownex Model of the RPS and IPS for Event Analysis	006558	Rev 1 05/15/2023	Cross Reference

Document Title Cross References: X-energy documents that <u>may</u> impact the content of this document. References: X-energy or other documents that <u>will not</u> impact the content of this document		Document No.	Rev./ Date of Issuance	Cross Reference/ Reference
[53]	Preliminary Scoping Xe-100 Input Data and Boundary Conditions Report	006088	Rev 1 01/12/2023	Cross Reference
[54]	Xe-100 Safety Analysis Summary Report	000850	Rev 2 August 30, 2021	Cross Reference
[55]	M.C. Potgieter, Flownex Validation Report: Node – Case 10: Volume blow down, M-Tech Industrial	FNXVV-VAL-0003.2	Rev 1 January 2023	Reference
[56]	Design Information Transmittal, Updated Reactor Component Temperature with Non-Local Power Generation in 180-degree CDF Model	005891	Rev 1 09/19/2022	Cross Reference
[57]	Preliminary Accuracy Reporting on Flownex Validation Cases: Bias Calculation Approach	006402	Rev 1 02/16/2023	Cross Reference
[58]	W.A. Landman, E. van Heerden, J.P. van Ravenswaay and G.P. Greyvenstein, Conference Paper: Flownet Nuclear Architecture, Implementation and Verification & Validation, International Congress on Advanced Nuclear Power Plants (ICAPP) Conference		May 4-7, 2003	Reference
[59]	W. van Niekerk, G. Greyvenstein, J. van Ravenswaay, J. Labuschagne, J. Swift, Comparison of the Thermal-Fluid Analysis Code Flownex with Experimental Data from the Pebble Bed Micro Model, 3rd International Topical Meeting on High Temperature Reactor Technology, October 1-4, 2006, Johannesburg, South Africa.		October 1-4, 2006	Reference
[60]	Flownex Validation Manual: Pipe Element – Case 22: Transient in branched network, M-Tech	FNXVV-VAL-0004.5	Rev 1 February 2023	Reference
[61]	Flownex Validation Manual: Pipe Element – Case 24: Transient in a branched network (continued), M-Tech	FNXVV-VAL-0004.7	Rev 1 April 2022	Reference
[62]	J.P. van Ravenwsaay, G.P. Greyvenstein, W.M.K. van Niekerk and J.T. Labuschagne, Verification and Validation of the HTGR Systems CFD Code Flownex, 2nd International Topical Meeting on High Temperature Reactor Technology, Beijing, China		September 22-24, 2004	Reference
[63]	M-Tech Industrial Verification and Validation document summary for Flownex)		09/2021	Reference

Document Title Cross References: X-energy documents that may impact the content of this document. References: X-energy or other documents that will not impact the content of this document		Document No.	Rev./ Date of Issuance	Cross Reference/ Reference
[64]	C.G. du Toit, G.P. Greyvenstein, F.N. Emslie and P.G. Rousseau, Acceptance Procedure for Thermo-Hydraulic Simulators : An Example, 2000. https://flownex.com/legacy/fnxdocs/conferencepapers/c019.pdf		2000	Reference
[65]	M.C. Potgieter, Flownex Validation Manual: Node – Case 1: Inlet temperature step of a fixed adiabatic volume – Case 2: Step in heat transfer to a fixed volume – Case 3: Fixed volume with constant inlet mass flow – Case 7: Sharp edged T-junction – Case 8: Jet pup model," M-Tech Industrial	FNXVV-0003.3	Rev 4 October 2017	Reference
[66]	C.G du Toit, Benchmark results for basic thermo-hydraulic models, PBMR-0007		1999	Reference
[67]	EPRI, GOTHIC Thermal Hydraulic Analysis Package User Manual, Version 8.4(QA)		May 2022	Reference
[68]	EPRI, GOTHIC Thermal Hydraulic Analysis Package Technical Manual, Version 8.4(QA)		May 2022	Reference
[69]	Software QA Computer Code GOTHIC Validation Plan	009435	Rev 1 04/22/2024	Cross Reference
[70]	M.C. Potgieter, Flownex Validation Manual: Node – Case 4: Sudden Mass Injection into Tank, M-Tech Industrial	FNXVV-0003.4	Rev 3 October 2017	Reference
[71]	R. Laurens, Flownex SE Verification & Validation Status for Clients, M-Tech Industrial	FNXVV-0001.11	Rev 2 May 2020	Reference
[72]	DIT Xe-100 In-Progress Design Updates for D2 Flownex Model	006892	Rev 1 02/28/2023	Cross Reference
[73]	International Atomic Energy Agency, Heat Transport and Afterheat Removal for Gas Cooled Reactors Under Accident Conditions, Vienna, https://www-pub.iaea.org/MTCD/Publications/PDF/te_1163_prn.pdf	IAEA-TECDOC-1163	2000	Reference
[74]	EPRI, GOTHIC Thermal Hydraulic Analysis Package Qualification Report, Version 8.4(QA)		May 2022	Reference

	Document Title **Cross References: X-energy documents that <u>may</u> impact the content of this document.** **References: X-energy or other documents that <u>will not</u> impact the content of this document**	**Document No.**	**Rev./ Date of Issuance**	**Cross Reference/ Reference**
[75]	Startup and Shutdown System, System Design Description Service Receipt Inspection Report	001672	Rev 3 01/08/2024	Cross Reference
[76]	Siemens Energy Heat Flow Diagrams (HBD_p_10757)			Reference
[77]	CL Wheeler et al. COBRA-NC: A Thermal-Hydraulic Code for Transient Analysis of Nuclear Reactor Components. Technical report, U.S. Nuclear Regulatory Commission, Washington, D.C., 1986. NUREG/CR-3262, PNL-4710		1986	Reference
[78]	DS Rowe et al. GOTHIC Design Review, Final Report. Technical report, Electric Power Research Institute, 1993. Palo Alto, CA.		1993	Reference
[79]	CA Meyer et al. ASME Steam Tables. American Society of Mechanical Engineers, New York, 1983.		Fifth Edition 1983	Reference
[80]	GJ Van Wylen and RE Sonntag. Fundamentals of Classical Thermodynamics. John Wiley & Sons Inc.		Second Edition 1973	Reference
[81]	Xe-100 Civil Structures Reconfiguration Effort to Support Dow Gate 6 Work Plan	009647	Rev 2 03/22/2024	Cross Reference
[82]	Preliminary Flownex Turbine Building with Air Cooled Condenser Scoping Model Report,	005559	Rev 2 06/20/2023	Cross Reference
[83]	Flownex Fuel Temperature Validation Exercise Report Using HTR-10 Benchmark - Heat Transfer Phenomena (Conduction, Convection and Radiation)	K- 640207/RP/0010	Rev 0 July 2022	Reference
[84]	XE-100 Licensing Topical Report Reactor Core Design Methods and Analysis	006889	Rev. 1 04/04/2024	Reference

Appendix A Flownex Model Theory Overview

A.1. Introduction

Flownex is developed within an ASME NQA1 accredited quality system. Flownex is also validated and verified within the X-energy Quality system. As can be seen below, Flownex has been audited based on mostly nuclear standards and quality procedures, which are some of the most stringent regulations.

- In 2007 the National Nuclear Regulator (NNR) of South Africa reviewed the Flownex Software V&V status and found it to be acceptable to be used to support the design and safety case for the PBMR.
- NQA1:2008 accredited by Westinghouse USA.
- 2009: ISO 9001 audited and approved.

In 2022, X-energy conducted an audit of M-Tech to evaluate M-Tech's capability to provide Flownex software in accordance with X-energy procurement document requirements for use in nuclear safety-related applications. The scope of the audit was limited to the QA program elements applicable to the development, maintenance, and delivery of Flownex software specified in 10 CFR 50 Appendix B, 10 CFR Part 21, ASME NQA-1-2015 and the M-Tech Quality Assurance Manual. The audit concluded the M-Tech QA program, as currently constituted, is effectively implemented as it applies to the Flownex program. [33]

A.2. Governing Equations

Three conservation laws govern the transport processes occurring in thermal-fluid networks and transport processes in general. These are:

- Conservation of mass.
- Conservation of momentum.
- Conservation of energy.

These are fundamental laws of nature that are universally applicable in natural and man-made systems. The conservation laws are described in the language of mathematics by partial differential equations. The differential equations form a system of coupled equations that must be solved using a suitable solution algorithm. An essential part of the solution process is the specification of realistic BCs for the network and in the case of dynamic simulations, realistic initial conditions. Additional equations are introduced to complete the system of governing equations mathematically, i.e., there must be as many independent equations as there are unknown variables. The variables that Flownex solves are usually referred to as the dependent variables and are variables of particular interest in the design and analysis of thermal-fluid networks. The variables are, amongst others, flow velocity, pressure, and temperature. Flownex presents the calculated distributions of these variables and many additional variables in a formatted result file and in additional graphical format in the event of a dynamic (transient) simulation. In addition to the basic dependent variables, Flownex also provides results for the heat transfer rates for certain elements, which are calculated from the solution of the dependent variables. Additional equations are solved for the advanced functionalities of Flownex, for example the shaft dynamics of turbomachinery and the functioning of controllers.

When dealing with the analysis of transport processes, a reference frame is required to use as a basis from which the governing equations can be constructed and described. Two popular reference frames are commonly used in fluid dynamics namely the Lagrangian reference frame and the Eulerian reference frame.

The conservation equations formulated in the Lagrangian reference frame are not particularly suitable for modelling thermal-fluid systems. However, they do explain the physical meaning of the equations in easy-to-understand mathematical terms. The equations are therefore converted to the Eulerian reference frame (see A.2.1), which is more suitable for numerical analysis.

A.2.1. Eulerian Reference Frame [39]

The Eulerian reference frame considers a stationary fixed-volume control volume. Figure 1 shows a schematic representation of a fixed control volume Eulerian reference frame. The fluid crosses the control surface unlike the fluid parcel in the Lagrangian reference frame.

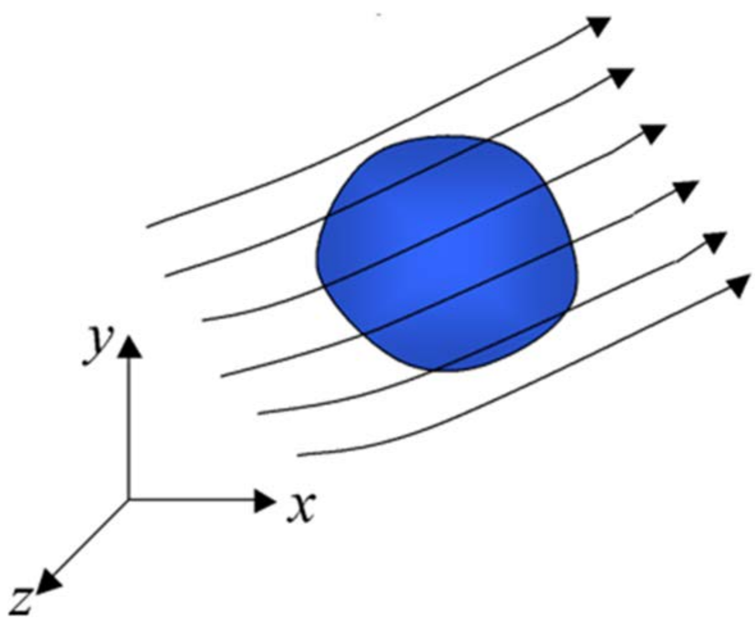

Figure 1: Fixed Control Volume in Eulerian Reference Frame

To convert the equations from the Lagrangian reference frame to the Eulerian reference frame the Reynolds transport theorem is applied, Equation A.1.

$$\frac{DN}{Dt} = \oint_{CS} \eta\left(\rho\vec{V}\cdot d\vec{A}\right) + \frac{\partial}{\partial t}\int_{CV} \rho\eta\, dv \tag{A.1}$$

In Equation A.1, N denotes a general extensive property and η is its intensive counterpart. *dA* is the incremental outwards facing area vector on the control surface. For each of the equations (conservation of mass, momentum, and energy) discussed in the following paragraphs, the quantities substituted into the Reynolds transport equation are indicated in parenthesis.

A.2.1.1 Conservation of mass

$(N = m, \eta = 1)$

$$\frac{Dm}{Dt} = \oint_{CS} \left(\rho \vec{V} \cdot d\vec{A} \right) + \frac{\partial}{\partial t} \int_{CV} \rho dv = 0 \tag{A.2}$$

Equation A.2 describes a balance of the change in fluid mass inside the control volume and the mass flowing across the control surface. Equation A.2 is commonly referred to as the continuity equation or mass conservation equation. The mass inside the control volume can only be changed by either an inflow or outflow of mass through the control surface in the absence of mass sources inside the control volume. Figure 2 shows the mass flow through the control surface of the stationary control volume. Note that the area vectors are always oriented outwards, pointing away from the control volume. The velocity vectors are aligned with the flow streamlines. The mass flow $\dot{m}$ through the control surface $\vec{A}$ is given by Equation A.3.

$$\dot{m} = \oint_{CS} \rho \vec{V} \cdot d\vec{A} \tag{A.3}$$

Equation A.3 implies that the mass flow out of the control volume is positive due to the outwards oriented area vector; therefore, the surface integral in Equation A.2 denotes the net efflux of mass through the control surface. The volume integral in Equation A.2 denotes the rate of increase of mass inside the control volume.

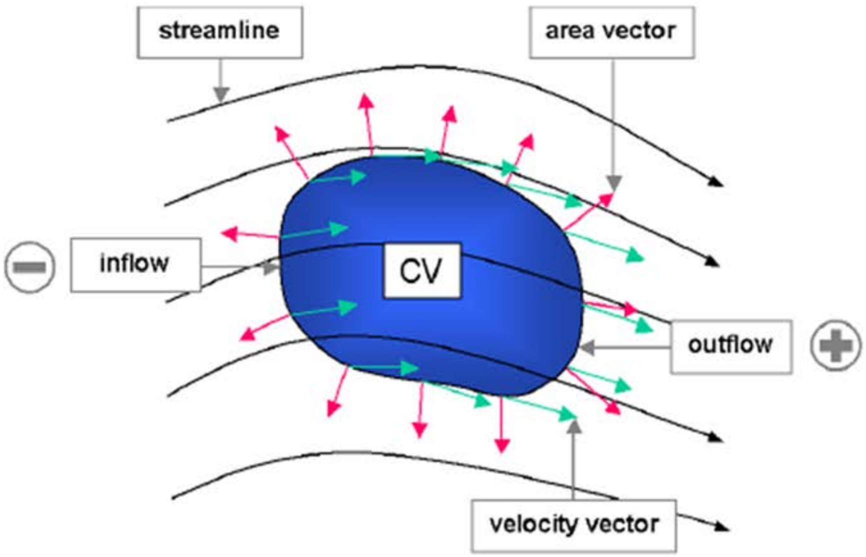

Figure 2: Mass Flow Through Control Surface

Equation A.2 is written in integral form, containing both a volume and surface integral. By shrinking the control volume in the Eulerian reference frame to a differential volume and converting the surface integral into a volume integral by applying the Gauss divergence theorem, the differential form of the continuity equation is obtained, Equation A.4.

$$\frac{\partial \rho}{\partial t} + \vec{\nabla} \cdot \left(\rho \vec{V} \right) = 0 \tag{A.4}$$

A.2.1.2 Conservation of Momentum

The momentum equation for an arbitrary finite-volume control volume in the Eulerian reference frame is given by Equation A.5. The momentum equation has the same general form as the continuity Equation A.2 except that in the momentum equation the resultant force on the control volume is introduced on the right hand side of and the velocity is advected with the mass flow through the control surface. The surface integral in Equation A.5 represents the net efflux of momentum out of the control volume through the control surface. Furthermore, the linear momentum inside the control volume is considered instead of only the mass as in the case of the continuity equation.

$$\left(N = m\vec{V}, \eta = \vec{V} \right)$$

$$\frac{D(m\vec{V})}{Dt} = \oint_{CS} \vec{V} \left(\rho \vec{V} \cdot d\vec{A} \right) + \frac{\partial}{\partial t} \int_{CV} \rho \vec{V} dv = \sum \vec{F} \tag{A.5}$$

The volume integral in Equation A.6 therefore represents the rate of increase of momentum inside the control volume. The force term on the right-hand side of Equation A.6 consists of both the body forces acting on the fluid inside the control volume and the surface forces acting on the control surface. Equation A.6 can therefore be written in terms of the surface and body forces.

$$\oint_{CS} \vec{V}\left(\rho\vec{V}\cdot d\vec{A}\right) + \frac{\partial}{\partial t}\int_{CV}\rho\vec{V}dv = \oint_{CS}\bar{T}\cdot d\vec{A} + \int_{CV}\vec{B}dv \qquad \text{(A.6)}$$

In Equation A.6, $\bar{T}$ denotes the stress tensor per unit area acting on the control surface and *B*, the body force acting on the fluid inside the control volume. The stress tensor contains the contributions of both shear stresses on the control surface due to friction forces for example, and normal stresses due to the pressure on the control surface. One example of an important body force is the gravitational force acting on the fluid inside the control volume. Similar to the continuity equation the momentum equation can also be converted from integral form to differential form by contracting the control volume to a differential volume and converting the surface integrals in Equation A.7 into volume integrals using the Gauss divergence theorem.

Equation A.7 is a vector equation describing the conservation of linear momentum in three- dimensional space.

$$\frac{\partial\left(\rho V\right)}{\partial t} + \vec{\nabla}\cdot\left(\rho\vec{V}\vec{V}\right) = \vec{\nabla}\cdot\bar{T} + \vec{B} \qquad \text{(A.7)}$$

Conservation of Energy

Equation A.8 represents the energy conservation equation for a fixed volume control volume in the Eulerian reference frame. Equation A.8 is written in terms of the general rate of heat transfer $\dot{Q}$ to the fluid inside the control volume and the rate of work *W*� performed by the fluid inside the control volume on the environment.

$$\left(N = me, \eta = e = u + {}^{1}{}_{2}V^2 + gz\right)$$

$$\frac{D(me)}{Dt} = \oint_{CS} e\left(\rho\vec{V}\cdot d\vec{A}\right) + \frac{\partial}{\partial t}\int_{CV}\rho e dv = \dot{Q}_H - \dot{W} \qquad \text{(A.8)}$$

The heat transfer to or from a control volume can take place through three different processes: Conduction, Convection, and Radiation. Each of these processes can occur simultaneously in a system, complicating the analysis of such a system.

A. Conduction

Conduction is the mode of heat transfer where a temperature difference is present in a solid material or fluid when there is no bulk motion present. Conductive heat transfer always occurs from a region of higher temperature to a region of lower temperature. Figure 3 shows a schematic representation of the conductive heat transfer process.

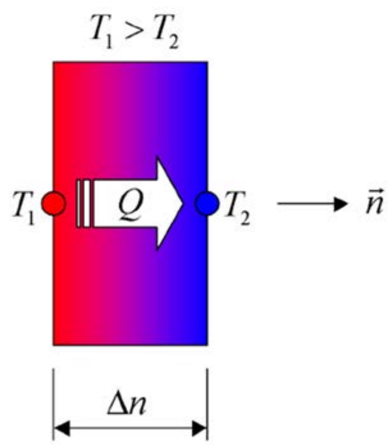

Figure 3: Conduction Heat Transfer

The amount of heat conducted through the solid material or fluid is given by Equation A.9.

$$Q_H = -kA\frac{\partial T}{\partial n} \tag{A.9}$$

The heat transfer is in the opposite direction to the temperature gradient, as heat transfer always occurs from a higher to a lower temperature region. Conductive heat transfer is also known as diffusive heat transfer, as the heat transfer mechanism is fundamentally a result of the random motion of molecules at different energy levels.

B. Convection

Convective heat transfer is caused by energy transferred by the bulk motion of a fluid in addition to diffusive heat transfer by molecular motion. Figure 4 shows a schematic representation of the convective heat transfer mechanism. Heat is transferred from a surface to a fluid moving across the plate at a bulk temperature lower than the temperature of the surface. If the bulk fluid temperature is higher than the surface temperature, the heat transfer will be reversed, and heat will be transferred from the fluid to the surface.

The convective heat transfer coefficient, λ, determines the amount of heat transferred from the surface to the fluid or vice versa. The heat transfer coefficient is often a complex function of the surface geometry and boundary layer. The heat transferred through convection from a surface to a fluid or vice versa is determined by Equation A.10.

$$Q_H = \lambda A\left(T_S - T_\infty\right) \tag{A.10}$$

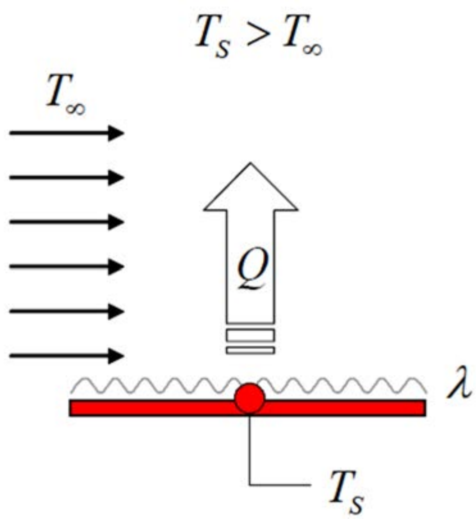

Figure 4: Convective Heat Transfer

In the formulation of Equation A.10 the assumption was made that heat transfer from the surface to the fluid is positive while heat transfer from the fluid to the surface is negative. Equation A.10 is also known as Newton's Law of Cooling.

C. Radiation

Heat transfer through radiation is a result of energy transported by magnetic waves. Figure 5 shows a schematic representation of the radiation heat transfer mechanism where heat is transferred from a high temperature surface to a lower temperature surface. While heat transfer by conduction and convection requires a material, radiation heat transfer does not. In fact, radiation heat transfer occurs most effectively in a vacuum.

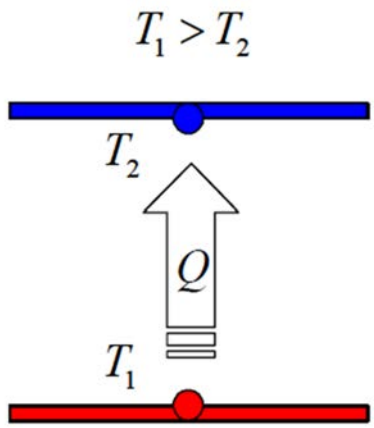

Figure 5: Radiation Heat Transfer

The radiation heat transfer between two surfaces at different temperatures is given by Equation A.11 where σ is the Stefan-Boltzmann constant and ε is the emissivity of the material.

$$Q_H = \varepsilon\sigma A\left(T_1^4 - T_2^4\right) \tag{A.11}$$

D. Work

Work is also a form of energy and is generally defined as a force undergoing a displacement:

$$W = \int_{r_1}^{r_2} F \cdot dr \tag{A.12}$$

Work is defined as energy in transition to or from a system when external forces acting on the system undergoes a displacement. Both the surface and body forces acting on the control volume can also perform work on the system. Both heat and work are only defined at the boundaries of a system. A system cannot contain either heat or work. Heat and work are only defined when it moves across the boundary of the system (control surface) and is therefore a transitional phenomena.

The energy equation can also be written in differential form by contracting the control volume to a differential volume. Equation A.8 then reduces to equation A13.

$$\frac{\partial(\rho e)}{\partial t} + \vec{\nabla}\cdot\left(\rho\vec{V}e\right) = \dot{Q}_H - \dot{W} \tag{A.13}$$

A.2.2. Fluid Properties

Fluid properties, such as the fluid density ρ and viscosity μ, form an integral part of governing equations. The viscosity forms part of the stress tensor $\bar{T}$ on the right hand side of Equation A.6. In order to solve the governing equations these fluid properties must be known. Various options are available to determine the fluid properties that are usually also functions of other variables for example the temperature, pressure and velocity.

When the fluid density is constant throughout the flow field the flow is considered incompressible. The flow of liquids can be considered incompressible for most engineering applications. Gasses on the other hand can be considered incompressible only under special circumstances for example under low velocity flow conditions. The gas density can be determined from equations of state such as the ideal gas law, in terms of the fluid temperature and pressure, which forms part of the solution. For non-ideal gasses a compressibility factor *Z* may be introduced, which is a function of pressure and temperature.

The gas density may be expressed according to the ideal gas law as follows:

$$\rho = \frac{p}{RT} \tag{A.14}$$

A.3. Two-Phase Flow

Two-phase flow is a phenomenon that occurs mainly as a result of one of the following processes:

- Flashing
- Boiling
- Condensation

The three processes mentioned are typically present in a one-fluid two-phase flow system. Figure 6 shows the different processes as applicable to a one-fluid two-phase flow system on a pressure – enthalpy diagram.

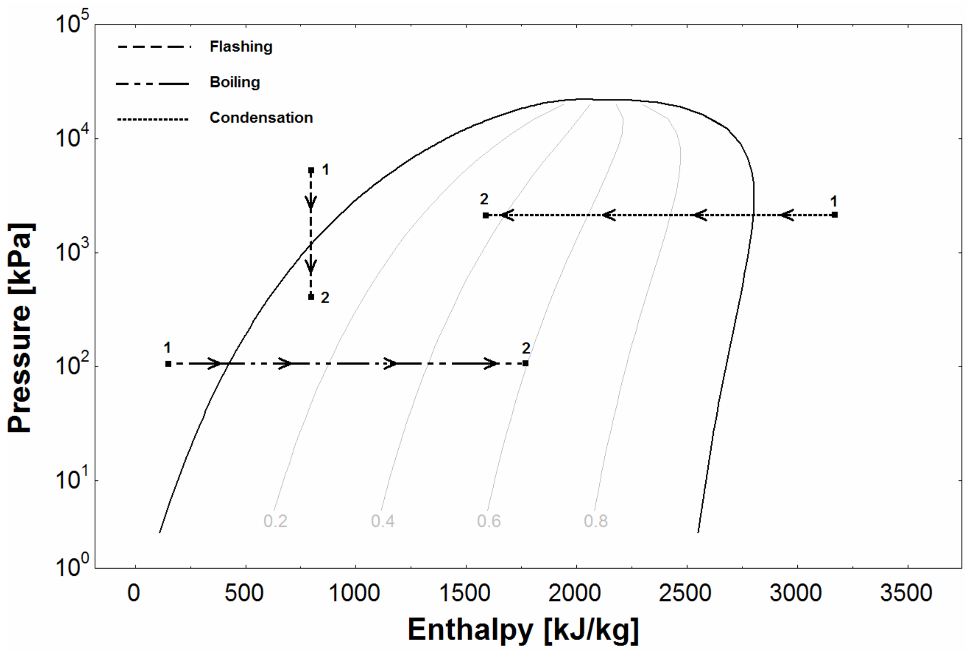

Figure 6: Pressure - Enthalpy Diagram Showing Flashing, Boiling, and Condensation Processes

Flashing takes place when the pressure of a fluid is reduced (adiabatic process) below the saturation pressure for the given temperature. Boiling occurs when heat is added to the system and the fluid reaches the liquid saturation temperature for the given pressure (illustrated for isobaric process). Condensation takes place when the vapor is cooled down and the vapor saturation temperature is reached (illustrated for isobaric process). Two-phase flows are governed by mass, momentum, and energy conservation equations. A number of constitutive equations are also used to calculate the two-phase friction factor and heat transfer coefficient. The final process mentioned takes place when two immiscible fluids are mixed. Such two-phase flow systems are encountered in the oil industry or when air from the atmosphere enters into a liquid filled system from a leaking pipe or open valve.

Incondensable gas mixtures are defined as mixtures that contain both an incondensable gas and a liquid-vapor mixture. A typical example is the situation found in condensers/evaporators with air entrainment. In this case, the air would be the incondensable gas with the saturated steam present in liquid and vapor phases. Thermo-dynamic conditions determine in which of three possible states the mixture exists:

- Liquid-vapor mixture with incondensable gas
- Super-heated vapor containing only vapor and the incondensable gas

This equation is used to calculate various thermo-dynamic properties of such a mixture are located in Reference [39]. The properties that can be calculated are the partial pressures, enthalpy, mixture density, temperature, vapor mass fraction and entropy.

Appendix B GOTHIC Model Theory Overview

B.1. Introduction

GOTHIC is an integrated, general purpose thermal-hydraulics software package for design, licensing, safety and operating analysis of nuclear power plant systems, confinement buildings and system components. Applications of GOTHIC include evaluation of SSCs response to the full spectrum of high energy line breaks within the design basis envelope and a wide variety of systems evaluations involving multiphase flow and heat transfer, gas mixing and other thermal hydraulic behavior. Applications may include, but are by no means limited to, pressure and temperature determination, equipment qualification profiles and inadvertent system initiation, and degradation or failure of engineered safety features. As a general purpose tool, GOTHIC can be used for a wide variety of plant operations support issues involving single and multiphase heat transfer and fluid flow provided that the application is consistent with the underlying physical basis and assumptions and the- code validation basis. [67] [68]

B.2. GOTHIC BASE MODEL THEORY

B.2.1. Governing Equations

The conservation equations solved by GOTHIC are written in integral form. This form is closely related to the finite volume numerical method used to solve the equations. The equations are written for a fixed volume bounded by area. The volume may be the entire region of interest or a portion of the total volume, although, in practice, the volume corresponds to one of the finite volumes of the computational grid. The specific equations for the following parameters can be found in the EPRI document titled "GOTHIC Thermal Hydraulic Analysis Package Technical Manual" [68] dated May 2023. The equations are for multidimensional analysis with simplifications made for lumped parameter analysis and junction flows.

B.2.1.1 Mass Conservation

Mass conservation equations are solved for: liquid, each drop field, ice, mist, steam and each noncondensing gas component as well as each liquid component in the liquid and each drop field. The steam/gas mixture, hereafter referred to as the vapor phase, can be in the form of bubbles or a continuous vapor region. The liquid phase can be in the form of pools, films or large chunks found in slug flow. The drop phase can consist of any number of interacting drop fields and each drop field is treated as a separate phase. The general form of the mass balance is:

$$\underbrace{\frac{\partial}{\partial t}\int_V \Theta\alpha_\phi\rho_{\phi\varsigma}dV}_{\text{storage}} = \underbrace{-\int_{A_f}\Psi\alpha_\phi\rho_{\phi\varsigma}\vec{u_\phi}\cdot\vec{n}\,dA}_{\text{convection}} + \underbrace{\int_{A_f}\Psi\alpha_\phi\rho_\phi D^c_\phi\vec{\nabla}\left(\frac{\rho_{\phi\varsigma}}{\rho_\phi}\right)\cdot\vec{n}\,dA}_{\text{diffusion}}$$
$$+\underbrace{\int_{A_w} s^c_{\phi\varsigma}dA}_{\text{boundary source}} + \underbrace{S^c_{\phi\varsigma}}_{\text{interphase source}} + \underbrace{E^c_{\phi\varsigma}}_{\text{equipment source}} + \underbrace{C^c_{\phi\varsigma}}_{\text{combustion source}} \tag{B.1}$$

The subscript φ refers to the phase and takes on the values *v* (vapor), *l* (liquid), d_f (drops for field *f*) and *i* (ice). It is assumed that the mist occupies no volume in the vapor phase so α_v is used for α_φ in the mist mass balance. The subscript ζ refers to a component of the vapor ($\zeta = s$ for the steam component, $\zeta = n$ for a single component of the noncondensing gas mixture, and $\zeta = g$ for the noncondensing gas mixture). Θ is the volume porosity and Ψ is the area porosity factor. The porosity factors range from 0 to 1 with a value of 1 for a completely unobstructed volume or Area. α is the volume fraction, ρ is the density, $\vec{u}$ is the velocity, $\vec{n}$ is outward normal to the surface dA, A_f is that portion of the total surface area in contact with adjacent fluid volumes, D^c is the mass diffusion coefficient, including turbulence effects, s^c is the mass source per unit area generated at, or passing through, bounding wall A_w, S^c is the mass source due to interaction with other phases (e.g., evaporation, condensation, drop entrainment deposition), E^c is the mass source from engineered safety equipment and C^c is the mass source from hydrogen combustion.

B.2.1.2 Energy Conservation

Energy conservation equations are solved for three fluid phases: each drop field, liquid and vapor/mist, and for solid thermal conductors with or without surface ice. The fluid energy equation is solved for enthalpy, so the equation is written in terms of enthalpy rather than internal energy. The fluid energy equation is:

$$\underbrace{\frac{\partial}{\partial t}\int_V \Theta\alpha_\phi\left(\rho_\phi(h+ke)_\phi - P\right)dV}_{\text{storage}} = \underbrace{-\int_{A_f}\Psi\alpha_\phi\rho_\phi(h+ke)_\phi\,\vec{u_\phi}\cdot\vec{n}\,dA}_{\text{convection}} \underbrace{-\int_V P\frac{\partial}{\partial t}(\Theta\alpha_\phi)\,dV}_{\text{work}}$$
$$+\underbrace{\int_{A_f}\Psi\alpha_\phi\rho_\phi c_{p\phi}D^e_\phi\vec{\nabla}T_\phi\cdot\vec{n}\,dA}_{\text{thermal diffusion}}$$
$$+\underbrace{\sum_\zeta\int_{A_f}\Psi\alpha_\phi\rho_\phi D^c_\phi\vec{\nabla}\left(\frac{\rho_{\phi\zeta}}{\rho_\phi}\right)h_{\phi\zeta}\cdot\vec{n}\,dA}_{\text{gas component diffusion}}+\underbrace{\sum_k\int_V\Theta\lambda_k q_k\alpha_\phi\Phi_{k\phi}dV}_{\text{tracer decay}}$$
$$+\underbrace{\int_{A_w}s^e_\phi dA}_{\text{boundary source}}+\underbrace{S^e_\phi}_{\text{interphase source}}+\underbrace{E^e_\phi}_{\text{equipment source}}+\underbrace{C^e_\phi}_{\text{combustion source}} \tag{B.2}$$

h is enthalpy, ke is the kinetic energy, P is the static pressure, D^e is the thermal diffusion coefficient, λ_k is the decay rate for tracer k (*fission/s-mol*), q_k is the decay energy release per fission event, s^e is the energy source per unit wall area, S^e is the interphase energy source, E^e is the equipment energy source and C^e is the energy source from hydrogen combustion. Kinetic energy is included or neglected by user selection, and all other energy forms not explicitly represented above are neglected. Viscous dissipation is also neglected. The kinetic energy is defined as $ke_\varphi = u^2_\varphi/2$. All components of the vapor are assumed to be at the same temperature. The enthalpy in the vapor energy is the mixture energy of the steam, noncondensing gas mixture and the mist. Each drop field has its own energy balance. The energy transported with the mass through mass diffusion is included only for the vapor. The ice energy is included in the energy balance for the underlying conductor.

Additional decay heat is added to the fluid from radioactive decay of tracers on surfaces and in filters. For surface tracer decay, the associated heat is added to the fluid (liquid or vapor phase) that is in contact with the surface, with tracers on the wet and dry portions of a conductor tracked separately. For tracer decay in filters, the associated heat is added to the downstream fluid. If there is no flow through the tracer, the decay heat is equally split between the two volumes on either side of the filter.

The energy equation for the solid conductors is:

$$\underbrace{\int_{V_{cn}} \rho_{cn} c_{p,cn} \frac{\partial T_{cn}}{\partial t} dV_{cn}}_{\text{storage}} = \underbrace{\int_{A_i} D^e_{cn} \vec{\nabla} T_{cn} \cdot \vec{n}\, dA}_{\text{diffusion}} + \underbrace{\int_{A_b} s^e_{cn} dA}_{\text{boundary source}} \qquad \text{(B.3)}$$

The subscript *cn* refers to a particular conductor, V_{cn} is the volume of the conductor or portion of a conductor, A_i is the surface area of V_{cn} internal to the conductor, D^e is the diffusion coefficient (conductivity) and A_b is the external bounding surface area of the conductor which may be in contact with one or more of the fluid phases. If there is ice on one or both surfaces of the conductor, it is treated as any other material layer in the conductor for the conduction solution. Conductors in GOTHIC cover only 1D heat transfer; no heat is transferred to neighboring conductors.

B.2.1.3 Momentum Conservation

Momentum conservation equations are solved for three phases: each drop field, liquid and vapor. The general form of the equation is:

$$\underbrace{\frac{\partial}{\partial t} \int_{V} \Theta \alpha_\phi \rho_\phi \vec{u_\phi} dV}_{\text{storage}} = -\underbrace{\int_{A_f} \Psi \alpha_\phi \rho_\phi \vec{u_\phi} (\vec{u_\phi} \cdot \vec{n})\, dA}_{\text{convection}} + \underbrace{\int_{A_f} \Psi \alpha_\phi \underline{\sigma}_\phi \cdot \vec{n}\, dA}_{\text{surface stress}} + \underbrace{\int_{V} \Theta \vec{g} \alpha_\phi \rho_\phi dV}_{\text{body force}}$$
$$+ \underbrace{\int_{A_w} \vec{s^{m}_\phi} dA}_{\text{boundary source}} + \underbrace{\vec{S^{m}_\phi}}_{\text{interphase source}} + \underbrace{\vec{E^{m}_\phi}}_{\text{equipment source}} \qquad \text{(B.4)}$$

$\underline{\sigma}$ includes the static pressure and the viscous and Reynolds stress terms, $\vec{g}$ is the gravitational acceleration, $\vec{s^{m}}$ is the momentum source per unit wall area, $\vec{S^{m}}$ the momentum source due to interphase exchange (drag and phase transition) and $\vec{E^{m}}$ is the momentum source from equipment. All components of the vapor are assumed to move at the same velocity. The density in the vapor momentum equation includes the steam and gas component densities, (each at their own partial pressure) and the mist macroscopic density (i.e., mist mass per unit vapor volume).

B.2.1.4 Drop Number Concentration and Surface Area

For each drop field, i, the drop count balance is:

$$\frac{\partial}{\partial t}\int_V \Theta N'''_{d_f} dV = -\int_{A_f} \Psi N'''_{d_f}\overrightarrow{u_{d_f}} \cdot \overrightarrow{n}\, dA + S^N_{d_f} + E^N_{d_f} \tag{B.5}$$

where N_d mmm is the number of drops in field f per unit volume, S^N is the drop number source due to agglomeration, deposition and entrainment and E^N is the drop number source from engineered safety equipment (e.g., nozzles).

The equation for surface area is:

$$\frac{\partial}{\partial t}\int_V \Theta A'''_{d_f} dV = -\int_{A_f} \Psi A'''_{d_f}\overrightarrow{u_{d_f}} \cdot \overrightarrow{n}\, dA + S^A_{d_f} + E^A_{d_f} \tag{B.6}$$

where $A_{df}{}^{m}$ is the drop surface area in field f per unit volume, SA is the drop surface area source coming from agglomeration, deposition, entrainment, evaporation and condensation and EA is the drop surface area source from engineered safety equipment (nozzles). The drop number and area densities are used to track the average drop diameter and geometric standard deviation.

B.2.1.5 Reduced Equations for Lumped Parameter Volumes

The computational grid can be made up of a combination of subdivided volumes (with 1-, 2- or 3-dimensional rectangular meshes) and lumped volumes (one computational cell per volume). For a mesh of lumped parameter cells and junctions, mass and energy balances are maintained for the lumped volumes and momentum balances are maintained for the junctions which serve as the only flow connections to lumped volumes. Junctions are also used to connect subvolumes to lumped volumes and may be used to connect two sub- volumes. The lumped parameter approach involves some simplifying assumptions resulting in reduced conservation equations. In this section the mass and energy balances for lumped parameter volumes are presented.

A. Mass Conservation

To emphasize the fact that flow paths are the only flow connections to a lumped volume, the integrals for the convective terms are replaced by summations over all the junction connections to the volume in the following equations.

$$\frac{\partial}{\partial t}\int_V \alpha_\phi \rho_{\phi\zeta} dV = \sum_{\{j\}V} \alpha_\phi \rho_{\phi\zeta} \overrightarrow{u_\phi} \cdot \overrightarrow{n} A_j + \int_{A_w} s^c_{\phi\zeta} dA + S^c_{\phi\zeta} + E^c_{\phi\zeta} \tag{B.7}$$

where {*j*}V is the set of junctions connected to the volume and A_j is the junction area. The junction velocities are not actually vector quantities, but the vector notation is retained to give the correct sign on the convection terms, i.e., $\overrightarrow{u_\phi} \cdot \overrightarrow{n} = \pm u_\phi$. The volume and area porosity factors are not included in the lumped volume balances equations. Therefore, the specified volume represents the free volume and the junction areas are the actual flow areas.

B. Energy Conservation

Energy conservation equations are solved for three phases; drops, liquid and the vapor, and for the solid thermal conductors. The fluid energy equation is

$$\begin{aligned}\frac{\partial}{\partial t}\int_V \alpha_\phi \rho_\phi (e+ke)_\phi dV \quad &= -\sum_{\{j\}V} \alpha_\phi \left(\rho_\phi (e+ke)_\phi + P\right) \overrightarrow{u}_\phi \cdot \overrightarrow{n} A_j \\ &-\int_V P \frac{\partial}{\partial t}(\Theta \alpha_\phi) dV + \int_{A_w} s^e_\phi dA_{I_\phi} + \sum_k \int_V \Theta \lambda_k q_k \alpha_\phi \Phi_{k\phi} dV + S^e_\phi + E^e_\phi\end{aligned} \tag{B.8}$$

In lumped parameter analysis, the turbulent diffusion coefficients will be zero even if the turbulent option is selected because there are no velocity gradients available for their calculation. Therefore, mass and thermal diffusion across the junctions are not included in the above lumped parameter mass and energy balances. However, for junctions that connect subdivided volumes, turbulent mass diffusion across the junction (and its associated energy transfer) is included. Thermal diffusion across junctions is not included in any case.

C. Momentum Conservation

While a lumped parameter volume has mass and energy, there is no flow field such as would exist in a subdivided volume. Therefore, momentum equations are not solved for lumped parameter volumes. Instead, where lumped parameter volumes are connected by junctions, momentum balances are solved for each junction.

B.2.1.6 Liquid Components

GOTHIC can track the propagation and storage of solid, liquid or dissolved components in the liquid and droplet fields. Two types of liquid components are available: solid particles and dissolved gas. Both are referred to as liquid components but the treatment varies depending on the type.

B.2.1.7 Equations of State

A. Vapor

The Dalton model is used for the steam/gas mixture. In this model, it is assumed that each component exists at the volume and temperature of the mixture. The total pressure is then equal to the sum of the component partial pressures, expressed as

$$P_v = \sum_{\zeta} P_{v\zeta} \tag{B.9}$$

where $P_{v\zeta}$ is a vapor component partial pressure.

All components of the vapor phase are assumed to be at the same temperature, and the perfect gas law is used to obtain the density of the noncondensing vapor components. Thus, for the noncondensing components, we have

$$T_{v\zeta} = T_{vs} = T_v \tag{B.10}$$

and

$$\rho_{v\zeta} = \frac{P_{v\zeta}}{R_{v\zeta} T_{v\zeta}} \tag{B.11}$$

where $R_{v\zeta}$ is the gas constant for gas component ζ.

The total vapor density and enthalpy are calculated from

$$\rho_v = \sum_{\zeta} \rho_{v\zeta} \tag{B.12}$$

and

$$h_v = \frac{1}{\rho_v} \sum_{\zeta} h_{v\zeta} \rho_{v\zeta} \tag{B.13}$$

B. **Drops and Liquid**

The static pressure in the drops and in the liquid are assumed to be the same as the total pressure

$$P_l = P_d = P \tag{B.14}$$

The temperature and density of the water in drops are obtained from

$$\rho_d = \rho_{st}(h_d, P) \tag{B.15}$$

and

$$T_d = T_{st}(h_d, P) \tag{B.16}$$

with

$$h_d = e_d + \frac{P}{\rho_d} \tag{B.17}$$

Similarly, the liquid density and temperature are given by

$$\rho_l = \rho_{st}(h_l, P) \tag{B.18}$$

and

$$T_l = T_{st}(h_l, P) \tag{B.19}$$

with

$$h_l = e_l + \frac{P}{\rho_l} \tag{B.20}$$

C. Liquid Component

It is assumed that the enthalpy of the liquid component is given by

$$h_{c_k} = (c_p)_{c_k}(T_l - T_0) \tag{B.21}$$

where c_p is the specific heat for the component (assumed constant) and T_0 is the reference temperature. It is assumed that T^0 = 32°F.

For the liquid momentum balance the liquid density is replaced by the mixture density defined as

$$\rho_{lt} = (1 - \chi_{l,c,tot})\rho_l + \sum_{k=1}^{N_{sp}} (\chi_{l,c}\zeta_c\rho_c)_k \tag{B.22}$$

This is only for solid particle components and only considers suspended particles. Settled particles are assumed to not impact the liquid momentum. Settled particles include both those that are resting on a horizontal face as well as those that are falling through a cell but have not yet come to rest. A separate velocity is calculated for falling particles while the suspended component travels with the liquid velocity. Therefore, only the suspended portion should be considered when quantifying the impact of the solid particle components on the momentum of the continuous liquid field.

For the liquid or droplet field momentum balance the droplet density is replaced by the mixture density defined as

$$\rho_{d_f t} = (1 - \chi_{d_f c_{tot}})\rho_{d_f} + \sum_{k=1}^{N_{sp}} (\chi_{d_f c_k}\rho_{d_f c_k}) \tag{B.23}$$

D. Mist

GOTHIC solves for the mist density per unit vapor volume, referred to as the macroscopic mist density. The thermodynamic density of the water that constitutes the mist droplets is also needed. Under the assumption that the mist temperature is equal to the saturation temperature at the steam partial pressure, the mist thermodynamic density is obtained from:

$$\rho_{mt} = \rho_{st}\left(P_v, T_{sat}\left(P_{vs}\right)\right) \tag{B.24}$$

where T_{sat} is the saturation temperature at the steam pressure, P_{vs}.

The mist enthalpy is obtained from:

$$h_m = h_{st}\left(P_v, T_{sat}\left(P_{vs}\right)\right) \tag{B.25}$$

E. Pressure Adjustment for Vapor Phase

In calculating the vapor and gas properties, the total pressure of the vapor P_v is nominally equal to the total pressure P which is also the cell center pressure. However, when the height of the liquid pool is greater than half the cell height, the cell vapor pressure should be reduced by the head of the liquid above the cell center. An input option is available that implements this correction and, when it is requested, steam and gas properties are evaluated with the pressure of the vapor phase defined as

$$P_\nu = \left\{ \begin{array}{ll} P - \rho_l g \Delta X\left(\alpha_l - 0.5\right) & \text{if } \alpha_l > 0.5 \\ P & \text{if } \alpha_l \leq 0.5 \end{array} \right\} \tag{B.26}$$

B.2.1.8 Source Terms

External mass, energy and momentum sources, such as a specified source from a line break, are included in the convective terms of Equations B.1, B.2, and B.3. The boundary source terms in the conservation equations above include heat and momentum sources and sinks due to bounding walls, e.g., convection heat transfer from conductor surfaces and wall drag on the fluid.

A. Mass Source

Surface mass source terms include mass sources and sinks due to a phase change at a non-fluid surface. For example, condensation heat transfer on conductors results in a mass sink for the steam and a mass source for the liquid. The boundary source terms for the mass balances are shown in following Equations.

$$\int_{A_w} s_v^c dA = \sum_w \Gamma_{w_v} \tag{B.27}$$

$$\int_{A_w} s_l^c dA = \sum_w \Gamma_{w_l} \tag{B.28}$$

$$\int_{A_w} s_d^c dA = 0 \tag{B.29}$$

Where Γ_w is the phase change resulting directly from heat transfer to the wall and the summation is over all conductors thermally connected to the volume.

B. Energy Source

The boundary source terms for the fluid energy equations include convection and radiation heat transfer from walls and the energy associated with any surface mass source terms. It is assumed that all wall heat transfer is between the walls and the liquid and vapor phases. There is no heat transfer directly between the walls and the drops. The boundary source terms for the energy equations are shown in:

$$\int_{A_w} s_v^e dA = \sum_w Q_{w_v} \tag{B.30}$$

$$\int_{A_w} s_l^e dA = \sum_w Q_{w_l} \tag{B.31}$$

$$\int_{A_w} s_d^e dA = 0 \tag{B.32}$$

Where Qw includes the sensible heat flux from the wall to the fluid and also the energy carried by Γw.

For the solid conductors, the surface heat flux is either specified or it is calculated from known conductor and fluid temperatures and heat transfer coefficients. The boundary source term for the conductor energy equation, including the sensible heat flux and the latent heat associated with Γ_w, is:

$$\int_{A_w} s^e_{cn} dA = -Q_{w_v} - Q_{w_l} + Q_{w_s} + Q_{w_r} \tag{B.33}$$

where Q_{w_s} is the wall heat calculated from specified wall BCs and where Q_{w_r} is the net energy gain from wall to wall radiation exchange.

C. Momentum Source

The boundary momentum source includes friction and form drag due to walls, orifices and obstructions. The boundary source term for the momentum equation is

$$\int_{A_w} s^m_{\phi} dA = D_{\phi} \tag{B.34}$$

Where D_{φ} is the total wall, form and orifice drag force.

B.2.1.9 Interphase Source Terms

The interphase source terms include the mass, energy and momentum transfer from one phase to another due to vaporization, condensation, drop entrainment and deposition and ice melting. Vaporization, condensation and ice melting are the result of combined heat and mass transfer at the interfaces. Drop entrainment and deposition are due to mechanical effects. The source terms for phase transition are obtained by mass and energy balances for the interfaces. It is assumed that no mass or energy is stored at the interface. For the phase change at the vapor/liquid interface, or at the vapor/drop interface, the energy balance for the interface is

$$\int_{A_I} q''_I = \Gamma_I \Delta h_I \tag{B.35}$$

where q''_I is the net heat flux to the interface from both phases, Γ_I is the net rate of vaporization (condensation, if it is negative), and Δh_I is the effective heat of vaporization.

B.2.1.10 Laminar Leakage

GOTHIC includes a laminar leakage model for lumped parameter volumes and subdivided volumes. This model is intended to simulate the leakage through very narrow cracks where the flow can be characterized as laminar. Leakages from larger holes, which is generally turbulent, can be modeled using junctions with appropriate loss coefficients or with the turbulent leakage model.

B.2.1.11 Turbulent Leakage

GOTHIC includes a turbulent leakage model for lumped parameter volumes and subdivided volumes. This model is intended to simulate the leakage through larger cracks and holes where the flow can be characterized as turbulent.

For steady turbulent flow of a perfect gas through an opening with area A, Equations B.36 through B.38 are assumed to hold.

$$P_u - P_{wu} = \frac{Y_c K_c F^2}{2A^2 \rho_u} + \frac{F^2}{2A^2 \rho_{wu}} \tag{B.36}$$

$$\frac{dP_w}{dx} = \frac{f}{2DA^2} \frac{F^2}{\rho_w(x)} + \frac{d}{dx}\left(\frac{F^2}{A^2 \rho_w(x)}\right) = \frac{fRF^2}{2DA^2} \frac{T_w(x)}{P_w(x)} + \frac{F^2}{A^2} \frac{dv_w(x)}{dx} \tag{B.37}$$

$$P_{wd} - P_d = \frac{Y_e K_e F^2}{2A^2 \rho_{wd}} - \frac{F^2}{2A^2 \rho_{wd}} \tag{B.38}$$

Where:

P_u is the upstream pressure

P_d is the downstream pressure

P_{wu} is the pressure just inside the wall on the upstream side

P_{wd} is the pressure just inside the wall on the downstream side

$P_w(x)$ is the pressure profile inside the wall, $x = 0$ at the upstream wall surface

ρ_u is the upstream density

ρ_{wd} is the density of the fluid in the wall just upstream of the expansion loss

$\rho_w(x)$ is the fluid density profile inside the wall

$v_w(x)$ is the fluid specific volume inside the wall

F is the steady flow rate

D is the hydraulic diameter (assumed constant)

f is the friction factor (assumed constant)

R is the gas constant

$T_w(x)$ is the temperature profile through the wall

K_c is the contraction loss coefficient for flow entering the wall

K_e is the expansion loss coefficient for flow exiting the wall

Y_c is the compressibility factor for the contraction

Y_e is the compressibility factor for the expansion

The second term in each of the above equations represents the reversible pressure loss or gain due to acceleration or deceleration. It is assumed that the flow through the leak is not choked.

B.2.1.12 Drop Leakage

For either laminar or turbulent leakage, the upstream drops may be optionally included in the leakage flow. The following assumptions apply for both leakage models:

1. The option to include or not include the drops in the leakage has no direct impact on the calculated vapor phase leakage rate.
2. Each drop field moves with the vapor phase through the leak without 2-phase slippage.
3. Drops are included in the leakage only when the leakage is toward the sink pressure BC or specified sink volume.

For drop field n, the drop mass transfer rate associated with the vapor phase leakage is:

$$F_{d_n} = \frac{F_v}{\rho_v{}^*} \frac{\alpha_{d_n}{}^*}{\alpha_v{}^* + \alpha_d{}^*} \rho_{d_n}{}^* \tag{B.39}$$

where the superscript * refers to an upstream value.

The drop field energy and any tracers and liquid components in the drop field are transported with the drops.

If the leakage sink is a pressure BC, the leak drop mass, energy, tracer and liquid components are included in the respective loss to BCs.

If the leakage sink is a volume, the accumulated leakage is relaxed into the sink volume. The source rate for any entity, R, associated with the drop field leakage is given by

$$\dot{R}^{n-1} = \frac{R^{n-1}}{\Delta t_{leak}} \tag{B.40}$$

$$R^n = R^{n-1} - \dot{R}^{n-1} \Delta t_{n-1} \tag{B.41}$$

where Δt_{leak} is the relaxation time interval (assumed at 10 s), and the superscript refers to the time step number.

B.2.1.13 Tracer Conservation

GOTHIC solves a set of tracer transport equations that track the molar inventory of each tracer in vapor and liquid phases and each drop field in each cell. The user may define of tracer type that is optionally tracked in the vapor, liquid and/or conductor surfaces. If a tracer type is tracked in the liquid, it is automatically tracked in the liquid phase and each drop field.

The tracer inventory is also tracked in filters (both generalized and charcoal filters). The effects of radioactive decay can be optionally included.

Basic assumptions for the tracer conservation equations are:

1. Tracers do not have any mass or volume.
2. Tracers have no effect on the thermodynamic or thermal hydraulic transport properties of the carrier fluids.
3. Tracers move at the same speed as the carrier fluid.
4. For drop entrainment, deposition and agglomeration, the tracers are transferred with the transferred mass.
5. The diffusion of any particular tracer is not affected by the presence of other tracers.

B.2.2. Flow Paths

Flow paths, also referred to as junctions, are used to hydraulically connect any two computational cells. The flow paths may represent doorways, pipe or instrument penetrations, pipes, duct work, and so forth. These hydraulic connections are in addition to the vertical and lateral flow connections for 1-, 2- and 3-dimensional meshes that give the sub volume face velocities. Momentum equations for the vapor, droplets and liquid are solved for each junction. The junction momentum equations are consistent with those used for the sub volume face velocities and 3D Connectors except that the effects of viscous and turbulent shear are not included. The following parameters are calculated to adequately represent the movement within the flow path (between each computational cell). The equations and information for these parameters are found in Reference [68].

B.2.2.1 Momentum Conservation

Figure 7 shows a junction between two volumes, labeled 1 and 2, with overflow liquid from the pool in volume 2 displacing the vapor in volume 1. Although the figure shows vapor and liquid residing in the junction, it is important to note that the mass of fluid in the junction is not accounted for in the overall mass balance for the system. For purposes of mass balancing, there is no mass stored in the junctions and mass taken out of one volume via a junction is immediately placed in the connecting volume. However, for the purpose of calculating the inertia of the junction flow, an approximate junction fluid mass is calculated.

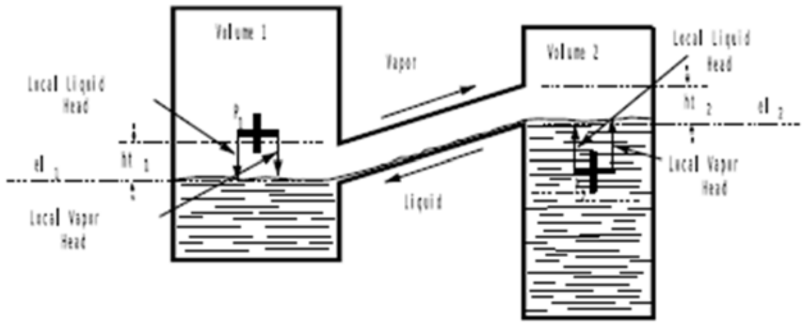

Figure 7: Junction Parameters

Junctions are physically characterized by their cross-sectional area, A, length, L, end elevations, el_1 and el_2, and end spanning heights, ht_1 and ht_2. By convention, positive flow is from volume 1 to volume 2. The momentum equation solved for each phase, φ, is

$$\underbrace{AL\frac{d(\hat{\alpha}_\phi \hat{\rho}_\phi w_\phi)}{dt}}_{\text{inertia}} = \underbrace{\hat{\alpha}_\phi A (P_1 + PL_{1\phi} - P_2 - PL_{2\phi})}_{\text{pressure gradient and local gravity head}} + \underbrace{\hat{\alpha}_\phi \hat{\rho}_\phi g A (el_1 - el_2)}_{\text{junction gravity head}} + \underbrace{E^m_\phi}_{\text{equipment source}} + \underbrace{MF_{1\phi} - MF_{2\phi}}_{\text{momentum fluxes}} + \underbrace{D_{w_\phi}}_{\text{wall drag}} + \underbrace{D_{I_\phi}}_{\text{interfacial drag}} \tag{B.42}$$

B.2.2.2 Pool Height and Vapor Fraction

For flow out of a cell through a junction, donor phase fractions are determined from the liquid level. For lumped parameter volumes, liquid level is based on the simplistic assumption that the liquid is in a pool below the drop/vapor mixture. For subdivided volumes, liquid height may be adjusted by the presence of bubbles in the pool. An effective pool height and pool vapor fraction is calculated from the vertical liquid and vapor velocities through the pool, cell fluid properties, cell phase volume fractions and cell geometric parameters.

B.2.2.3 Junction Volume Fractions

There are two sets of phase fractions relevant to junctions. These are the donor cell phase fractions which are used to determine mass balance flows through junctions, and junction phase fractions which are used in the determination of junction inertia, gravitational head, and pressure forces. Donor cell phase fractions are discussed first since they drive the calculation for junction phase fractions.

The donor cell phase fractions are determined by the direction of the phase velocity and the location of the pool surface relative to the junction end elevation and spanning height, Figure 8 shows three example situations where a horizontal junction connects to a volume with a pool. The junction end elevations are input parameters that define the low point of a junction connection to a volume. The end spanning heights are also input parameters and define the high point, relative to the junction end height, of a junction connection to a volume. For the purpose of discussion, assume that the flow of all phases is out of the volume and, therefore, the donor cell values are determined by the conditions in the volume shown. If the pool surface is below the end elevation, such as depicted in Figure 8 part a, then the donor phase fraction for the liquid is set to zero, and the phase fractions for the vapor and drops are set to their relative fractions in the vapor/drop mixture.

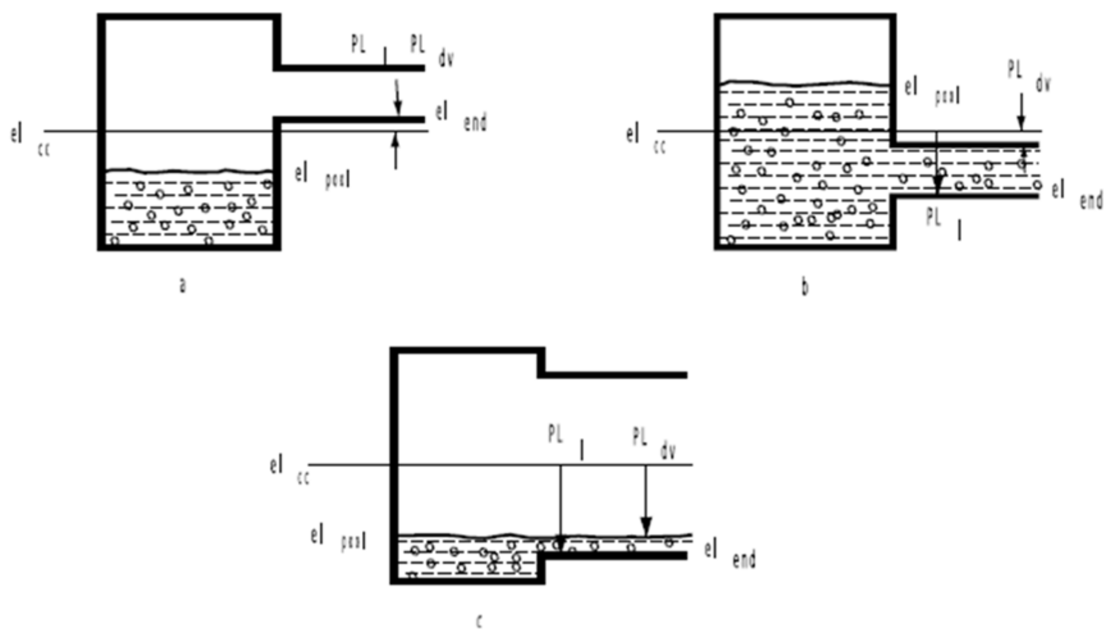

Figure 8: Junction and Pool Interaction

B.2.2.4 Flow Path Gravity Heads

The static pressure is calculated at the vertical center of each volume. In order to correctly calculate buoyancy induced flows in lumped parameter modeling, the variation in the static pressure within each volume is estimated to give the pressure loads at the junction ends.

Flow path gravitational head is split into two parts: head across the flow path (flow path head) and head from the cell center to the flow path end elevation (local head). The flow path head for phase φ is simply the flow path phase density, $\hat{\rho}_{\varphi}$, times the difference in the flow path end elevations as noted in Equation B.43.

The local gravitational head depends on the relative locations of the pool surface, cell vertical center and the flow path end elevations. The local gravitational head terms account for the pressure variation within a cell due to gravity. Separate local head terms are defined for each end of the flow path and they depend only on the conditions within the cells at the flow path ends. For the liquid phase, the local head is the static head from the cell center to flow path end elevation. Referring again to the three possible cases shown in Figure 8, the local liquid heads are given by:

$$\begin{aligned} \text{case a:} \quad PL_l &= \rho_{dv} g \left(el_{cc} - el_{end}\right) \\ \text{case b:} \quad PL_l &= \rho_{pool} g \left(el_{cc} - el_{end}\right) \\ \text{case c:} \quad PL_l &= \rho_{dv} g \left(el_{cc} - el_{pool}\right) + \rho_{pool} g \left(el_{pool} - el_{end}\right) \end{aligned} \tag{B.43}$$

B.2.2.5 Momentum Transport

The momentum flux terms in the flow path momentum equation are included so that flow paths can be used to connect compartments with 1-, 2- or 3-dimensional meshes while maintaining consistency with the momentum equations for the subdivided mesh. With these terms, flow paths can be used to connect two subdivided volumes and the results will be nearly identical to those obtained by modeling the entire two volume region with a single subdivided volume. Originally, this feature was included to permit complex region modeling with a collection of subdivided volumes interconnected by flow paths. With the release of version 7.0, the preferred approach to modeling complex geometries was a combination of subdivided volumes and 3D flow connectors. The flow path momentum transport features continue to be useful for modeling piping systems.

B.2.2.6 Intrinsic Pressure Loss

Modeling with GOTHIC subdivided volumes allows simulations in complex geometries with internal obstructions. The subdivided volumes can be connected together and to lumped volumes with Flow Paths or 3D connectors. The numerical treatment of the momentum equations in subdivided volumes results in irreversible losses for flow around obstructions and through area changes. These losses occur even if all surfaces are set to the slip conditions and are referred to here as intrinsic losses. The equivalent irreversible loss factors are reasonably close to the handbook values that are available for simple geometries. This relieves the user of the need to specify local loss factors for geometry variations within subdivided volumes.

B.2.2.7 Critical Flow Model

For any flow path, except those connected to flow BCs, the user may select a critical flow option. If the option is selected, the flow rate through the flow path is limited by that calculated using a critical flow model. Two models are available. One model uses a set of tables that were obtained from analytic models for water/steam mixtures. The other model solves the thermodynamic relationships directly for the maximum flow rate.

B.2.3. Engineered Safety Equipment

The base model of GOTHIC contains a variety of equipment that may exist within the plant and is part of the operation for safety and emergency response. These are referred to components and include the list equipment listed below. Each component group is treated as a single component (e.g., pumps and fans). For this example, if a pump is referred to, it would also include the fan; however, only one component class can be located on a flow path. A fan, recombiner, and valve can be assigned to a flow path.

- Pumps and fans
- Valves and doors and vacuum breakers
- Pressure Relief Valves (PRVs)
- Heat exchangers
- Spray nozzles
- Coolers and heaters
- Volumetric fans
- Filter Systems
- Dryer/Demisters
- Filters
- Charcoal Filters
- Recombiners
- Ignitors

Technical descriptions and mathematical models for each component are contained in Reference [68]. The mathematical models define the mass, momentum and energy source terms associated with the component.

B.2.4. Conductors

Conductors are used to model heat sinks such as concrete walls and floors and structural steel in containment buildings. Conductor geometries that can be modeled in GOTHIC are flat plates, hollow tubes, solid cylinders (rods) and hollow or solid spheres with conduction in one or two dimensions with an optional ice layer on the surface. Thermal radiation exchange among conductor surfaces can also be modeled.

For two-dimensional conduction in flat plate geometries the energy balance (Equation B.3) reduces to

$$\rho_{cn} c_{cn} \frac{\partial T_{cn}}{\partial t} = \frac{\partial \left(k_{cn} \frac{\partial T_{cn}}{\partial x} \right)}{\partial x} + \frac{\partial \left(k_{cn} \frac{\partial T_{cn}}{\partial z} \right)}{\partial z} + Q'''_{cn} \tag{B.44}$$

and for cylindrical geometries it is

$$\rho_{cn} c_{cn} \frac{\partial T_{cn}}{\partial t} = \frac{1}{r} \frac{\partial \left(k_{cn} r \frac{\partial T_{cn}}{\partial r} \right)}{\partial r} + \frac{\partial \left(k_{cn} \frac{\partial T_{cn}}{\partial z} \right)}{\partial z} + Q'''_{cn} \tag{B.45}$$

where the specific heat (c_{cn}) and the conductivity (k_{cn}) may be functions of space and the local temperature (T_{cn}) and Q''_{cn} is the local internal heating rate. The conductors can be made up of layers of varying materials. The conductor density (ρ_{cn}) is assumed constant for each type of material. For solid cylinders a zero heat flux condition is assumed at the center line. For surfaces normal to the x-direction (or r-direction), the possible boundary conditions include:

1. Specified temperature, *T(t)*
2. Specified heat flux, $q''(t)$
3. Convection, condensation and thermal radiation heat transfer,

$$Q''_w = Q''_{cond} + Q''_{conv_v} + Q''_{conv_l} + Q''_{rad} \tag{B.46}$$

where Q''_w is the total heat flux from the wall to the vapor, liquid and other surfaces and Q''_{cond} is the heat from the wall associated with a change of phase, Q''_{convv} and Q''_{convl} are the heat rates to the liquid and vapor phases, respectively, and Q''_{rad} is the net heat rate to other surfaces via radiative exchange.

For heat transfer in the z-direction, the only BCs allowed are time dependent specified temperature or heat flux. There is no radiant heat transfer to the conductor surfaces normal to the z-direction.

One material region in a conductor can be designated as a gap. Gaps can have no more than one temperature node. The effective conductivity of the gap can be calculated.

B.2.5. Source Terms

B.2.5.1 Interface Source Terms

The interface source terms are calculated by performing mass, momentum, and energy balances for the interfaces. It is assumed that there is no storage of any of these quantities at the interfaces. Seven interface combinations are considered; liquid/vapor, drops/vapor, ice/vapor, ice/liquid, drops/liquid, mist/vapor, and mist/(drop or liquid). Interchange at these interface combinations is due to heat transfer with a corresponding phase change and mechanical interaction resulting in interfacial mass and momentum transfer.

B.2.5.2 Wall Source Terms

Wall source terms include convection and radiation heat transfer, condensation and boiling at the wall and friction and orifice drag. The equations along with the correlations derived from the equations used to calculate these source terms are listed below.

A. Mass and Energy Source Terms

The available options for calculation of the energy source for each conductor available for selection by the user are:

1. Convection
   - Natural Convection
   - Forced Convection
   - Specified Convection
2. Radiation
3. Condensation
   - Direct Condensation
   - Tagami Blowdown
   - Specified Condensation
   - Mist/diffusion layer model
4. Specified Revaporization
5. Built-In Heat Transfer Package
6. Thermal BCs

B. Momentum Source Term

The Momentum source terms include the fluid drag due to wall friction and losses through orifices or across obstructions. Additional drag can be caused by the following.

1. Floor Drag
2. Wall Adhesion
3. Compressibility Option which includes orifice vapor phase compressibility, liquid and drop phase flashing, and nozzle vapor phase compressibility
4. Steam Injection into a Condensing Bowl

B.2.6. Drop Fields

Any number of drop fields can be used to track and simulate drop behavior in a GOTHIC model. It is assumed that the drops for a given field in a given cell have a log normal size distribution and that within each cell, each field is characterized by an average drop diameter and the geometric standard deviation (GSD).

Depending on the field option settings, the drop behavior may include agglomeration and deposition by various mechanism, evaporation, condensation and entrainment from pools and films. The combined effect of these mechanisms causes the average drop diameter and the GSD to change as the transient progresses.

If the drops are from a single source, (e.g., spray system or break), a single drop field is typically adequate to model the drop behavior. If the drops are from multiple sources (e.g., drops from a break followed by drops from spray system), the difference in the average diameter of the two drop source makes it difficult to model the drops with a single field. When the two fields are combined together in a single, the average drop diameter results in drop behavior that is not truly representative of either field. In these cases, multiple drop fields are recommended. Multiple drop fields may also be useful where there is interest in tracking the distribution of a constituent with a particular drop source combined with other drop sources.

B.2.7. Stress and Diffusion Terms

The stress tensor in the surface stress term of the momentum equation includes the effects of static pressure, viscous shear and turbulent diffusion of momentum. The components of the mass and energy diffusion that are due to turbulence are closely related to that for turbulent momentum diffusion. Inclusion of both molecular and turbulent diffusion in the mass diffusion coefficient and in the energy diffusion coefficient is optional in GOTHIC.

The fluid-fluid shear stress terms are applied only to the continuous phase. When the flow is primarily drop/vapor, the stresses are applied to the vapor phase. When the flow is bubble/liquid, the stresses are applied to the liquid phase. The stress tensors are calculated for each phase but are ramped to zero when the phase becomes discontinuous.

B.2.8. Fluid Properties

Formulas for calculation of ice, liquid, steam, gas component, and vapor mixture properties and the corresponding table data are coded in GOTHIC S. References are provided for most of the properties. There are a few properties, however, for which no specific reference is available. In most cases where a reference is not available, the properties in question were built into COBRANC [77] when it was acquired as the starting point for the development of FATHOMS and GOTHIC S, as outlined in Section 1.3 of Reference [9]. Therefore, these property correlations and tables in GOTHIC S have received considerable scrutiny over many years of applications. In addition, as part of the GOTHIC Design Review [78], many property correlations and tables in GOTHIC S were compared to other sources of property data [79] [80] and found to agree quite well.

Sections 14.1, 14.2 and 14.3 of Reference [68] describe the fluid property equations coded into GOTHIC S for the solid (ice), liquid (water) and vapor (steam) phases of water. GOTHIC also includes an option to use table based properties for water, as well as alternate fluids. Table based properties are discussed in Section 14.4 of Reference [68].

B.2.9. Finite Volume

The finite-volume for the mass, energy and momentum balances are written such that they may be solved on a rectangular mesh or in lumped parameter form. On a rectangular mesh, the full three dimensional form of the momentum equations is solved.

Mass and energy balances are maintained for each finite volume. Lumped parameter finite volumes are defined by the total free volume, height, and hydraulic diameter. The actual shape of a lumped volume is unspecified. Subdivided volumes can be divided into any number of finite volumes on a rectangular grid. The finite volumes in a subdivided volume are defined by the x, y and z dimensions, and volume and area porosity factors. The porosity factors are values between zero and 1. The volume porosity is the fraction of the cell volume occupied by the fluid. The area porosity factors specify the fraction of each cell face area that is open to flow.

B.2.10. Solution Algorithm

The general flow of the solution scheme is shown in Figure 9. Only the major elements of the algorithm are represented in the diagram.

GOTHIC models three types of phases (vapor, liquid and drops) and one, two or all three can be included in a model. The list below describes the solution procedure when all three phases are included. When one or more phases is excluded, the corresponding equations are not solved and the coefficients relating to the missing phases are zero. Details on the following solutions are found in Section 17 of Reference [68].

- Solution of the Momentum Equations
- Linearization of the Mass and Energy Equations
- Solution of the Pressure Matrix
- Unfolding of Primary and Secondary Variables
- 3D Flow Connectors
- Network Solutions
- Leakage
- Oscillating Flow Control
- Time step Control
- Damping and Ramps
- Phase Change Rate Limits
- Variable Limits

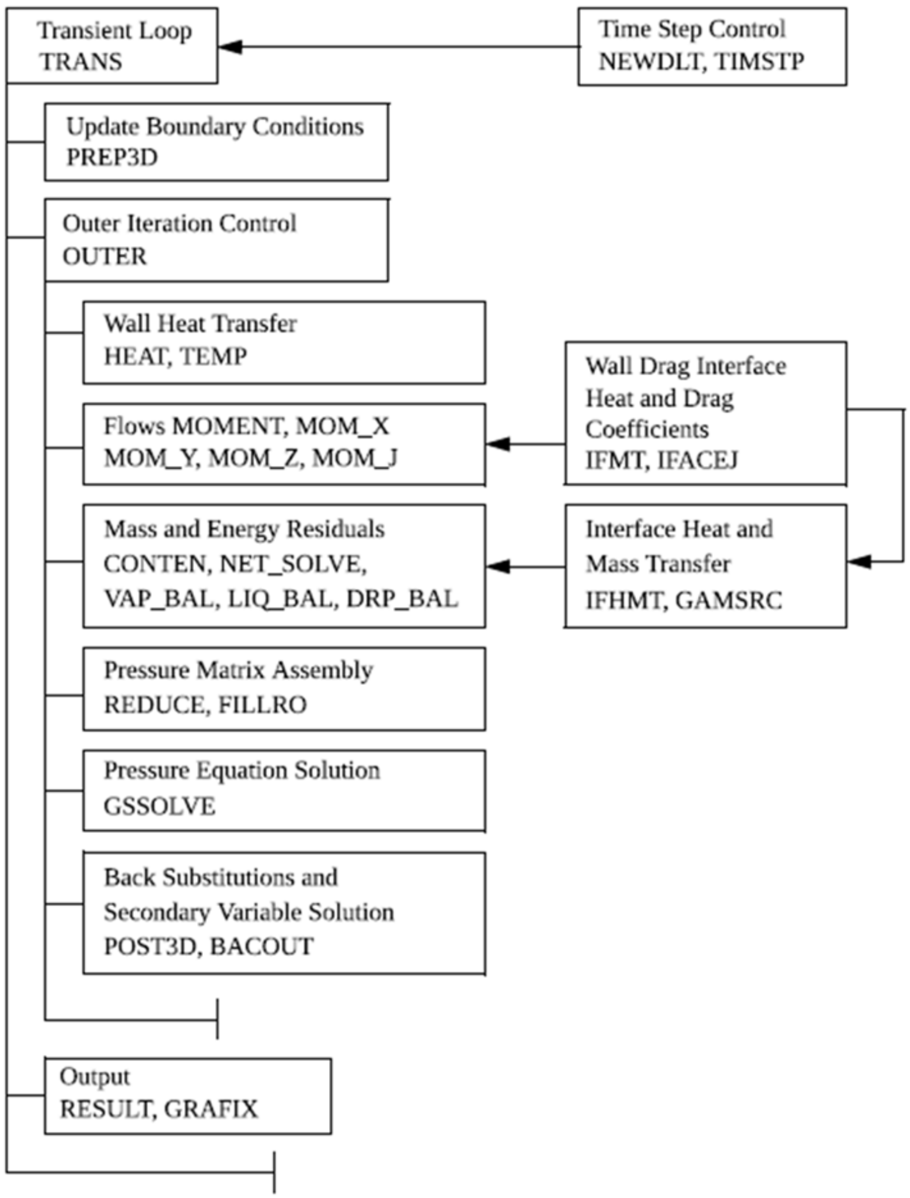

Figure 9: GOTHIC Solution Scheme Flow Diagram

Appendix C Flownex Model

The Flownex Model is used to calculate mass flows, temperatures, and pressures in the reactor core during expected operational modes and states, as well as under accident conditions. It is used for both steady state and transient simulations. It provides a common base of model inputs, components, solver settings, and formatted reporting to reduce duplication of work and unify the presentation of analysis results. Individual analysts will use and modify this base model as appropriate for the scope of analyzed events.

C.1. Description

A Flownex model file was prepared to serve as a common base model for Xe-100 safety analysis event transients. The model is derived from upstream mass and energy balance models and integrated models and includes many simplifications and modifications to facilitate usage for the safety analysis team. [6]

Challenges to model stability and rising model complexity of the Steady State integrated model introduced difficulties when applying the model to postulated Xe-100 plant transient events. The full model contains many details that did not impact the core concerns of safety analysis, and therefore represented an opportunity to tailor the model for the specific needs of the safety analysis team. This report documents the actions taken to simplify the model, along with the associated justifications. This result is a model that retains all necessary details but is more stable and robust in the target operating regimes.

Providing a common base model prevents duplicate work and error traps that could occur if each analyst was responsible for all changes and allows for greater configuration control.

A model file is provided that includes pre-defined starting points for event analysis, as well as reporting and visualization tools to promote presentation consistency and robust postprocessing. Analysts may initiate their respective events from a known-good set of operating conditions.

The final base model file will contain all the changes described in the following sections, along with various snaps that provide starting points for the event analysis. Guidance is documented for best practices on how to work with the model and perform common functions. [6] Snaps are a “snapshot” of the plant model state that is used for the initial conditions of a simulation.

C.2. Summary of Methodology

The process documented within this report starts with a base Flownex model. The performance of this base model is insufficient for general safety analysis in terms of execution time and convergence characteristics. The model was stabilized using the following general principles to simplify and stabilize the model. [4] [5] [6]

A. Two-phase tanks to the extent practical need to be removed from the system. These components are found to cause significant convergence issues.

B. The Flownex model is intended for short-term analysis of the Xe-100 on the scale of approximately 1 hour. Components that have approximately constant conditions over this time frame are disabled and replaced with BCs.

C. Disable components and systems that are not used for Safety Analysis scenarios. (Components are disabled rather than deleted in this approach, such that the original model structure can be re-enabled if needed for a specific event. Analysts can re-enable those components and refer to upstream model documentation to apply appropriate values.)

D. In Flownex all piping has a flow, even if it is infinitesimally small. The presence of infinitesimally small flows leads to frequent flow reversals and significant convergence issues. Efforts are made to eliminate these components or to allow larger but still negligible flows in these components. (e.g., opening valves by very small amounts or adding BCs to induce small flows).

E. The turbine, extraction steam, and turbine drains were replaced with simplified representations.

F. Pumps/circulators in low flow or reverse flow conditions are the source of significant convergence issues. Efforts are made to address or eliminate these conditions.

G. Calibration of convergence parameters to balance model execution speed with model stability.

H. General bug fixes in the control systems.

I. Adding monitoring utilities for the analyst (graphs and diagnostic information) to determine the status of the model more easily.

J. Definition of a snap for initiating safety analysis cases at 100[%] Full Power (FP).

K. Provide a unified set of graphs and reports for analysts to visualize results of the event transient, promoting consistency in style and form across all Flownex safety analysis work.

Model changes are made incrementally, saving intermediate snaps often and comparing the steady state solution results at 100% power to previous known-good results before moving on to the next change. All significant changes to model structure, nodalization, or fluid usage were followed by a new steady state solution. An Excel report showing key parameters was used to compare important results across solutions. The results should remain unchanged unless the modification affects a specific part of the model in an expected way.

C.3. Flownex Model

The safety analysis team is primarily utilizing the safety analysis specific Flownex model to capture the short-term transient response of the plant, focusing on the primary system conditions and key secondary side systems such as the SG. The model [6] is built in a modular fashion, such that the boundaries between subsystems are well-defined. The Flownex model is comprised of sub-models. Each sub-system was built and characterized by itself and then integrated with the other sub-system models. During the characterization of the models the interface conditions were kept constant.

The baseline reference for the structure, and vast majority of component inputs, are the Steady State mass and energy balance Flownex models of the Xe-100 reactor [31], HPB and SG [48], DA tank [26], and turbine [32] as well as the RPS/IPS modeling [52]. Significant additional systems, functionality, and numerous model components were added in areas to capture additional phenomena needed to support the event transients. All additions, deletions, and modifications to the reference models are documented in this report along with justification for each change.

C.3.1. Modeling Assumptions

The following assumptions are a consolidated list that are the most impactful. Modelling assumptions, simplification justifications, and engineering judgement that are embedded in the safety analysis model are discussed in the relevant sections. [6]

A. The water supplied by the DA tank to the feedwater (FW) pump is assumed to be at constant conditions over the anticipated timespan of the analyzed transients. Logic is included to cut off supply if the mass imbalance over time is such that it would exhaust the tank inventory.

B. Pump curves for the high pressure feedwater pumps (HPFWP) from upstream references do not include data on operation at low speeds. An artificial 0 rpm pump curve was added to improve numerical stability.

C. Density changes of graphite due to irradiation are not accounted for in the graphite material property adjustments. Since irradiation damage doesn't affect the mass of graphite, just the volume a given mass occupies, it does not significantly affect the heat transfer calculated by Flownex.

D. Fuel pebbles are assumed to make an average of 6 passes through the core during their lifetime. This is consistent with upstream neutronics analysis.

E. When calculating the graphite material properties accounting for a given amount of irradiation damage, the automation script assumes that all irradiation occurs at the current temperature of the graphite solid nodes when the script is run. The user must ensure that the network is in an appropriate state before running the script. The recommended methodology uses the Steady State conditions with fresh graphite as the state to use.

F. A constant factor of $1.37E21 ncm2/dpa$ is used to convert between units of fluence to match the graphite properties model inputs with the output from VSOP.

G. Structural graphite material property tables calculated by the automation script peg the value at the end of each curve, instead of extrapolating outside of its bounds. It does this by entering a duplicate point at the beginning and end of each property curve with the same value as the bound.)

H. The effect of xenon on reactor reactivity is not included in this model, consistent with upstream references. This will mainly impact long term transients where re-criticality may be a factor as xenon decays.

I. A reactor SCRAM is modeled as first inserting only the RSS rods until their depth is equal to the Reactivity Control System (RCS) rods, then both banks of rods inserting together. This must be done to align with the input tables that were generated from VSOP. It results in a slower overall negative reactivity insertion that what would happen if both rod banks dropped from their current positions immediately.

[[

]]P Control rod insertion is accompanied by safety rod insertion during a simulated SCRAM, adding additional negative reactivity, and xenon transients are not included with this model that could challenge shutdown reactivity margin.

J. The SCRAM insertion rate is approximated from design documents. [[
]]P

K. The design of the check valves upstream of each circulator is not well-defined. Inputs were chosen to result in a smooth closure during low-flow transients so that the behavior matches that which is expected using engineering judgement.

L. The default discharge coefficient for restrictors modeling break areas where the fluid is expected to be a vapor is 1.0. The value is 0.61 for liquids. Analysts may adjust this as applicable for the event under consideration.

M. [[
]]P

N. The outlet conditions and pressure response of the multi-stage turbine assembly is approximated by a set of linear (or piece-wise linear) response curves based on vendor data and upstream model conditions. The input data used a constant set of main steam input conditions, and thus the response may differ under different main steam conditions. No data was available for that operating regime. It is assumed that the quasi-Steady State simplified response adequately represents the turbine during the analyzed scenarios. No inertial effects are modelled during turbine trip or rundown.

O. Relief valve piping in the PLPRS and the SG are modelled in upstream references using current pipe run estimates from plant design. Any pressure drop between the piping and the valves is assumed to be representative.

P. Reactor Pressure Vessel temperatures are reported by aggregating the nodal results from the appropriate components. The heat transfer coefficients for convection, radiation, and conduction are unchanged from the upstream model. More detailed analysis will be conducted outside of event transient analysis to determine the validity of the RPV temperatures, but analysts may report this as best-available data.

Q. Waterhammer effects are not considered when developing this model, as it is outside the current scope.

R. The Distribution Control System (DCS) structure, tunings, and design is an area of active development, with work still in an in-process state. Due to the preliminary nature of this work, a point-in-time snapshot of the control system design was used in the base model after consultation with the controls team due to the preliminary nature of the work on the base model.

This is the best available information that is considered representative of the control design at the current time.

S. Many aspects of helium circulator design remain under development. Low-speed circulator fan curves have been added to the model, scaled from the nominal vendor curves using centrifugal pump scaling relationships. The added low-speed curves ensure model stability during circulator coastdown following a trip. For zero-speed conditions, a generic stabilizing fan curve has been included to simulate the flow resistance of idle impellers. Since engineering data on idle impeller resistance is not yet available, small resistance values based on engineering judgment have been applied. Circulator check valves close under low-RPM conditions, so most scenarios would not be affected by the selected resistance values. The coastdown is modeled as a frictionless, inertial coastdown using vendor-supplied inputs.

C.3.2. Reactor

The preliminary reactor scoping model includes components contained in the Nuclear Island (NI) and NIAB and interfaces with the SG in the RB and RCCS in the NIAB. The Reactor scoping model extends from the RPV top head, down to the bottom of the defueling chute. Radially the model extends past the RB concrete all the way to the soil. [31]

The boundaries between the reactor scoping model and interfacing models are defined in Table 2.

Table 2: Boundary and Interfaces

Boundary/interface	Location
Reactor Inlet/SG Outlet	Cold Helium leaving the SG enters the Reactor
Reactor Outlet/SG Inlet	Hot Helium leaving the reactor travels to the SG

The Reactor model's BCs were removed. The reactor inlet interfaces with the SG outlet and the reactor outlet interfaces with the SG inlet to form the HPB. The cold leg of the RCCS standpipes (both train A and B) interfaces with the outlet of the RCCS model, and the hot leg interfaces with the inlet to the RCCS model. [4]

C.3.2.1 Geometry

[[

]]P

The Kugeler-Schulten convection correlation, [[ ]]P is used when solving for the convective heat transfer between the pebbles and the helium. For the effective pebble bed conductivity between the pebbles, the Zehner-Schlünder model is used, with A3-3 graphite as the conductive material [28].

[[

]]P

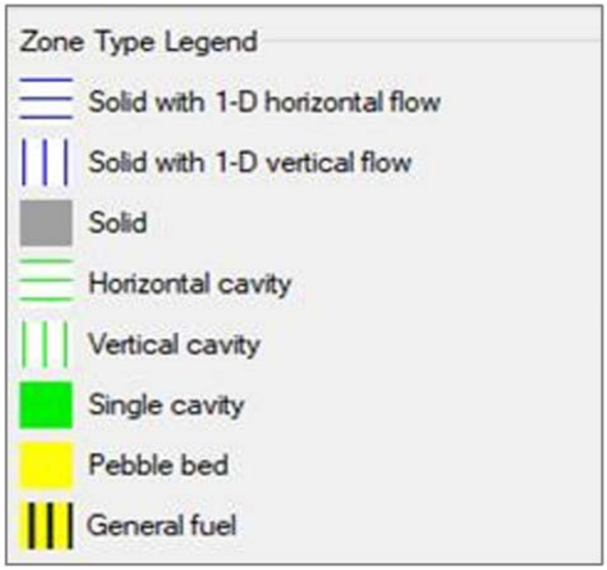

Figure 12: Zone Type Legend Single Cavities With "P" are Connection Ports

C.3.2.2 Material Allocations

Table 4 provides the material allocated to each zone and Figure 13 shows the regions where different materials are located within the reactor core. The temperature-dependent material properties are assumed to be representative of the end-of-life stage. The air below the bottom of the RPV and concrete is approximated as a solid with the conduction of air. Specific information on the allocated material and material properties (TRISO Particles, Graphite, Metallics, Soil and Concrete, and Insulation) is in the Preliminary Flownex Reactor Scoping Model Report [31].

[[

]]P

[[

]]P

C.3.2.3 Neutronics

The neutronics script requires inputs that are read from input files. The reactor heat distribution input files are derived from Reference [9] and the point kinetics parameters are derived from Reference [10]. Below is a brief discussion of these and the decay heat and RCS rod worth for the Xe-100 [31]. Xenon feedback is currently not included in this model; it will be added in future releases of the model.

A. Heat Distribution

[[

]]P

B. Decay Heat

The decay heat curve is given by equation (C.1) [45]:

$$\dot{Q_d} = Q_0\,[(1 - \sum_{k=1}^{5} \beta_k) \sum_{k=1}^{5} \beta_k e^{-\lambda k t}] \tag{C.1}$$

The delayed neutron fraction and decay constants, for 100 [%] Maximum Continuous Rating (MCR), are read from a file called decay_heat.txt. The decay fraction and decay constants used, for nominal conditions starting at 100 % MCR, are shown in Table 6 [10]. Reference [10] states the curve is not valid past 48 hours.

[[

]]P

C. Delayed Neutron Precursors

The delayed neutron precursors used, for nominal conditions starting at 100 % MCR, are given in Table 7 and taken from Reference [10]. Reference [10] also provides off nominal precursor inputs.

[[

]]P

D. Feedback Coefficients

The reactivity feedback, in pcm, for the fuel, moderator and reflector is calculated using Equation (C.2) [31]. a, b, and c in Equation (C.2) are the feedback coefficients. $Tref$ is the volumetric averaged temperature at steady state and T is the current volumetric averaged temperature used for feedback.

$$\rho(T, Tref) = -a(T - Tref) + -(T2 - T2ref) + -(T3 - T3ref) \tag{C.2}$$

The reference temperature, $Tref$, is calculated at steady state conditions and the reactivity feedback is calculated from this temperature. Once the steady state temperature has been calculated, the core can be initialized at a different power level without recalculating the previously calculated $Tref$. This allows the reactor model to be used for different transient scenarios. Table 8 gives the reactivity parameters for nominal conditions [10]. Reference [10] also provides off nominal feedback coefficients inputs.

[[

]]P

Only the volume of the Uranium Oxy-Carbide (UCO) is used to calculate the volume averaged reference temperature for the fuel feedback. The volume of the TRISO shell and all the pebble graphite volume is used to calculate the volume averaged reference temperature for the moderator feedback. The volume of all the graphite outside of the core is used to calculate the volume averaged reference temperature for the moderator feedback.

E. RCS Rod Worth

[[

]]P

F. Boundary Conditions.

BCs for the reactor model are provided in Table 9.

[[

]]P

Helium from the Pure Fluids database was used as the fluid for the HPB. The RCCS is water-cooled; thus, using water as the cooling medium for the reactor cavity and gap between the RCCS and concrete.

C.3.2.4 Results

A. Materials

Table 10 provides the calculated mass of each zone. There will be some inaccuracies with some of the component masses, as the Flownex model is axisymmetric and some of the finer details of various components cannot be captured, e.g., fasteners, flanges, and spacers. The main goal is to capture most of the thermal mass that is within the reactor.

[[

]]P

B. Reactor Results

When using the BCs from Table 11, it was found that the Reactor Outlet Temperature (ROT) was higher than the prescribed 750.0 [°C], so the helium flowrate was adjusted so the ROT is 750.0 [°C]. The main results are shown in Table 11. It should be noted that Reference [10] did not specify what volumes were used for averaging, nor did it include the defueling chute. Reference [10] used a heat map, so any heat generation in the reflector or other components are reflected in the heat map.

[[

]]P

C.3.3. Steam Generator

The SG Model includes components contained in the NI and NIAB in the RB and Turbine Building (TB) on the Conventional Island (CI) side. [29]

The design inputs and BCs of the SG model will be used for analysis of the Xe-100 nuclear power plant, as well as to provide the steady state results of the model that forms the expected conditions of the SG during normal, full power operation. The SG model is one of the constituent sub-models that make up the plant mass and energy balance model. [29]

The SG model contains both the primary (helium) loop which interfaces with the reactor model and the Helium Service System (HSS) model, and the secondary (water/steam) loop which interfaces with the DA model, the turbine building model, and the startup and shutdown system model. [29]

The boundaries between the SG model and its neighboring models are defined in Table 12.

Table 12: Model Boundaries

Boundary/interface	Location
SG/Reactor model	Reactor side of the hot and cold helium ducts, immediately inside the reactor pressure boundary
SG/HSS	Outlet off the high pressure HSS nozzle and inlet of the low pressure HSS nozzle
SG/DA	Piping between the redundant feedwater isolation valves (FWIVs)
SG/TB	14 m beyond the second main steam isolation valves
SG/SSS	**Same as DA**

C.3.3.1 Inputs and Assumptions

The inputs and assumptions are summarized below:

A. Inputs

1. Reactor Conditions – Helium will be supplied to the reactor at 260°C and 6.0 MPa. Helium exiting the reactor will have a temperature of 750°C.
2. Steam Conditions – The SG will produce steam at 565°C and 16.5 MPa.
3. [[

]]P

B. Assumptions

[[

]]P

C.3.3.2 Steam Generator Model

A. Geometry

Figure 15 shows the flow path in the SG. Note that this figure does not reflect the new riser configuration or the SG nodalization.

[[

]]P

B. Boundary Conditions

[[

]]P

In order to achieve these required conditions, a series of other BCs are adjusted by the SG system. These BCs include primary flowrate, which is controlled by helium circulator speed, FW flowrate which is controlled by the FW pump speed and FW temperature which can be controlled by the DA system. These parameters are adjusted over the course of tuning the model and thus are considered as model results rather than inputs.

To improve the accuracy of the model, and to better match with neighboring models, these BCs are not simultaneously stipulated in the model. The pressure conditions are defined in key locations and a series of steady-state controller scripts change the adjustable parameters until the temperatures are met.

C. Fluids Modeled

For the primary side fluid, helium from the Flownex pure fluid library was selected. On the secondary side, the two-phase water with incondensable gas (air) was selected. While the use of helium as the primary side is self-explanatory, the inclusion of air with the two-phase water in the secondary side will allow for more realistic simulations, as some air may infiltrate the secondary loop during normal operation.

D. Primary Side Components

Table 15 shows primary side component inputs in the order of flow direction. The primary loop is modeled as a continuously flowing loop including a heavily simplified reactor which models the heat addition and pressure drop that occur in the core. The helium circulators are preceded by check valves. The PRV located at the bottom of the SG is preceded by an isolation IV. The RPV interfaces with the RB. The components are identified in Table 15. The Low-Pressure (LP) and High-Pressure (HP) nozzles interface with the HSS.

[[

]]P

E. Primary Side Pressure Drop

A summary of the expected pressure drop around the primary loop is provided in Table 16. Pressure drop values are found using CFD results and application of experimental correlations for specific geometries. Whenever possible, CFD results are used as they provide a more application specific analysis of the expected pressure drop. However, some areas of the model do not yet have CFD pressure drop results. Such cases are sourced using correlations from the *Handbook of Hydraulic Resistance* by I. E. Idelchik.

[[

]]P

The pressure losses in all piping components are calculated automatically by Flownex. This is achieved by specifying the loss type (Darcy-Weisbach) pipe roughness for each component. Certain other features of the flow path such as bends, tees and area changes have associated form losses which must be added manually.

G. Secondary Side Components

The secondary side of the model (outside of the SG components) is still under development; however, it will be capable of delivering steam to the Turbine or to a process steam facility. Table 17 provides the preliminary component inputs for the secondary side of the SG in Figure 16.

Table 17: Secondary Component Inputs

Component	Label
FWIV A/B	1a
FW Line After FWIV	2a
SG flow restrictor	3a
Lower transition tubes	4a
SG tubes	5a
SG compensation tubes	6a
MSIV	7a
Backup MSIV	8a

H. Secondary Side Nodalization

Figure 16 shows the Flownex model for the SG secondary side. The SG FW lines interface with the NIAB, where they flow down to the bottom of the SG. [[ ]]P After the FR, there is a tube transition region before the SG helical tubes are reached. After the SG tubes, there is a tube compensation and transition before reaching the tubesheet and reducing elbow (header). Two separate steam lines leave the SG before the steam PRV[2], IV and NRV are reached. The two separate steam lines feed into a header that feeds the Main Steam Line (MSL) and the SSS lines. The MSL interfaces with the TB on the CI side. The SSS interfaces with the DA that is in the NIAB.

[2] Steam side PRV has not been sized yet. The sizing requirements will come from the safety analysis. The set-point is 17.5MPa.

[[

]]P

C.3.4. Reactor Cavity Cooling System

The RCCS has the required safety function to "control decay heat removal" [21] . The RCCS SSCs in the reactor citadel provide the safety related passive means for heat removal for the RPV and reactor citadel walls during a DBE/DBA.

During DBE/DBAs the RCCS will ensure the reactor cavity walls will remain below 175°C, the RPV will remain below 540°C and reactor vessel internals will remain below 593°C. During normal operations the RCCS will ensure the reactor cavity walls will stay below 65°C per ACI 318. [33]

The RCCS model is still under development. The steady state model contains a general purpose and layout of the system. The liquid is single phase while in steady state with a network of pumps, pipes, and HXs removing a known quantity of parasitic heat loss from the RPV. Thus, for purposes of the safety analysis, only BCs are utilized.

C.3.5. Deaerator

The DA was removed from the Safety Analysis Model. The DA model developed in Reference [26] includes "components contained in the NIAB such as the HPFWP, FW flow control valves (FCV), IVs and Non-return valves (NRV). The DA model interfaces with the SG, SSS and TB." For the safety analysis model, modifications were made to compensate for the removal of the DA:

- The DA tank, and all upstream piping between the SSS and Turbine Bypass have been removed from the model. The DA is assumed to be a fixed temperature and pressure BC upstream of the HPFWPs and a fixed temperature BC downstream of the HPFWP recirculation lines. The temperature and pressure of the DA is represented by a BC as specified in Table 19 consistent with the Steady State value in [35]. The recirculation lines also were modified to discharge into a BC of the same conditions as the source. The rationale behind this modification is:
    - The DA tank is a large tank, which results in the conditions within the tank being relatively stable over the short term, which is the primary focus of the Flownex Safety Analysis model.
        - With the removal of the DA tank, the DA level controller and the DA temperature controller have also been removed as the components they act on are no longer present in the model. These systems are assumed to continue their functions for the simplified Safety Analysis model while the system has sufficient coolant inventory.
    - The removal of the DA tank component assumes that all steam through the turbine bypass and turbine goes to the DA tank.

C.3.6. Feedwater System

This FW inlet BC specifies the temperature and mass flow which are both controlled by individual scripts. The mass flow rate is controlled such that the SG outlet temperature (at node #10) is maintained. As such the FW temperature is controlled such that the reactor inlet temperature is also maintained. [29]

C.3.7. Turbine and Condenser

The heat balance data from the Steady State integrated report [35] for 100% to 25% power conditions for the Air Cooled Condenser (ACC) are applied in this model. Four curves are used and connected scripts [6] on the TB page.

The outlet temperature is determined based on the saturated conditions at the outlet of the turbine and the pressure given in [35]. The conditions given for the ACC turbine and condenser are given in Table 18 below. Note that the exhaust pressure data comes from [76] which is the vendor heat balance data. As shown by [76], the combination of active extraction steam lines changes based on power level, which results in a piecewise flow response. This is approximated by the stepwise application of a flow admittance to the flow resistance component from the *Turbine Flow Admittance* script. Admittance values were computed as the ratio of mass flow to pressure drop for each power level and applied to discrete ranges of mass flows. Note that the inlet pressures used were based on the preliminary inlet pressures of the Water-Cooled Condenser used in the previous iteration of this calculation. The inlet values in the Flownex model for [35] differ from those used previously in the Water Cooled Condenser model, but this will have negligible effect on the model as the turbine is ultimately a BC.

The multi-stage turbine components in the upstream reference models [82] and [35] are simplified down to a single turbine control valve, the turbine bypass valve (BV), the turbine stope valve, a flow resistance, and a set of lookup tables that serve as a BC for the turbine and condenser. The flow coefficient of the lumped valve is the sum of the individual valves. One byproduct of this is that the turbine power result becomes a direct relationship with steam mass flow, which is sufficient for the safety analysis event scope. The turbine mass flow used for power calculations is set to only use the steam portion of any two-phase flow based on the quality of the two-phase fluid. This prevents water flow skewing the turbine outputs.

[[

]]P

C.3.8. Startup/Shutdown System

The safety analysis base model includes a simplified representation of the SSS to simulate the effects of decay heat removal and sensible heat removal from the Xe-100 reactor. The purpose of the simulated SSS is to provide secondary heat removal when main loop cooling capabilities are unavailable. However, SSS fluid conditions, operational sequencing, and target SG conditions for cooldown have not been formalized in procedures at the time of this calculation's approval. Therefore, estimated or assumed values for SSS functionality are applied. [6]

The SSS is placed in service when specified by the prescribed PRA event sequence for a given transient. The SSS simulation has the effect of preventing further fuel heatup and bringing the plant to a stable, cooled-down condition. Fuel temperatures and the resulting dose calculations are the primary FOM for safety analysis, so SSS behavior is of secondary importance once fuel heatup is arrested and maximum fuel temperature (and dose) have occurred. SSS functionality is fully automated in the base model by the Flownex script. [6]

SSS cooldown is accomplished using BCs connected to the FW inlet and steam outlet sides of both SGs to simulate single-train or dual-train SSS operability. The SSS feedwater BCs (Figure 17) provide FW at a specified flow rate. As described in [75], the SSS pumps draw from a vented tank, so the supply water is always subcooled liquid. In the simplified representation in the base model, it is maintained at a fixed temperature. SSS feed flow rates are specified in concert with helium flow and SG outlet pressure to control the rate of heat removal and achieve a targeted fuel cooldown rate and/or maintain the SG in a watering condition.

[[

]]P

The SG outlet BCs (Figure 18) are specified-pressure type, initially maintained at normal steam pressure but isolated behind closed valves. With the IVs open and plant cooldown in progress, the specified pressure follows a linear program as ROT decreases. The program drives the SGs toward a watering condition after the targeted cooldown helium temperature is reached.

[[

]]P

Once activated, a script manipulates the steam and feed IVs, feed pumps, RCSS, helium circulators, and SSS outlet valves to initiate plant cooldown from any starting condition. The general sequence is as follows; depending on plant conditions at SSS initiation, actions for every step may not be required.

1. Trip the reactor / run back the circulators.
2. Trip the operating feed pump.
3. Open the SSS steam outlet valves, and simultaneously close the MSIVs and FWIVs.
4. Initiate SSS FW flow to restore adequate liquid water level in the SG tubes to support starting a circulator.
5. Start a circulator.
6. Allow SG tubes to pressurize by heat addition from the running circulator, initiating SSS steaming mode to remove decay and sensible heat and cool down the plant.
7. Transition to SSS watering mode following cooldown.

C.4. Flownex Model Boundary Conditions

A. Simplification Boundary Conditions

Table 19 lists all the BC components used in the simplified model for transient analyses. The listed values correspond to the parameters used to establish the 100% power controlled operating conditions. They are derived from the upstream [35] model conditions at 100% power.

Most of these BCs will remain unchanged during an event unless that event specifically requires a change. [[

]]P

B. Steady State Boundary Condition and Component Settings

The following BCs and component inputs must be set when performing a steady state solution, in addition to those listed in Section 2.11.2.A. The values shown in Table 20 are for 100% power conditions and match those used in [2]. [[

]]P

Appendix D GOTHIC Model

GOTHIC was developed and is maintained under Numerical Advisory Solutions, LLC QA Program that conforms to the requirements of 10 CFR 50 Appendix B and 10 CFR 50 Part 21. GOTHIC is a hybrid code that bridges the gap between CFD and standard thermal-hydraulic systems analysis codes. Lumped parameter and 3-D regions can be combined into a single model to allow for detailed analysis in regions of interest. As a result, assuming proper care is taken in development of the model, a relatively fast running simulation can be produced. These features allow for the development of models suitable for sensitivity studies and design change analyses. The purpose of this model is to provide a relatively fast running tool to provide insight into dose analysis, RCCS design changes, and RB design changes. [7]

D.1. Model Description

Thermal-hydraulic analysis is needed to address certain safety issues such as plant response following a LOCA; for designing plant systems; to predict performance of systems and components; to model the behavior of plant buildings; or for a wide variety of situations that involve the response of a system to applied mass and energy sources. In these analyses, the focus may be on the maximum pressure or temperature, pressure loadings on internal structures due to jet impingement or pressure gradients, local temperature variation, equipment temperatures, buildup of volatile gases or a variety of other conditions of interest.

The GOTHIC model includes the RPV, Cross-Over Pipe, and SG. The RCCS is modeled as a temperature dependent heat flux on the RPV outer surface based on results from a stand-alone GOTHIC RCCS model. Results for steady- state, CRWCS, and Depressurized Loss of Forced Circulation transients are presented in Reference [7].

D.2. Methodology

The GOTHIC8.4a(QA) model is an interim model that incorporates various assumptions and inputs that are subject to change as the Xe-100 system design evolves. The purpose of this model is to provide a relatively fast running tool to provide insight into dose analysis, RCCS design changes, and RB design changes. Using available data (along with various assumptions for data that has not yet been specified), a GOTHIC model of the reactor system was developed to include the RPV, Cross-over Pipe, and SG. After development of the base model, iterative runs were performed to allow tuning of various parameters so that the model would produce steady-state conditions close to target values [7].

The restart-data file from the final steady-state run was used to define the reactor system conditions for production of the following transients.

D.2.1. CRW (with long-term PLOFC)

A. Nominal case without uncertainties applied to key parameters.

B. Extreme case with uncertainties applied to all key parameters.

Note that the CRW includes a loss of forced circulation; therefore, the CRW, as analyzed in this report, is equivalent to a PLOFC with a power excursion occurring early in the event. As a result, the CRW will be bounding relative to the PLOFC.

D.2.2. DLOFC with SCRAM

A. Nominal case without uncertainties applied to key parameters.

B. Extreme case with uncertainties applied to all key parameters.

C. Case with reactor power uncertainty applied.

D. Case with decay heat uncertainty applied.

E. Case with pebble bed effective conductivity uncertainty applied.

D.3. GOTHIC Model

This section describes the components used for development of the GOTHIC Xe-100 reactor system model. Brief summaries and descriptions are provided in the body of this report.

D.3.1. Inputs

The GOTHIC Model Inputs used to develop the reactor system model (other GOTHIC models used similar inputs and, in some cases, additional inputs were used) are listed in Reference [7]. These parameters were assumed during development due to the incomplete specification of the Xe-100 design.

D.3.2. Assumptions

Listed below are assumptions employed in the development of the preliminary GOTHIC reactor system model along with assumptions applied to the CRW and DLOFC transient runs:

A. Heat transfer within the RPV and SG is assumed to be circumferentially symmetric.

B. The helium risers and control rod channels are thermally isolated from the side reflector.

C. The fuel pebbles are assumed to be evenly distributed across the width of the core, thus a reduction in the fuel pebble density next to the side reflector is not currently modelled.

D. The fuel pebble volumetric heat generation rate is assumed to be evenly distributed across the radius of the pebbles. For the model presented in this report, a spherical geometry was specified for the fuel conductors.

E. Heat conduction due to direct contact between the fuel pebbles and side reflector is assumed to be handled via the GOTHIC8.4a(QA) effective conductivity model.

F. The thermal conductivity of the fine-grain graphite [[ ]]^P in the reflectors corresponds to irradiated graphite.

G. For the transients presented in this document, the core axial and radial power distributions are assumed to remain constant through the duration of the transients.

H. Loss coefficients at the core "z" planes are used to represent core friction losses. The "z" plane loss coefficients were adjusted during steady-state to achieve a target 100% power/flow RPV pressure drop. A future version of the reactor vessel model will incorporate the KTA friction loss correlation to represent friction losses in the pebble bed.

I. Sufficient data to fully define homologous head curves for the helium circulators is not currently available. Available head data from the Flownex model was converted to homologous data and was found to be reasonably close to the GOTHIC built-in Semiscale homologous head curves; therefore, the Semiscale homologous head curves were used. No torque data is available; therefore, the Semiscale homologous torque curves were used. Circulator speed versus time for the circulator coast- down was obtained from the Flownex model. A comparison of the circulator mass flow rates showed that the GOTHIC flow rates are very similar to the Flownex circulator mass flow rates for a coastdown.

J. Break and PRV discharge flows are assumed to blowdown to volumes at atmospheric pressure.

K. The defuel chute region is included in the model; however, it is assumed to be inoperative (no flow and no heat generation).

L. The radiation from the fuel conductors to the side reflector is "smeared" over the entire length of the side reflector. Similarly, the radiation from the CB to the RPV is "smeared" over the entire length of RPV. This assumption will be addressed in a future revision of this calculation.

M. The core power history for the PLOFC with rod-withdrawal transients consists of unverified data.

N. Heat loss from the outer surface of the SG and cross-over pipe is not modelled.

O. The HPB PRV connected to the SG is being resized. The new valve size and design relief capacity are not captured in this report.

P. The size and relief capacities for the MSL safety relief valves have not yet been defined; therefore, simple open/shut valves have been assumed.

Q. For the [[ ]]P graphite, a thermal conductivity corresponding to high irradiation was assumed for the entire axial length of the reflector next to the core region. This is conservative relative to the Flownex model that employs an axial variation for the irradiation.

R. The most recent revisions of some references indicate minor dimensional changes within the reactor vessel system. These changes will have an insignificant effect on the transient results; therefore, they will be captured in the next iteration of the GOTHIC vessel model.

S. The provided VSOP decay heat curve does not extend out to the 30 days needed for the GOTHIC runs. A curve fit to the VSOP data is therefore used to estimate the remaining decay heat. Since this curve fit is as estimate of the very-long term decay heat, the 5.7% decay heat uncertainty was not applied to this extrapolated data for the PKPIRT cases.

D.3.3. GOTHIC Model Description

D.3.3.1 Volumes

Table 21 lists the GOTHIC volumes and provides a brief description of the reactor system region represented by the volume. Volume numbers with an attached "s" denote subdivided (3-D) volumes.

[[

]]P

A. **Core Volumes**

The pebble bed region of the core is modeled by Volume 4s in Table 20. The cone region of the pebble bed is not explicitly modelled; therefore, all fuel pebbles are assumed to occupy a cylindrical region. The pebble bed is divided radially into a central cylindrical region surrounded by four rings. The radial dimensions of the five radial fuel regions are set to be approximately equal to the radial dimensions used in the VSOP model documented in [36]. Each radial fuel region is, in turn, divided into 19 equally spaced axial nodes. Thus, the pebble bed is composed of 95 distinct nodes.

B. **Helium Volume in SG Tube Coil Region**

Volume 14s models the Helium space in the SG tube coil region. Heat transfer from the Helium is assumed to be evenly distributed across the diameter of tube coil region; therefore, only axial subdivisions were defined. Sensitivity studies were performed to determine the minimum number of axial nodes required to reproduce the desired heat transfer performance for the SG. The sensitivity studies indicate that 30 axial nodes were required to achieve acceptable heat transfer performance.

C. **Water/Steam Side of Tube Coils**

Volumes 24s, 25s, and 26s model the water/steam side of the SG tube coils. Heat transfer was assumed to be evenly distributed across the diameter of the tube coil region. Axially, these volumes were divided into 30 axial nodes to match the axial regions for the Helium side of the tube coils.

D.3.3.2 Flow Paths

The GOTHIC Flow Paths are summarized in Table 22.

[[

]]^{P}

D.3.3.3 Conductors

A. Conductors

Table 23 provides a summary of the conductors defined for the GOTHIC reactor system model. Conductor numbers with a “s” appended refer to subdivided conductors.

[[

]]P

1. **Pebble Bed Fuel Conductors**

The fuel conductors for the GOTHIC8.4a(QA) model were developed as follows:

a. For each of the 95 core sub-volumes, a single spherical conductor is defined. Thus, each fuel conductor represents the average fuel conditions for all the fuel pebbles in the sub-volume.

b. The surface area of each fuel sphere conductor is set equal to the total surface area of the fuel pebbles within the sub-volume connected to the conductor.

c. The radius of the fuel spherical conductor is set equal to the radius of a single fuel pebble.

d. The volumetric heat generation rate is adjusted by axial and radial power profiles from the 100% power steady-state VSOP model documented in [36].

e. After reactor SCRAM, the volumetric heat generation rates of the fuel conductors are adjusted to represent the decay heat generation. For the CRW event, the volumetric heat generation rates were adjusted to represent the core power produced by the CRW.

f. An effective thermal conductivity that represents pebble-to-pebble conductivity in combination with pebble-to-pebble radiation and pebble-to-reflector contact is specified for the pebble bed volume.

g. At the top and bottom outer surfaces of the pebble bed, fuel conductor-to-top reflector and "cone" reflector radiative heat transfer is specified.

h. The inner surfaces of the fuel conductors (representing the fuel sphere centers) are assigned a zero heat flux BC.

i. A fuel pebble bed convective heat transfer coefficient is assigned to the outer surface of the fuel conductors (see Table 24, Surface Option 7).

2. **Side Reflector Conductors**

The Helium gap between the outer graphite surface of the side reflector and the inner surface of the core barrel is not explicitly modelled as a separate volume. This is due to uncertainties concerning graphite expansion and fissuring due to radiation exposure along with uncertainties concerning Helium bypass around the graphite blocks into the Helium gap. Therefore, a composite conductor consisting of the side reflector graphite inner blocks, graphite outer blocks, Helium gap, and core barrel was defined.

The side reflector support rings and wedges are not explicitly modelled. Therefore, the thermal conductivity of the helium gap in the side reflector conductor was increased. Comparison of the GOTHIC and Flownex DLOFC results revealed that the GOTHIC model shows much higher thermal resistance across this gap; therefore, for the DLOFC transients an additional multiplier is applied to the thermal conductivity of the gap. This is justified by the fact that the side reflector support rings and wedges will provide conduits for heat transfer directly through the gap versus conduction through the helium layer. In addition, the Flownex model includes Helium bypass flow through this gap, whereas, in the GOTHIC model the Helium is stagnant.

B. Surface Options

GOTHIC surface options define heat transfer coefficients along with various heat transfer options. Conductors have two sides; therefore, a surface option is defined for each side of the conductor. Table 24 lists the Surface Options.

Table 24: Surface Options

SURFACE OPTION	DESCRIPTION
Surface Option 1 **Zero Flux**	This surface option defines a zero heat flux condition.
Surface Option 2 **Convective Reflector Inner**	This surface option defines the heat transfer characteristics for the inner surface of the side reflector next to the fuel pebble bed. This surface option incorporates the pebble bed effective conductivity.
Surface Option 3 **Convective Reflector Outer**	This surface option defines the heat transfer characteristics for the outer surface of the side reflector conductor (this corresponds to the outer surface of the core barrel).
Surface Option 4 **Convective He Out Reflector**	This surface option defines the heat transfer characteristics for the inner surface of the side reflector next to the He outlet plenum.
Surface Option 5 **Face Down**	This surface option defines the heat transfer characteristics for downward facing surfaces.
Surface Option 6 **Face Up**	This surface option defines the heat transfer characteristics for upward facing surfaces.
Surface Option 7 **Pebble Bed**	This surface option defines the heat transfer characteristics for the outside surface of the conductors representing the fuel pebble bed. Employing the KTA Heat Transfer Coefficient (HTC) would require programming a DLL to hook into GOTHIC. Therefore, for the GOTHIC model used in this report, an HTC of a form that allowed for direct input to GOTHIC was used.*
Surface Option 8 **SG Tube Interior**	This surface option defines the heat transfer characteristics for the inner surface of the SG tubes.
Surface Option 9 **SG Tube Exterior**	This surface option defines the heat transfer characteristics for the exterior surface of the SG tube coils. The Helium flow in this region is similar to flow on the exterior of a bank of horizontal tubes; therefore, the form of the convective HTC was set to match that for flow over a bank of horizontal tubes.
Surface Option 10 **RPV Vertical Wall**	This surface option defines the heat transfer characteristics for the vertical portion of the RPV outer wall.

SURFACE OPTION	DESCRIPTION
Surface Option 11 **"Generic Convective"**	A generic convective HTC for miscellaneous surfaces with complex geometries.
Surface Option 12 **Vessel Wall**	Defines heat flux for RPV outer surface as a function of RPV surface temperature. This represents heat removal from the RPV surface by the RCCS.
Surface Option 13 **Steam Pipe DN250**	Defines the HTC for the interior surface of the DN250 steam pipe.
Surface Option 14 **Steam Pipe DN350**	Defines the HTC for the interior surface of the DN350 steam pipe.
Surface Option 15 **FW Pipe DN150**	Defines the HTC for the interior surface of the DN150 FW pipe.

*** The correlation is :**

$$Nu = 2 + 1.1 Pr^{1/3} Re^{0.6}$$

where the non-dimensional Prandtl number (Pr) is defined as follows:

$$Pr = \frac{\mu C_p}{k}$$

where the Nusselt number is defined based on pebble diameter (d_p) and is given by:

$$Nu = \frac{h d_p}{k}$$

D.3.3.4 Boundary Conditions

Table 25 contains the BCs and a brief description.

Table 25: Boundary Conditions

BOUNDARY CONDITION	DESCRIPTION
1P - Blowdown	Pressure boundary condition that collects flow from the DLOFC break. This boundary condition is set to atmospheric pressure.
2F – FW Intact In	Flow boundary condition that supplies FW to the intact FW/steam circuit.
3F – FW Faulted In	Flow boundary condition that supplies FW to the faulted FW/steam circuit.
4P – Press Control	Pressure boundary condition that maintains RPV pressure during steady-state initialization. This boundary condition is isolated from the RPV during transient runs.
5P – PRV Discharge	Pressure boundary condition that captures discharge from the PRV.
6P – Steam Out	Pressure boundary condition that collects steam flow from the SG.
7P & 8P– Intact & Faulted MS SRV	Pressure boundary conditions that provide blowdown sinks for the MSL SRVs.

D.3.3.5 Components

A. Valves

Table 26 contains a listing of the valves and a brief description.

[[

]]P

B. Pumps – Helium Circulators

Homologous head and torque curves are used in GOTHIC to define the performance of pumps and fans. A limited amount of Helium circulator head data and no torque data is available in the Xe-100 Flownex documentation; therefore, construction of homologous curves suitable for input to the

GOTHIC model is not possible. The limited amount of the head data was translated to homologous data and compared to types of homologous curves built into GOTHIC. This data comparison revealed that the available head data was similar to that supplied for the Semiscale pump available in GOTHIC; therefore, the Semiscale homologous head curves were specified for the circulators. No torque data for the circulators was available; therefore, the Semiscale homologous torque data was also specified and pump coastdown data from the Flownex model was used. During steady-state initialization, the rated head of the Helium circulators was adjusted to achieve the target steady-state Helium flow.

D.3.3.6 Trips

Table 27 lists the Trips specified for the GOTHIC reactor system model:

[[

]]P

D.3.3.7 Control Variables

The list of Control Variables specified for the GOTHIC reactor systems model are specified in Table 28.

Table 28: GOTHIC Control Variable Summary

CONTROL VARIABLE	GOTHIC MODEL DESIGNATION	DESCRIPTION
1C	Axial Positions	Sets up array of axial positions for the core sub-volumes
2C	Chan1 Axial Power	Uses axial position pulled from 1C to look up axial power in Table 1T (axial power profile for Fuel Channel 1). The result is multiplied by the radial power factor for Fuel Channel 1 to give the total power for each fuel conductor in Fuel Channel 1.
3C	Chan2 Axial Power	Same as 2C for Fuel Channel 2 sub-volumes
4C	Chan3 Axial Power	Same as 2C for Fuel Channel 3 sub-volumes
5C	Chan4 Axial Power	Same as 2C for Fuel Channel 4 sub-volumes
6C	Chan5 Axial Power	Same as 2C for Fuel Channel 5 sub-volumes
7C	Vessel DP	Calculates RPV ΔP in kPa
8C	Time after Rx trip	Tracks time after reactor SCRAM
9C	Decay On?	Determines if reactor has SCRAMed
10C	Decay Heat	Determines decay heat using time after reactor SCRAM
11C	Chan1 w/ Decay	If reactor has SCRAMmed, applies decay heat to Fuel Channel 1 conductors
12C	Chan2 w/ Decay	If reactor has SCRAMmed, applies decay heat to Fuel Channel 2 conductors
13C	Chan3 w/ Decay	If reactor has SCRAMmed, applies decay heat to Fuel Channel 3 conductors
14C	Chan4 w/ Decay	If reactor has SCRAMmed, applies decay heat to Fuel Channel 4 conductors
15C	Chan5 w/ Decay	If reactor has SCRAMmed, applies decay heat to Fuel Channel 5 conductors
16C	Integrated PRV Flow	Tracks integrated mass flow out of the PRV (kg)
17C	Integrated Break	Tracks integrated mass flow out of the 65 mm DLOFC break (kg)
18C	Power vs Time	ASME data
19C	BC 2 Temperature	ASME data
20C	BC 2 Pressure	ASME data

CONTROL VARIABLE	GOTHIC MODEL DESIGNATION	DESCRIPTION
21C – 26C	Flows	Miscellaneous controllers for pulling data for output for ASME data requests.
27C	Lower Head Temp	ASME data
28C	Power Ramp Table	Defines power ramp for steady-state runs
29C-33C	Chan1-5 Power Ramp	Defines power ramps for the 5 core radial channels for steady-state runs
34C-56C	RPV Level Temp	Pull RPV outer surface temperatures for each RPV axial level & convert to ^{o}C
57C	Sum Weighted RPV T's	Sum up RPV temperatures weighted by axial heights
58C	Avg RPV Temp	Calculates average RPV surface temperature
59C	RPV Avg Heat Flux	Pulls RPV exterior surface heat flux as a function of average RPV surface temperature
60C	Int Steam-Steam Side	Calculates integrated steam flow from steam side of SGTR break
61C	Int Liq-Steam Side	Calculates integrated liquid flow from steam side of SGTR break
62C	Int Drop-Steam Side	Calculates integrated drop flow from steam side of SGTR break
63C	Int Steam-FW Side	Calculates integrated steam flow from FW side of SGTR break
64C	Int Liq-FW Side	Calculates integrated liquid flow from FW side of SGTR break
65C	Int Drop-FW Side	Calculates integrated drop flow from FW side of SGTR break
66C	Int MS SRV Intact	Calculates integrated flow from main steam SRV on intact FW/steam circuit
67C	Int MS SRV Faulted	Calculates integrated flow from main steam SRV on faulted FW/steam circuit
68C	Local Vap Temp Core	Sets up array of vapor temperatures for each of the 95 core volumes
69C	Reflector HTC	Calculates side reflector HTC for each side reflector sub-conductor based on local helium temperature
70C	Time after Circ Trip	Calculates elapsed time following circulator trip
71C	He Circ Trip?	Determines if circulator trip has occurred
72C	SG HTC Ratio	Calculates ratio for adjusting SG tube HTC multiplier to account for circulator coastdown
73C	SG HTC Multiplier	Pull SG tube HTC multiplier
74C	SG HTC	Calculates final SG tube HTC multiplier with adjustment for helium circulator coastdown

D.3.3.8 Table Functions

The list of Table Functions specified for the GOTHIC reactor systems model are specified in Table 29.

Table 29: GOTHIC Data Tables Summary

Table	GOTHIC Model Designation	Description
1T	Chan 1 Axial	Fuel Channel 1 Axial Power Profile
2T	Chan 2 Axial	Fuel Channel 2 Axial Power Profile
3T	Chan 3 Axial	Fuel Channel 3 Axial Power Profile
4T	Chan 4 Axial	Fuel Channel 4 Axial Power Profile
5T	Chan 5 Axial	Fuel Channel 5 Axial Power Profile
6T	Decay Heat	Decay heat versus time
7T	Eff K por-Fuel	Pebble bed effective conductivity versus temperature with porosity adjustment
8T	Circ Coastdown	He Circulator speed versus time for He Circulator coast-down
9T	FW Coastdown	Relative FW flow versus time for FW coast-down
10T	Steady-State FW Flow Ramp	Specifies FW flow ramp for steady-state runs
11T	Steady-State Circ Ramp	Specifies Helium circulator startup ramp for steady-state runs
12T	Steady-State Power Ramp	Specifies core power ramp for steady-state runs
13T	SG Tube HTC Multiplier	Multiplier for SG tube HTCs
14T	RPV-RCCS Flux	Specifies RPV surface heat flux as a function of RPV average outer surface temperature
15T	MS Vlv Open	Open travel curve for main steam isolation valves
16T	MS Vlv Close	Close travel curve for main steam isolation valves
17T	MS Vlv Cd Mult	Main steam isolation valves Cd multiplier curve
18T	TSV Close	TCV/TSV close travel curve

Table	GOTHIC Model Designation	Description
19T	SGTR FW Intact	FW inlet flow to intact FW/steam circuit for SGTR event
20T	SGTR FW Faulted	FW inlet flow to faulted FW/steam circuit for SGTR event
21T	Control Rod Withdrawal	Core power curve for CRS
22T	No Scram	Core power curve for no scram event
23T	SG HTC Ratio	SG tube HTC adjustment ratio that accounts for helium circulator coastdown
24T	Spare1	Spare table with 100 data points
25T	Spare2	Spare table with 100 data points
26T	Spare3	Spare table with 100 data points
27T	Spare4	Spare table with 100 data points
28T	Spare5	Spare table with 100 data points
29T	Specific Heat Multiplier	Specifies multiplier for specific heat
30T	Gap Cond Multiplier	Specifies multiplier for reflector-core barrel gap thermal conductivity.

D.3.3.9 Materials

The list of Control Variables specified for the GOTHIC reactor systems model are specified in Table 30.

[[

]]P

D.4. GOTHIC Steady-State and Transient Cases

This Section lists some of the steady-states and transients cases run with the GOTHIC vessel model. More detail on the results are found in Reference [2].

D.4.1. Steady States Cases

The following steady state cases were run.

A. CRW Nominal Steady-State
B. CRW Extreme Steady-State
C. DLOFC Nominal Steady-State
D. DLOFC Extreme PKPIRT Steady-State
E. DLOFC Effective Conductivity PKPIRT Steady-State
F. DLOFC Reactor Power PKPIRT Steady-State

D.4.2. Transients Cases

The following Transient Cases were run.

A. CRW Transients
    - A CRW with all PKPIRT parameters set to nominal values.
    - A CRW “extreme” case where all PKPIRT parameters are set to conservative values.
B. DLOF Transients

- A DLOFC with all PKPIRT parameters set to nominal values.
- A DLOFC “extreme” case where all PKPIRT parameters are set to conservative values.
- A DLOFC with the pebble bed effective conductivity reduced by 5%.
- A DLOFC with the core power increased by 2%.
- A DLOFC with the decay heat increased by 5.7%.
- A DLOFC with the side reflector thermal conductivities increased by 20%.